Applied Catalysis B: Environmental 181 (2016) 156–196

Contents lists available at ScienceDirect

Applied Catalysis B: Environmental

journal homepage: www.elsevier.com/locate/apcatb

Review

Development of nickel based catalysts for the transformation of natural triglycerides and related compounds into green diesel: a critical review

Christos Kordulis[a,b,*], Kyriakos Bourikas[c], Mantha Gousi[a], Eleana Kordouli[a], Alexis Lycourghiotis[a]

[a] Department of Chemistry, University of Patras, GR-26504 Patras, Greece
[b] Foundation for Research and Technology, Institute of Chemical Engineering Science (FORTH/ICE-HT), Stadiou str., Platani, P.O. Box 1414, GR-26500 Patras, Greece
[c] School of Science and Technology, Hellenic Open University, Tsamadou 13-15, GR-26222, Patras, Greece

ARTICLE INFO

Article history:
Received 13 May 2015
Received in revised form 17 July 2015
Accepted 24 July 2015
Available online 26 July 2015

Keywords:
Ni catalysts
Green diesel
Renewable diesel
Selective deoxygenation (SDO)
Triglycerides
Vegetable oils
Animal fats
Biofuels
Stand-alone process

ABSTRACT

The accumulation of greenhouse gases in the atmosphere resulting from the extensive use of fossil fuels and the depletion of oil reserves due to the increasing demands for energy compel the progressive replacement of fossil fuels by renewable energy sources among which biomass. Triglycerides-based biomass such as plant oils, animal fats, waste cooking and micro-algal oils should be upgraded by transesterification, cracking/hydrocracking and selective deoxygenation (SDO) to provide, respectively, biodiesel (fatty acid methyl esters), the so-called organic liquid product (mixture of hydrocarbons in the range of gasoline, kerosene and diesel) and green diesel (hydrocarbons in the diesel range). Problems related to the production, storage and use of the already produced biodiesel shifts the research to the second and third upgrading route. Intensive work in the last ten years has shown that the noble metals (mainly palladium) and the NiMo, CoMo and NiW sulphide catalysts supported on high surface area carriers, are promising concerning SDO for producing green diesel in the context of a stand-alone process of natural triglycerides.

However, the high cost of the noble metal catalysts and the eventual S-contamination of the end product when using the aforementioned sulfided catalysts have rise intensive parallel research in the last three years for developing low cost Ni-based non-sulphide catalysts. The research effort in this area seems to focus on the following issues: (i) effect of supports, nickel loading and promoters on the catalytic performance of Ni-based non-sulphide catalysts, (ii) SDO pathways over these catalysts, (iii) effect of preparation method on their catalytic performance, (iv) comparison of nickel catalysts with other metallic and sulphide catalysts, (v) development of nickel phosphide catalysts, (vi) development of NiMo, CoMo or NiW non-sulphide catalysts (reduced, carbides, nitrides) and (vii) deoxygenation in low or no hydrogen containing atmosphere.

In the present article we critically review the contributions relevant to each one of the aforementioned subjects for obtaining a synthetic picture concerning the progress pointed out so far and the future perspectives as well.

© 2015 Elsevier B.V. All rights reserved.

Contents

* Corresponding author. Fax: +30 2610994796.
E-mail address: kordulis@upatras.gr (C. Kordulis).

http://dx.doi.org/10.1016/j.apcatb.2015.07.042
0926-3373/© 2015 Elsevier B.V. All rights reserved.

1. Introduction

The planet is facing a great energy crisis due to the depletion of oil reserves. On the other hand, the accumulation of greenhouse gases in the atmosphere resulting from the extensive use of fossil fuels results to the increase of the earth temperature and thus to climate change. These compel the use of renewable energy sources among which biomass [1]. The production of biofuels (bioethanol, biodiesel, green gasoline, green kerosene, green diesel, synthetic fuels from biomass, fuels from upgrading of bio-oils, biogas, biohydrogen, biomethane and biological hydrogen) is actually a promising alternative for confronting the above problems [2–34]. These are schematized in Fig. 1. In fact, bio-fuels offer a possible route for the mitigation of CO_2 emissions as the CO_2 emitted upon fuel combustion is removed from the atmosphere during bio mass growth. Furthermore, the development of renewable biofuels can reduce dependency on foreign oil supplies.

Triglycerides-based biomass such as plant oils (e.g., soybean, palm, sunflower, safflower, cottonseed, rapeseed, peanut, coconut, corn, camelina and Jatropha oils) and animal fats can be used for the production of biodiesel and green diesel [10–15]. The competition between foods and biofuels sources and the world food crisis have raised interest in developing alternative low-cost feedstocks (waste cooking and micro-algal oils) [9,35–46]. The advantage of using cooked oils, the cheapest feedstock, in the protection of water environment is obvious, besides the bio-fuel production. However, the free fatty acid content in waste cooking oil is very high and this become difficult the biodiesel production using this feedstock [47]. Fortunately, this is not the case for the green diesel production. In any case the amounts of the cooked oils are not sufficient. Thus, the transition to oils produced from microalgae seems to be very promising as it can contribute to a reduction in land requirements. Microalgae present certain advantages. Some kinds of them are exceedingly rich in oils. They reproduce themselves completing an entire growth cycle every few days. These can generate as much as 30–100 times more energy per hectare compared to terrestrial crops. They do not require fresh water as they can grow in salt or even contaminated water at sea or ponds. The cultivation of algae does not require the use of herbicides or pesticides. One kilogram of dry algal biomass absorbs about 1.83 kg of CO_2. Thus, the production of microalgae biomass may help bio-compensation of CO_2 emissions from wastes resulting to the improvement of the air quality [48–54]. However, serious technological problems related to the microalgae oil production should be solved before they become realistic candidates for bio-fuels production.

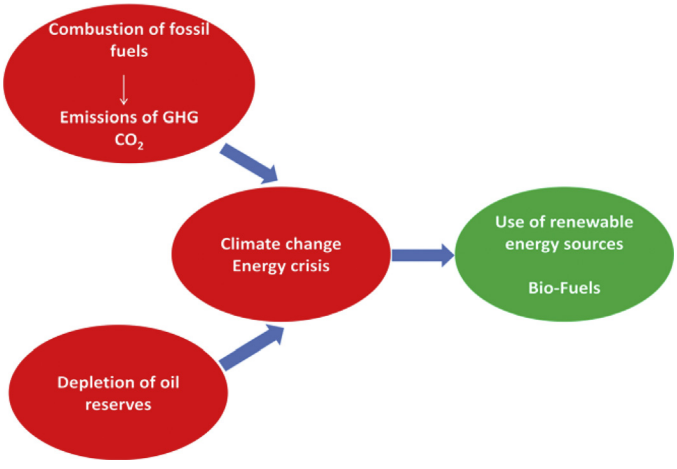

Fig. 1. The energy crises and the climate change compel to use of renewable energy sources.

Three main routes are followed for upgrading the natural triglycerides (Fig. 2). The first one is the transesterification with an alcohol, usually methanol, resulting to fatty acid methyl esters (FAME, biodiesel) and glycerol [55]. It is catalyzed by homogeneous basic catalysts (e.g., NaOH). The basic solutions are much more active than the acidic ones which also catalyse transesterification [56–59]. This quite simple process takes place under mild conditions allowing small scale production practically everywhere. This is perhaps the most important advantage of biodiesel. However, the production of biodiesel presents three main weaknesses. Plant oils with relatively high acidity, namely with relatively high concentration in free fatty acids, are not proper for transesterification catalyzed by basic solutions. This is because the basic catalyst reacts with the free fatty acids resulting to the formation of soaps. Moreover, the cations of the basic catalyst may contaminate the glycerol, decreasing thus its value, and the diesel produced as well. The use of acidic solutions will eliminate the danger for the aforementioned contaminations but, as already mentioned, the catalytic activity exhibited by acidic solutions are significantly smaller than those exhibited by the basic ones, the process equipments should be resistant to corrosion and a neutralization step should be added in the process. The above problems motivated research for developing bifunctional solid catalysts which would allow the usage of oils with relatively high acidity [60–64]. A second problem concerns the increasing accumulation of glycerol which is the main sub-product of the biodiesel production. The research focuses to the development of novel applications based on glycerol. An interesting prospect is the production of hydrogen by steam reforming of glycerol catalyzed by transition metal nanoparticles supported on γ-alumina [5,65–68]. Another interesting prospect would be the transformation of the syngas produced into methanol that could be used in transesterification making it greener. The reaction would be catalyzed by $Cu/ZnO/Al_2O_3$ catalysts [69–72]. Finally, biodiesel suffers from several drawbacks including relatively low thermal and oxidation stability. Moreover, the detergent properties of FAME cause elution of impurities and plugging of some parts of the fuel system whereas the relatively high solubility of water in FAME can cause relatively larger corrosion of metal parts. Similar problems cause the presence of FAME in diesel mixtures

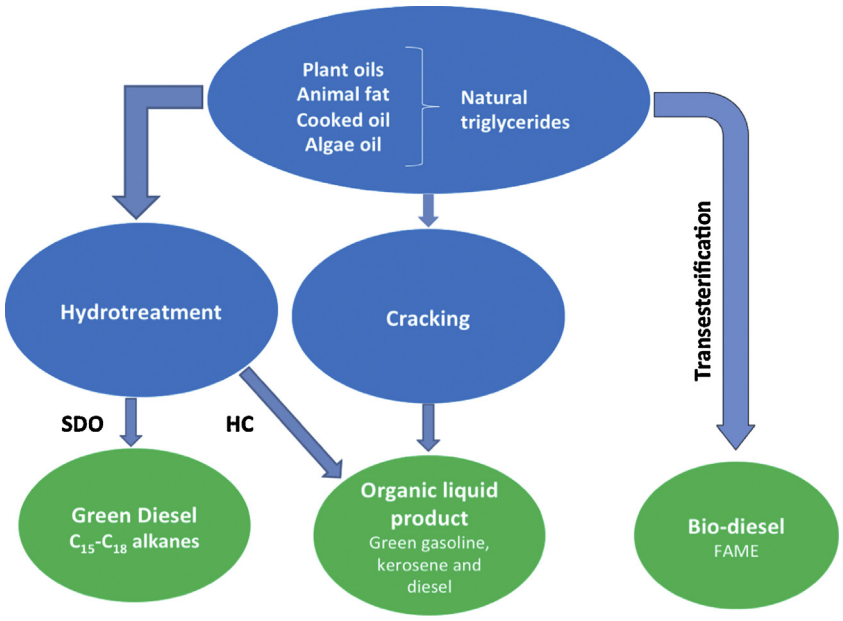

Fig. 2. Main routes for upgrading natural triglycerides.

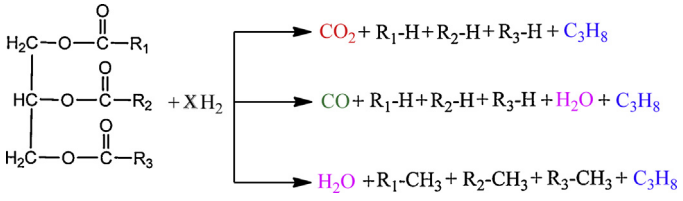

Fig. 3. Main reactions involved in the selective deoxygenation of natural triglycerides.

upon storage. The above limit the use of biodiesel to low concentration biodiesel–diesel mixture up to 7 vol% [73].

In view of the above the direct transformation of triglycerides into hydrocarbons, instead of FAME, seems to be a very promising alternative to transesterification. In this context, two alternative upgrading processes are intensively studied; the cracking/hydrocracking and the selective deoxygenation (SDO) of natural triglycerides. The subject has been recently presented in excellent review and general articles [38,74–83]. The cracking/hydrocracking (Fig. 2) performed over acidic catalysts results to the so-called organic liquid product, namely a mixture of hydrocarbons (in the gasoline, kerosene and diesel range) with traces of shorter chain oxygenates as well as hydrocarbon gases (C_3–C_5) and coke [74 and references there in, 84–91]. The hydrocarbons obtained by cracking of triglycerides consist, besides paraffins, of naphthenes and aromatics obtained by secondary reactions. This process is usually catalyzed by acidic zeolites. A serious problem with the process is the rapid catalysts deactivation own to coking. Moreover, the primary cracking products should be integrated in the context of production of green fuels and chemicals. The production of the organic liquid product can be obtained also by hydrocracking. The presence of hydrogen somewhat protects the active phase of the catalysts used (supported metal or sulfide) [74,90,91][74 and references there in, 90,91].

The third very promising route for upgrading of natural triglycerides is the so called selective deoxygenation (SDO) realized by hydrotreatment (Fig. 2). This involves three different reactions (Fig. 3) resulting to hydrocarbons (green or renewable diesel) in the range of petro-diesel.

In decarboxylation, deCO_2, oxygen is removed in the form of CO_2. In decarbonylation, deCO, oxygen is removed in the form of water and CO. In both cases the resulting alkanes have one carbon atom less than the corresponding fatty acid bound in the triglyceride. These routes cannot be easily distinguished from each other due to the easy reaction of CO_2, CO and hydrogen on the surface of the catalyst. In hydrodeoxygenation, HDO, oxygen is removed exclusively in the form of water. In this case the alkanes produced have the same number of carbon atoms as the corresponding fatty acid bound in the triglyceride. In all cases propane is produced as gaseous by-product. The above processes constitute the SDO resulting to hydrocarbons with almost the same number of carbon atoms. Depending on the experimental conditions and the catalyst used the CO and CO_2 produced in the gas phase may react with hydrogen to form CH_4 and CO respectively whereas the propane could be cracked to smaller hydrocarbons. Therefore, the determination of the gaseous phase composition is not sufficient to discriminate deCO_2 from deCO. Thus in many articles both reactions are symbolized as deCO_x. In contrast, the determination of the liquid composition at various reaction times have shown that usually, the first, rather rapid step, of SDO involves the saturation of the double bonds of the aliphatic chains followed by the easy formation of propane and the carboxylic acids involved in the triglycerides via hydrogenolysis of the of the C—O bonds. The fatty acids produced are then transformed into hydrocarbons following the aforementioned routes. This transformation is usually realized in more than one step involving the rate determining step. This is the reason for which in many cases carboxylic acids are used as probe molecules instead of plant oils or monoesters [92–96]. A detailed description of the SDO reaction pathways will be presented in a subsequent section, mainly with respect to the nickel based catalysts. In some cases condensation by-products are formed from the released carboxylic acids (symmetrical ketones and esters). Moreover, in some cases of SDO one can observe the formation of hydrocarbons with a number of carbon atoms considerably smaller than that of the fatty acids bound in the triglycerides. This is due to the fragmentation of the carbon chains of triglycerides. The extent of the effect depends on the acidity of the catalyst used and experimental conditions. High reaction temperature and low hydrogen pressure favor the aforementioned fragmentation shifting the SDO to hydrocracking.

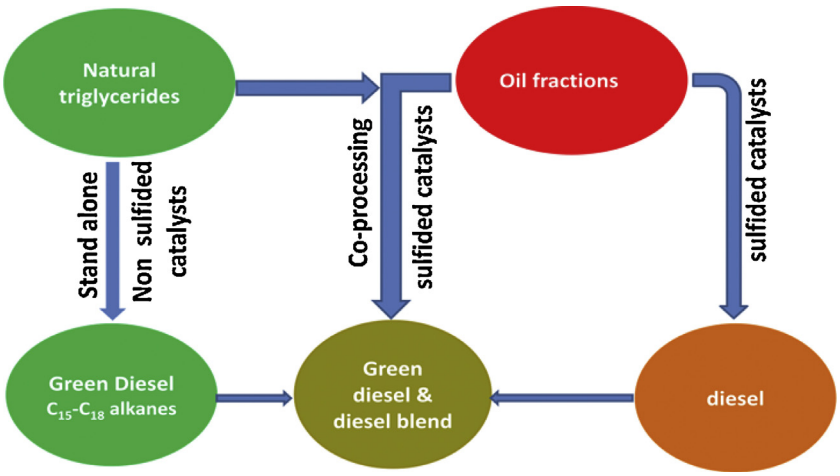

Fig. 4. Hydrotreatment strategies for industrial production of green diesel by SDO of natural triglycerides.

Two alternative approaches are investigated for the industrial production of green diesel by hydrotreatment of natural triglycerides via SDO (Fig. 4).

Following the co-processing of triglycerides with petroleum fractions, the plant oil is blended with the gas oil and the mixture is hydrotreated for the simultaneous selective deoxygenation/hydrodesulphurization [97–103]. Sulphided CoMo/γ-Al_2O_3, NiMo/γ-Al_2O_3 and NiW/-γAl_2O_3 catalysts are used in the frame of the co-processing approach. The reaction takes place in the range of 250–360 °C, usually in the presence of hydrogen (pressure in the range 7–150 bars). Both HDO and deCO_x take place on the surface of hydrotreating catalysts. It seems that HDO (deCO_x) is favoured on the surface of MoS_2 (NiS_x or CoS_x). Moreover, increase in the hydrogen pressure favours HDO whereas increase in the reaction temperature favours deCO_x. The monometallic sulfided catalysts were proved to be less active than the bimetallic ones (NiMo > Mo > Ni). Increasing the degree of unsaturation of aliphatic chains the products contained relatively high concentrations of cyclic hydrocarbons. In order to maintain the catalysts in their sulphided form we blend a triglyceride-rich feedstock with a petroleum fraction which contains sulphur compounds (e.g., straight-run gas oil). Although co-processing seems an attractive strategy has to be dealt with many parameters such as the sulphur content in the final products, the separation of carbon oxides from the recycle gas and the deactivation of catalysts due to the presence of water and carbon dioxide. Moreover, it is not so easy to obtain simultaneously the optimum process conditions and catalysts for both SDO and hydrodesulphurization. Thus, the second strategy stated below seems to be more promising.

Following the stand-alone process of triglycerides, the hydrotreatment of plant oil takes place separately from the hydrotreatment of the petroleum fractions. There are two commercial stand-alone applications; the Universal Oil Products (UOP) renewable diesel based on vegetable oils and/or grease with trade name green diesel [104] and the NesteOil Corporation one based on vegetable oils and/or animal fats with trade name NExBTL (NExt generation Biomass-to-Liquid) [105]. In these cases the green diesel produced could be used alone or blended with the diesel produced after the hydrodesulphurization of the gas oil.

Various oils, triglycerides, monoesters, fatty and smaller carboxylic acids are used in the studies attempting to investigate the catalytic behavior in the context of stand-alone process. Noble metals supported on high surface area carriers have been extensively studied in the frame of stand-alone approach [74]. It seems that the supported Pd nanoparticles are very active and selective for deCO_x. Carriers with high specific surface area (γ-alumina, silica, titania, active carbons) have been used for the preparation of the metallic catalysts. The choice of the support affects selectivity, mainly the eventual formation of condensation products (ketones and esters produced through condensation of the fatty acids). It seems that carriers with too high acidity favor fragmentation. On the other hand carriers with too low acidity are related with rather low activity [74]. Although we need more systematic work concerning the carriers, the work done so far evidences that high specific surface area and medium—carefully regulated acidity may be the most important parameters for the choice of the support in the case of the noble metals. In spite of their high activity the noble metals are quite expensive and sensitive to some oxygenated compounds present in the feed. Thus, recent efforts for development of much less expensive metallic catalysts, like nickel based catalysts, are actually very useful. These efforts are reviewed in the present contribution (Fig. 5).

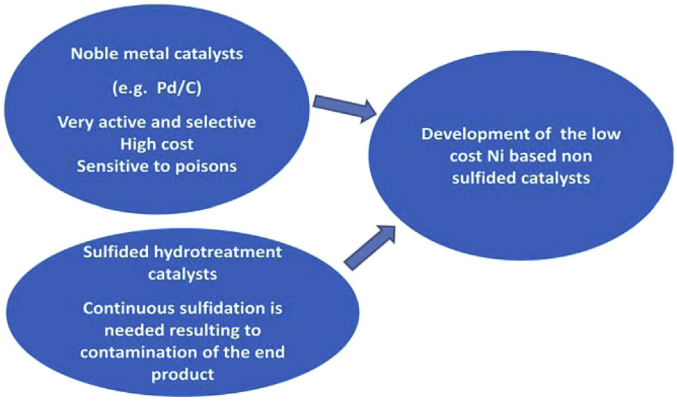

Fig. 5. From the noble metals and the NiMo, CoMo and NiW sulfided catalysts to the low cost Ni based non-sulphided catalysts in the context of the stand-alone approach.

The sulfided NiMo, CoMo and NiW hydrotreatment catalysts supported on γ-alumina have been also proposed even in the frame of the stand-alone approach. This is because it is rather well established that the sulfided catalysts are more active than the corresponding non-sulfided ones. It is therefore necessary to maintain the catalysts in their sulphided form. This is obtained by introducing in the feed a compound rich in sulphur (e.g., dimethylsulfide). However, this is a serious draw back from the view point of the sulphur contained in the end products. This is the reason for which various efforts have been recently reported to develop non-sulfided NiMo,

CoMo and NiW hydrotreatment catalysts (Fig. 5). These efforts are also reviewed in the present contribution.

2. Objectives

A large number of papers published in the last decade deals with the SDO over heterogeneous catalysts. These mainly deal with noble metal catalysts (Pd, Pt) [106–109], as well as with NiMo, NiW and CoMo sulphided catalysts. These papers have been very recently reviewed in eleven articles covering various aspects of the subject [38,74–83]. However, no one of these contributions focuses on the development of nickel based catalysts and non-sulphided NiMo, NiW and CoMo catalysts for the title transformation. This is reasonable as a very small number of original papers (of about five) devoted to the above catalysts had been published before 2012. The situation has been drastically changed in the last three years, where the research is turned to the non expensive aforementioned catalysts. Thanks to the intensive work in this period a picture started to be synthesized concerning the catalytic behavior of this kind of catalysts.

In the present article we critically review the very recent contributions in the subject focusing on the following issues which reflect corresponding research trends: (i) effect of supports, nickel loading and promoters on the catalytic performance on the nickel metallic catalysts, (ii) SDO pathways over nickel metallic catalysts, (iii) effect of preparation method on catalytic performance of the nickel metallic catalysts, (iv) comparison of nickel metallic catalysts with other metallic and sulphided catalysts, (v) development of nickel phosphide catalysts, (vi) development of NiMo and NiW non-sulphided catalysts, and (vii) Stability of nickel metallic catalysts.

3. Survey of the SDO literature relevant to the nickel based catalysts

3.1. An outline of the relevant contributions

In the following we attempt for a first time a survey of the very recent literature relevant to the SDO over nickel based catalysts. To the extent of our knowledge the first effort to investigate SDO over nickel supported catalysts was reported at 2006 by Snåre et al. [94]. The very low catalytic performance obtained, much probably due to the absence of hydrogen in the reactants, was perhaps the main reason for which the second work concerning the metallic nickel supported catalysts was published after three years [95]. Nevertheless, an increasing number of contributions devoted to nickel based non-sulphided catalysts was reported, mainly in the last two years. Fig. 6 illustrates the increasing rate of contributions in the subject.

The careful study of the contributions reported so far allows emerging the research trends relevant to the development of nickel based catalysts for the SDO of natural triglycerides and model compounds. These are illustrated in Table 1.

3.2. The effect of support, nickel loading and promoters on the catalytic performance in the nickel metallic catalysts

Several papers published so far deal with the influence of the support on catalytic behaviour of the supported nickel metallic nanoparticles (Table 2). A systematic effort to investigate the influence of the support was done by the group of Prof. Lercher. In the first paper of the series [110] they studied the SDO of stearic acid and Microalgae oil over nickel catalysts (of two Ni loadings) supported on two types of zeolites (HZSM-5 and HBeta) of varying Si/Al ratio using a batch reactor (Table 2, entry 1).

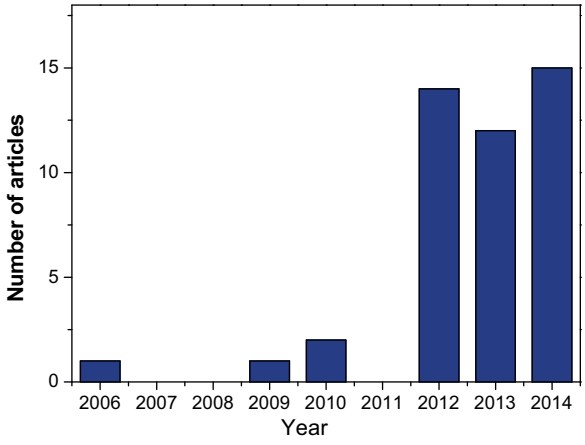

Fig. 6. Contributions reported for the nickel based non-sulphided catalysts in the last decade (2006–2014).

Table 1
Main directions of the research.

Research subject	References
The effect of supports, nickel loading and promoters on the catalytic performance of the nickel metallic catalysts	[95,96,110–119]
SDO pathways over nickel metallic catalysts	[110–114,119,128,131]
The effect of preparation method on catalytic performance of the nickel metallic catalysts	[132]
Comparison of nickel metallic catalysts with other metallic and sulphided catalysts and the effect of reaction parameters on catalytic behaviour	[144–148]
Development of nickel phosphide catalysts	[168–171,176–178]
Development of NiMo and NiW reduced catalysts	[181–188]
Development of NiMo and NiW carbide, nitride and phosphide catalysts	[216,221,224,226,227]
Influence of hydrogen partial pressure on the SDO over Ni catalysts-Stability of Ni catalysts upon SDO of natural triglycerides	[111,176,178,183,188,230-232]

Relatively high Si/Al ratio or Ni content leads to a relatively low acid site concentration on the catalytic surface. Full conversion of stearic acid was obtained over a 10% Ni/HZSM-5 (Si/Al = 45) catalyst, but severe cracking of the produced alkanes (43% selectivity to C_{17} and C_{18}) was observed own to its high acidity. By using 10% HZSM-5-supported Ni catalysts with higher Si/Al ratios (120 or 200), thus lower acidity, the cracking was gradually suppressed and the selectivity to C_{17} and C_{18} alkanes increased to 84 and 93%, respectively. However, the decrease in the acidity causes considerable decrease in the conversion. Full conversion of stearic acid was practically obtained over the four Ni/Beta catalysts studied. The selectivity to cracking products was limited at values lower than 0.7%. The above results visualize the critical role of the support, mainly of its acidity, on the activity and the selectivity for hydrocarbons with 17 or 18 carbon atoms. An interesting and rather unexpected point for nickel catalysts is that octadecane was the main product over all nickel catalysts studied (selectivity: 41.1–84.6%) whereas heptadecane was produced in very small amounts (selectivity: 6.1–14.8 %). One would attribute this observation to the zeolite nature of the supports in conjunction with the relatively low reaction temperature adopted in this study.

The authors hydrotreated microalgae oil over a 10%Ni/HBeta catalyst (Si/Al = 180) which had been proved quite promising in the SDO of stearic acid. After 8 h of reaction time, they obtained 78 wt% yield for liquid alkanes (60 wt% for octadecane and 10% for

Table 2
An overview of the reactant, catalysts, preparation, characterization and reaction conditions for the SDO of triglycerides and related molecules over nickel metallic nanoparticles supported on various carries.

Entry/Refs.	Reactant	Catalyst/preparation	Characterization	Reactor and reaction conditions
1/[110]	(Microalgae oil, stearic acid), in dodecane.	Three catalysts: 10%Ni/HZSM-5, Si/Al = 45–200. Four catalysts: 5% or10%Ni/HBeta, Si/Al = 75 or 180. w.i. using commercial zeolites.	N_2-physisorption NH_3-TPD XRD	BR, mass of reactant: 1.0 g, solvent volume: 100 mL and mass of catalyst: 0.2 g, Temperature 260 °C, H_2 pressure: 40 bar, reaction time: 8 h, stirring rate: 600 rpm.
2/[111]	Stearic acid (mainly) or 1-octadecanol or microalgae oil in dodecane	3%Ni/ZrO_2 5%Ni/ZrO_2 10%Ni/ZrO_2 15%Ni/ZrO_2 10%Ni/TiO_2 10%Ni/CeO_2 10%Ni/SiO_2 10%Ni/Al_2O_3 i.w.i. using commercial supports	AAS N_2-physisorption NH_3-TPD TPD-CO XRD	BR for all reactants, FBR for microalgae oil reactant (1.0 g), dodecane (100 mL) catalyst (0.5 g), temperature 260 °C (in most of cases), hydrogen pressure 40 bar (in most of cases), reaction time 8 h and stirring rate: 600 rpm (BR), Liquid flow rate: 0.2 mL/min, gas flow rate: 50 mL/min (FBR).
3/[112]	Palmitic acid (mainly) or 1-octadecanol or palmityl palmitate in dodecane	Pt black, Pd black 5%Pt/C, 5%Pd/C, 5%Pt/ZrO_2, 5%Pd/ZrO_2 Raney Ni 3% Ni/ZrO_2, 5% Ni/ZrO_2, 10% Ni/ZrO_2, 15% Ni/ZrO_2, 5%Ni/Al_2O_3, 5% Ni/SiO_2, 5% Ni/HBEA (Si/Al = 180), 5% Ni/HZSM-5(Si/Al = 200) i.w.i. using commercial supports for the catalysts supported on oxides (zirconia was prepared in the lab)	AAS N_2-physisorption NH_3-TPD TPD-CO XRD	SBR for all reactants mass of catalyst:0.5 g, mass of reactant:1.0 g, dodecane: 100 mL, temperature: 260 °C, gas pressure: 12 bar (H_2, H_2–N_2 or N_2), gas flow rate: 20 mL/min, reaction time: 8 h, stirring rate: 600 rpm
4/[113,114]	Methyl palmitate	7% Ni/SiO_2 7% Ni/γ-Al_2O_3 2–9% Ni/SAPO-11 (Si/Al = 0.11, Al/P = 1) 7% Ni/HZSM-5 (Si/Al = 38) 7% Ni/HY(Si/Al = 2.91) i.w.i.	XRD SEM H_2-TPR NH_3-TPD N_2-physisorption H_2-chemisorption TGA	SBR, mass of catalyst: 1 g Mass of reactant: 30 g Temperature: 220 °C, pressure: 20 bar, H_2 flow rate: 50 mL/min, reaction time: 6 h, stirring rate: 1000 rpm
5/[115]	Palm oil	7% Ni/SAPO-11a 7% Ni/SAPO-11b 7% Ni/SAPO-11c i.w.i. using lab made supports	XRD SEM TPR-H_2 TPD-NH_3 N_2-physisorption H_2-chemisorption TGA	FBR, mass of catalyst: 1 g LHSV: 2.0 h^{-1}, temperature: 200 °C, pressure: 40 bar, H_2/liquid volume ratio: 1000
6/[116]	Palm oil	2–9% Ni/SAPO-11 i.w.i. using a lab made support	XRD SEM TPR-H_2 TPD-NH_3 N_2-physisorption H_2-chemisorption TGA	FBR, mass of catalyst: 2 g LHSV: 1.0 h^{-1}, temperature: 200 °C, pressure: 40 bar, H_2/liquid volume ratio: 1000
7/[117]	Methyl oleate reagent (70% in methyl oleate) in heptane (total ester content: 10%).	5% Ni/SBA-15 5% Co/SBA-15 5% Ni /Al-SBA-15 5% Co /Al-SBA-15 Si/Al = 68	XRD TEM H_2-TPR NH_3-TPD	FBR, mass of catalyst: 200 mg, temperature: 300 or 340 °C, pressure: 30 bar of H_2, WHSV: 20.4 h^{-1}.
8/[118]	Methyl hexadecanoate	Ni/HZSM-5 (Si/Al = 38) Ni content: 1, 3, 5, 7 & 9% w.i. using commercial support	N_2-physisorption XRD SEM NH_3-TPD	SBR, Catalyst loading: 3.0 g Reactant loading: 30 g Temperature: 160–220 °C H_2 pressure: 20–60 bar Stirring rate: 1000 rpm Reaction time: 1–6 h
9/[119]	Stearic acid in dodecane	5% Ni/γ-Al_2O_3 10% Ni/γ-Al_2O_3 15% Ni/γ-Al_2O_3 25% Ni/γ-Al_2O_3 10% Ni/SiO_2 10% Ni/HZSM-5 i.w.i.	XRD H_2-TPR NH_3-TPD N_2-physisorption H_2-chemisorption ICP-AES	BR, catalyst loading: 0.10–0.75 (w/v)%, reactant concentration: 0.11–0.18 kmol/m^3, temperature: 260–290 °C pressure: 13–14.5 bar, stirring speed: 1200 rpm

Table 2 (*Continued*)

Entry/Refs.	Reactant	Catalyst/preparation	Characterization	Reactor and reaction conditions
10/[95]	Biodiesel (consisted from methyl esters of fatty acids)	38% Ni/ZrO_2, 38% Ni/CeO_2, 38%(Ni–Cu)/ZrO_2, 38% (Ni–Cu)/CeO_2, 38% Ni/ZrO_2–CeO_2, 38% (Ni–Cu)/ZrO_2–CeO_2,. w.i. or c.p. Ni/Cu = 3.	N_2-physisorption XRD	FBR, 250–400 °C, 10 bar, H_2 (50%)–Ar (50%), flow rate = 20 L h^{-1}, LHSV = 2 h^{-1}, molar ratio of H_2/—CH_2— groups in biodiesel = 2.65
11/[96]	Biodiesel (consisted from methyl esters of fatty acids)	30.3% Ni–10.4% Cu/28% ZrO_2–17.5% CeO_2 29.9% Ni–13.6% Cu/CeO_2 9.76% Ni–2.64% Cu/ZrO_2 31.6% Ni/CeO_2 38.8% Ni/ZrO_2 c.p.	N_2-physisorption XRD TPR TEM	FBR, 290–400 °C, 10 bar, H_2 flow rate = 10 L/h Ar flow rate = 10 L/h Biodiesel flow rate = 3mL/h
12/[128]	Soybean oil	57.6% Ni/SiO_2–Al_2O_3 4.29 Pd/γ-Al_2O_3 2.4% Ni 11.8% Mo/γ-Al_2O_3(sulphided) 2.8% Co 7.6% Mo/γ-Al_2O_3(sulphided) All the catalysts used are commercial samples		BR, mass of catalyst: 2.5 g, mass of oil: 28.1 g Temperatures: 300, 350, 400, 440 °C Various initial pressures, mainly 92 bar.
13/[131]	Waste chicken fat	10% Ni/γ-Al_2O_3 Prepared by i.w.i.	N_2-physisorption XRD H_2-TPR	FBR, mass of catalyst 8.5 g reduced in situ H_2 pressure: 50 bar Temperature: 330 °C H_2/fat ratio: 1000 cm^3 cm^{-3} LHSV: 0.5–2 h^{-1}
14/[132]	Stearic acid or microalgae oil in dodecane	Four 5% Ni/HBEA (Si/Al = 75) prepared by impregnation, ion-exchange/precipitation, deposition–precipitation, and grafting of as-synthesized Ni nanoparticles	TEM H_2-TPR NH_3-TPD IR of adsorbed pyridine IR of adsorbed CO	BR, Reactant: 1.0 g of stearic acid or microalgae oil in 100 mL of dodecane Mass of catalyst: 0.2 g Temperature:260 °C H_2 pressure: 40 bar Reaction time: 8 h Stirring speed: 700 rpm.

heptadecane). Propane and methane were the main products in the vapor phase. The increase of temperature from 250 to 270 °C at 40 bar enhanced the liquid alkane yield from 68 to 78 wt%, and an increase of the hydrogen pressure from 15 to 60 bar at 260 °C led to a decrease of *n*-C_{17} and iso-C_{18} yields from 28 to 11 wt%, whereas the *n*-C_{18} yield increased from 23 to 61 wt%. Similar results were obtained using a continuous flow system with a trickle bed reactor. The effect of hydrogen pressure on selectivity can be explained in terms of the SDO pathways presented in the Section 3.3.

In the second paper of the series [111] the group of Lercher extended their study on the role of the support by investigating the impact of other oxidic supports (zirconia, titania, alumina and silica) on the SDO catalytic performance of nickel supported catalysts containing 10% Ni (Table 2, entry 2). The effect of loading (0, 3, 5, 10 and 15%) was also studied concerning the nickel catalysts supported on zirconia. The catalysts screening was obtained using the SDO of stearic acid as a model reaction. Moreover, the SDO of micro-algae oil was studied over a nickel catalyst supported on zirconia. Heptadecane was the main product over all nickel catalysts studied (selectivity: 51–96%) whereas octadecane was produced in very small amounts (selectivity: 0.4–5%). This indicates that nickel catalysts supported on oxidic carriers favor deCO_x with respect to HDO even at low reaction temperatures (260 °C). This clearly visualizes the critical role of the support if we take into account that the use of zeolites as supports favors HDO [110]. Presumably due to the low reaction temperature very small amounts of cracking products (selectivity: 0.9–3.4%) were produced over all the catalysts studied.

The effect of the oxidic supports on catalytic performance was investigated over catalysts containing 10% of nickel. The nickel catalysts supported on zirconia, titania and ceria showed almost complete conversion for the stearic acid and very high selectivity for heptadecane (87–96%). In contrast, the catalysts supported on alumina and silica exhibited considerable lower activity (conversion 63 and 45%, respectively). The high activities of the catalysts supported on slightly reducible supports (zirconia, titania and ceria) were attributed to the participation of the support surface on the reaction mechanism through defect oxygen sites. This will be discussed in the Section 3.3 dealing with the SDO mechanism. However, the relatively small activity obtained for the nickel catalyst supported on γ-alumina could be partly attributed to the small specific surface area of the support used in this study (80 m^2 g^{-1}) with respect to that usually exhibited by this support (200–400 m^2 g^{-1}). In our opinion testing nickel metallic catalysts supported on alumina with much higher specific surface area would be useful for evaluating this support. This is not the case for the silica which presents very low acidity which does not favor SDO. The almost complete conversion obtained for the nickel catalysts supported on zirconia, titania and ceria did not allowed a comparison between these supports. A decrease of the conversion by increasing the reactant to catalyst ratio (see Table 2, entry 2) would be useful for a precise discrimination to be obtained.

The same is valid concerning the effect of nickel loading for the nickel catalysts supported on zirconia where almost complete conversion of the stearic acid was obtained under the conditions adopted for catalysts evaluation. It was moreover found that the increase of Ni loading from 3 to 10% increases the selectivity of heptadecane from 51 to 96%. Further increase of nickel loading to 15% does not affect catalytic performance.

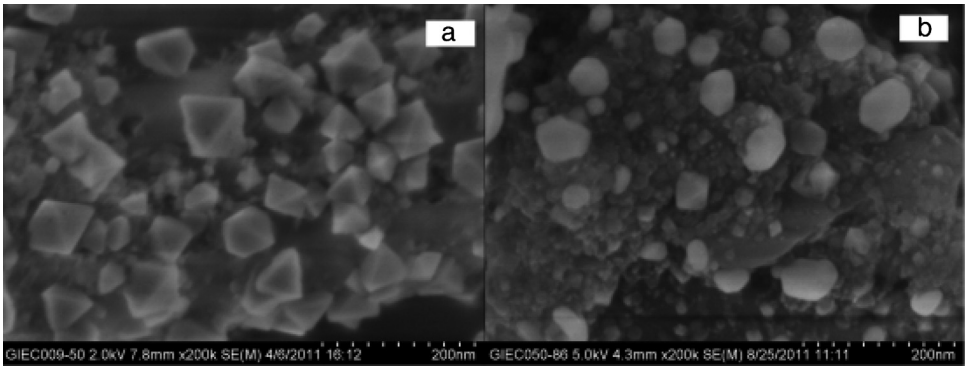

Fig. 7. SEM images of the fresh (a) and spent (b) Ni/SAPO-11 catalysts. Source: Ref. [114].

The very active 10% Ni/ZrO_2 catalyst was finally tested in the SDO of micro-algae oil. *n*-Heptadecane is the major product in the liquid phase and C_{13}-C_{21} hydrocarbons the minor ones. The yield obtained for the *n*-heptadecane and the total liquid alkanes was equal to 68 and 76%, respectively at 270 °C and hydrogen pressure 40 bar for reaction time of 8 h. Propane and methane were the main products in the vapor phase. These were formed respectively by the hydrogenolysis of oil triglycerides and the methanation of CO/CO_2. Similar results were obtained under the same conditions using a trickle bed reactor. It is remarkable that the catalyst does not deactivate for a time on stream equal to 72 h.

In the third paper of the series [112] the group of Lercher actually attempted to compare the most promising catalysts developed in the first and second work of the series as well as to compare the nickel with platinum and palladium catalysts. The SDO of palmitic acid was used as a probe reaction (Table 2, entry 3). The activity of the supported catalysts exhibited the following trend in terms of the initial SDO rates:

$$15\%Ni/ZrO_2 = 5\%Ni/HZSM\text{-}5(Si/Al = 200) > 5\%Ni/HBEA[d](Si/Al = 180) > 10\%Ni/ZrO_2 > 5\%Ni/ZrO_2 > 5\%Pd/ZrO_2 > 5\%Pt/ZrO_2 > 3\%Ni/ZrO_2 > 5\%Ni/Al_2O_3 > 5\%Ni/SiO_2 > 5\%Pt/C > 5\%Pd/C.$$

One may observe that the catalysts supported on the zeolites exhibited the highest catalytic activity among the catalysts with the same nickel content. Moreover, it seems that zirconia is better support compared to silica, alumina and active carbon, presumably due to the zirconia participation in the SDO (see Section 3.3). Moreover, it is rather unexpected that nickel is proved to be more active than platinum and palladium. Furthermore, one may observe that the activity of the nickel catalysts supported on zirconia increases with the nickel content.

The discovering of a promising support was also the main goal of the work reported by Zuo et al. [113,114] (Table 2, entry 4). They studied the SDO of methyl palmitate over nickel metallic catalysts supported on various carriers (SiO_2, γ-Al_2O_3, SAPO-11, HZSM-5, and HY). The catalysts tested contained 7% Ni. In all cases, the primary products were mainly composed of the gaseous CO, CO_2, dimethyl ether and C_1–C_4 alkanes, the liquid palmitic acid and alkanes with the carbon numbers of more than 5 as well as trace amounts (less than 0.01%.) of hexadecanal, hexadecanol and hexadecene intermediates. The conversion of the reactant over the nickel supported on silica catalyst was rather low (49.35%) whereas the conversion over the other catalysts was higher than 90%. However, the 7% Ni/HZSM-5 and 7% Ni/HY catalysts though very active were proved to be less selective towards the production of alkanes with long carbon chains (*n*-C_{15} and *n*-C_{16}) favoring extensive hydrocracking. The above are in full agreement to those reported by the group of Lercher [110–112] presented before. The most promising catalysts were proved to be the 7%Ni/γ-Al_2O_3 and 7% Ni/SAPO-11 which presented high activity and high selectivity towards the production of *n*-C_{15} and *n*-C_{16} alkanes under the relatively low reaction temperature (220 °C) and high pressure (20 bar) where the experiments have been performed.

The good catalytic performance of the 7% Ni/SAPO-11 and 7% Ni/γ-Al_2O_3 catalyst (high activity, prevention of cracking) was attributed to their medium acidity which follows the order: 7% Ni/SiO_2 < 7% Ni/SAPO-11 < 7% Ni/γ-Al_2O_3 < 7% Ni/HZSM-5 < 7% Ni/HY. The above results indicate again that a critical factor for obtaining the best SDO catalytic performance is the optimum acidity value of the support which allows the achievement of relatively high activity and low cracking (See Fig. 5 in Ref. [114]). Another factor presumably related to the good catalytic behavior exhibited by the catalyst supported on γ-alumina is that the supported nickel/nickel oxide particles are very small and thus no detectable by XRD. In contrast, larger nickel/nickel oxide particles (mean values for nickel particles: 20–27 nm) are formed above the other supports indicating lower nickel/nickel oxide dispersion. The nickel oxide particles supported on SAPO-11 (30–100 nm) are illustrated in Fig. 7a.

These, exclusively presented as the sharp-edged octahedral shape with one side attached to the surface of support and the other exposed to the air (Fig. 7a), are transformed to nickel spherical supported particles (20–80 nm) upon the hydrotreatment of the reactant (Fig. 7b).

The good catalytic performance exhibited by the 7% Ni/SAPO-11 catalyst synthesized using a rather medium specific surface area commercial support encouraged the same group to continue its study using hydrothermally synthesized nano-sized SAPO-11 supports with high surface area [115] (Table 2, entry 5). As compared to the commercial SAPO-11, the nano-sized SAPO-11 supports presented significantly enlarged surfaces and mesoporous volumes, which offered sufficient space and strong interactions for dispersing Ni. The SDO of palm oil demonstrated that the nano-sized SAPO-11 supported Ni catalysts showed high yield (80%) of liquid hydrocarbons, high isomerization selectivity (80%) and excellent stability. The outstanding catalytic performance of the Ni/SAPO-11 nanosized catalysts was attributed to appropriate acidity, higher Ni dispersion, balance of metal (Ni) and acid (SAPO-11) functionalities and fast diffusion for bulky palm oil and products.

In the context of the same effort a SAPO-11 support with small particles and large surface area and mesoporosity was also synthesized hydrothermally [116] (Table 2, entry 6). Using this support Ni/SAPO-11 catalysts with different Ni loadings (2, 7 and

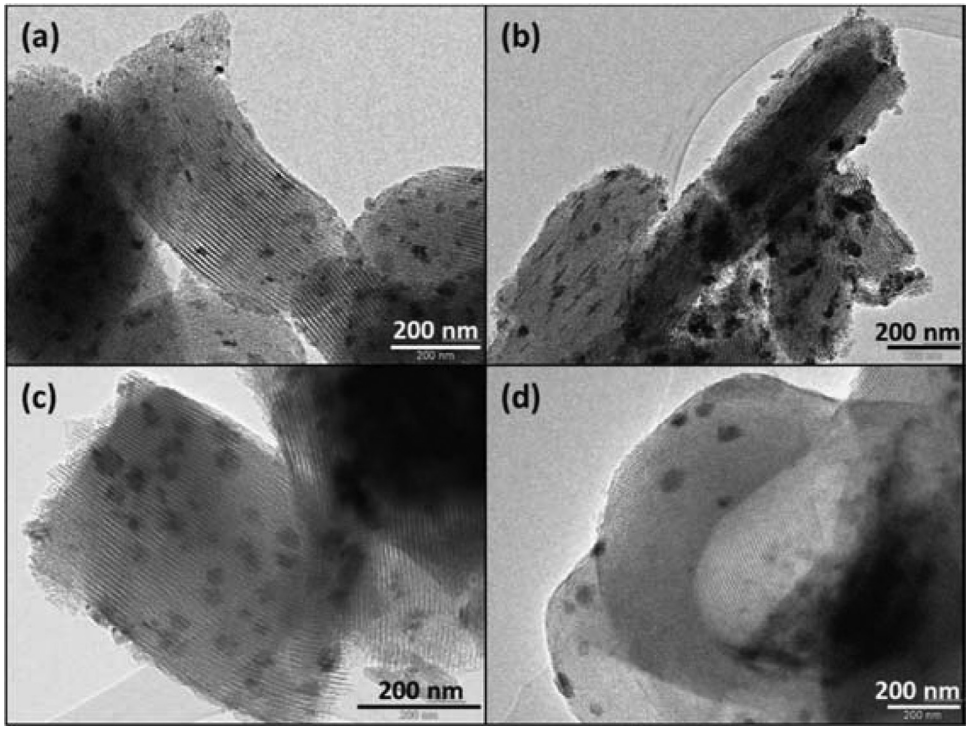

Fig. 8. TEM images of the catalysts in oxide form: (a) Ni/SBA-15, (b) Co/SBA-15, (c) Ni/Al-SBA-15 and (d) Co/Al-SBA-15. Source: Ref. [117].

9%) were prepared by wet impregnation. The catalytic behavior of the prepared samples was examined for the SDO of palm oil. At the Ni loading of 2 wt%, the liquid alkane yield of C_5–C_{18} was 60 wt% with the isomerization selectivity of 46%. Among the liquid alkanes, the selectivities to C_5–C_{14} and C_{15}–C_{18} chains were 18.7% and 70%, respectively, indicating that some cracking of long chain alkanes took place. In addition, gaseous CO and C_1–C_4 alkanes were detected with a total amount of 10.9%. As the Ni loading was increased to 7 wt%, the liquid alkane yield and isomerization selectivity were increased to 67.4% and 61.5%, respectively. As the Ni loading was further increased to 9 wt%, the liquid alkane yield remained at the same level, but the yields of C_5–C_{14} and C_1–C_4 alkanes were increased. This obviously shows that primary long chain alkanes were susceptible to cracking forming lighter compounds. The high isomerization selectivity of >83% achieved over the 9 wt%Ni/SAPO-11 catalyst indicated that a good balance between the metal Ni and acid SAPO-11 functions was reached in this sample. The catalytic performance tests revealed also the essential role of the reaction temperature on the liquid alkane yields, product distribution, and isomerization selectivities. Increase of reaction temperature enhances both isomerization and cracking.

An interesting work in the context of development of nickel metallic catalysts supported on different supports was reported by Ochoa-Hernandez et al. [117] (Table 2, entry 7). They studied the SDO of triglycerides over high specific surface area (558–700 $m^2\ g^{-1}$) nickel or cobalt metallic catalysts supported on pure or aluminum modified ordered mesoporous silica [M/SBA-15 and M/Al-SBA-15, (M: Ni or Co)]. Nickel oxide or cobalt oxide supported nanocrystallites inside or outside the support pores were detected by high angle XRD patterns. Moreover, the low angle XRD patterns and nitrogen adsorption isotherms evidenced the presence of an ordered mesoporous structure before and after incorporating the above oxides to the supports though a lower ordering degree of the pore networks was observed in the aluminum modified samples. The structure of the catalysts in the oxidic form is illustrated in Fig. 8. We may observe the well-ordered hexagonal array of cylindrical channels. Moreover, we may observe dark zones over and inside the mesoporous structure (elongated particles in channels direction) corresponding to NiO and Co_3O_4 nanoparticles. As these particles (30–50 nm) are significantly larger than the crystallite size obtained from the XRD (9.6–11.7 nm) it was concluded that these bulky particles are mainly polycrystalline.

The H_2-TPR profiles obtained for the nickel supported samples revealed the presence of NiO particles, which are more easily reducible to metallic nickel, as well as smaller particles located inside the pores of the SBA-15 which are more strongly interacted with the support surface. The H_2-TPR profiles obtained for the cobalt supported samples suggested the existence of Co species with smaller crystallite sizes and stronger metal-support interactions. The presence of aluminum increases the interactions between nickel or cobalt species and the support sites, indicating special interactions between these species and the Al sites. The ammonia TPD did not provide evidences for acidity in the SBA-15 based catalysts. In contrast, M/Al-SBA-15 catalysts presented mild acid sites. When cobalt was incorporated to the acidic support, the total acidity decreased. This was attributed to the cobalt deposition on some acid centers and/or existence of blocked channels. This was less pronounced in the nickel catalysts, probably due to the formation of additional Lewis acidic sites.

The oxidic catalysts were in situ reduced under a flow of pure hydrogen and then tested in a feedstock containing methyl oleate reagent in heptane. Normal paraffins in the range C_{15}–C_{18} were mainly produced with the *n*-heptadecane and *n*-octadecane to be the main products. In all cases the ratio $n\text{-}C_{18}/(n\text{-}C_{18}+n\text{-}C_{17})$ was lower than unit indicating affordance of $deCO_x$ with respect to HDO. This is rather expected for the nickel metallic catalysts. Regarding active phases, Co proved to be more active than Ni under the reaction conditions used in this study. This observation concerns the samples M/SBA-15 but not the samples M/Al-SBA-15 where equal activity was observed. More important is the effect of aluminum. The M/Al-SBA-15 catalysts are more active than M/SBA-15 ones

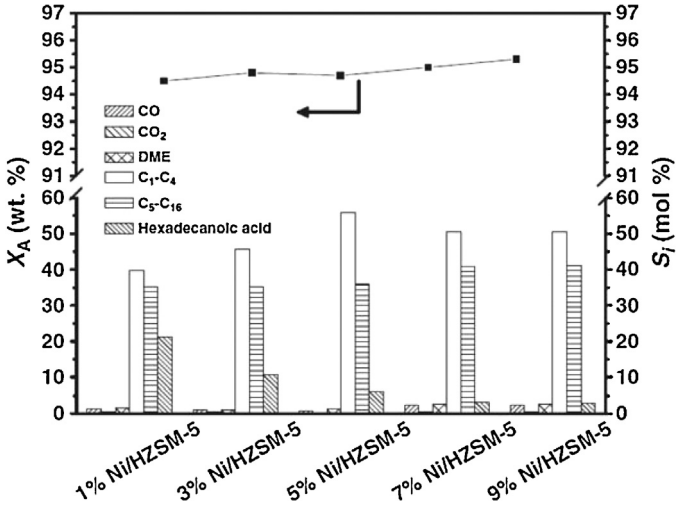

Fig. 9. Effect of Ni loading of Ni/HZSM-5 catalysts on the activity and product distribution in HDO of MHD. Reaction conditions: 220 °C, 40 bar H_2 and 160 min. Source: Ref. [118].

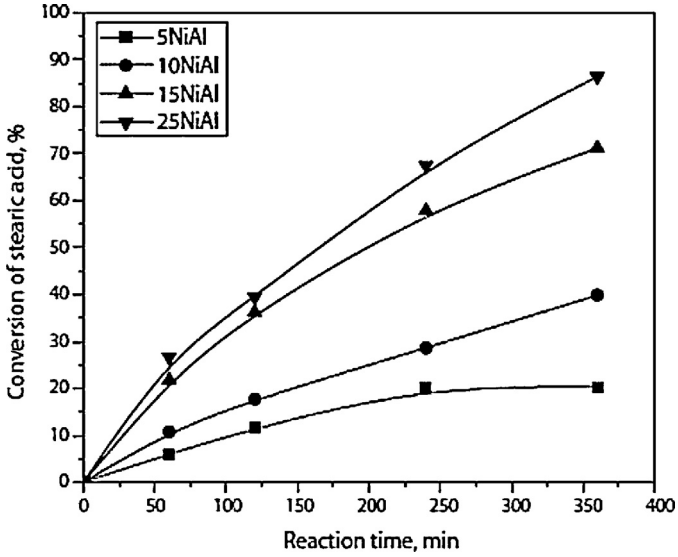

Fig. 10. Effect of Ni on stearic acid conversion. Conditions: concentration of stearic acid = 0.18 kmol/m^3, *n*-dodecane = 100 mL, catalyst loading = 0.5(w/v)%, temperature = 270 °C, initial hydrogen pressure = 8 bars. Source: Ref. [119].

and also more selective toward C_{18} at 300 °C. This could related to both, the presence of mild acid sites on the support surface, which may act synergistically with the active element, and the aluminum promotion of stronger interactions between the active elements and the support Al sites presumably indicating better dispersion of these elements. Besides, the presence of acid centers in the M/Al-SBA-15 catalysts favors the formation of significant proportions of non-linear hydrocarbons while SBA-15 based catalysts mainly produce n-paraffins. Specifically, high and stable conversions and elevated total yields to paraffins in diesel range are achieved using Co/Al-SBA-15. In addition, this material leads to the formation of relatively high $n\text{-}C_{18}/(n\text{-}C_{18} + n\text{-}C_{17})$ ratios (0.7–0.8), proving to be a very interesting hydrodeoxygenation catalyst. The above work are in line with the works reviewed before [110–114] for the view point that the incorporation of aluminum atoms in to the structure of silica increases the acidity providing more active catalysts. Moreover, this work indicates that future contributions devoted to the much less studied cobalt catalysts would be welcomed.

The work reported by Shi et al. [118] (Table 2, entry 8) focuses on the influence of Ni loading (1–9%) concerning the SDO performance of Ni/HZSM-5 catalysts. The hydrotreatment of methyl hexadecanoate was used as a probe reaction. The physicochemical characterization of the catalysts showed that at Ni loading below of 3%, the NiO is highly dispersed on the surface of HZSM-5, and gradually aggregates into relatively large particles of more than 100 nm as the Ni loading exceeds 3 wt%. Supporting Ni on HZSM-5 significantly changed its acidic properties. Highly dispersed Ni on HZSM-5 decreased the number of acid sites due to the blockage of HZSM-5 microchannels by NiO crystallites. As Ni loadings exceeded 5 wt%, large NiO particles formed on the surface of HZSM-5 and originated the strong acidic sites.

Fig. 9 represents typical catalytic results obtained over the catalysts studied. The conversion obtained is quite high and increases slightly with the nickel content. The increase in the nickel content increases the total selectivity of hydrocarbons whereas it decreases the selectivity of the intermediate hexadecanoic acid. The most important observation is the considerable fragmentation of the alkyl chains resulting to light hydrocarbons. This can be effortlessly attributed to the acidic character of the support again suggesting that we need less acidic carriers to obtain better selectivity for the hydrocarbons in the diesel range. It was also reported that the reaction mechanism involves hydrogenation, dehydration, decarbonylation/decarboxylation, cracking, and isomerization reactions.

Recently, Kumar et al. [119] (Table 2, entry 9) studied the influence of Ni loading on the SDO performance of Ni/γ-Al_2O_3 catalysts as well as the influence of the support nature by changing γ-Al_2O_3 with SiO_2 and HZSM-5 keeping Ni loading constant (10%). The nickel loading of the supported on γ-Al_2O_3 catalysts was 0, 5, 10, 15, and 25 wt%. The SDO of stearic acid was used as a probe reaction.

Inspection of Fig 10 shows that the conversion of stearic acid increases with increasing nickel loading. The relatively small increase in activity observed for increasing Ni loading from 15 to 25% could be attributed to the decrease in the specific surface area from 190 to 156 m^2/g and to the formation of bulk Ni in the sample 25NiAl. A similar dependence on nickel loading was reported by Palla et al. for the SDO of 1-octanol [120]. *n*-pentadecane, *n*-hexadecane, *n*-heptadecane, *n*-octadecane, and 1-octadecanol were identified with the *n*-heptadecane being primary product. This is in very good agreement with other studies already reviewed [111,112].

Fig. 11 shows the conversion of stearic acid obtained over Ni catalysts supported on γ-Al_2O_3, SiO_2 and HZSM-5 having the same Ni loading (10%). It is obvious that the activity of HZSM-5 supported catalyst has been proved much higher than that of the γ-Al_2O_3 and SiO_2 supported ones. However, in contrast to other studies [111–114] very small difference has been found concerning the activities of the later catalysts. It should be also stressed that no cracking products have been obtained over 10NiZSM-5, presumably due to the relatively low reaction temperature used. On the other hand, an enhancement of selectivity towards octadecane and/or octadecanol has been observed over this catalyst implying that HZSM-5 favors the HDO pathway with respect to alumina and silica. This observation is in line to the observation of Lercher et al. commented previously [110].

The works reviewed above deal with the effect of the support and Ni loading on the catalytic performance of nickel metallic catalysts. To the extent of our knowledge only two contributions dealing with the supports and the promoters as well have been reported by the same group. Specifically, Yakovlev et al. [95,96] (Table 2, entries 10 and 11) developed Ni and Ni-Cu catalysts supported on zirconia, ceria and zirconia–ceria for the SDO of the biodiesel in the context of an effort for its upgrading. In fact, biodiesel content in the mixed fuel is usually less than 20% because of its undesirable properties own to the presence of the methyl esters. Therefore, one

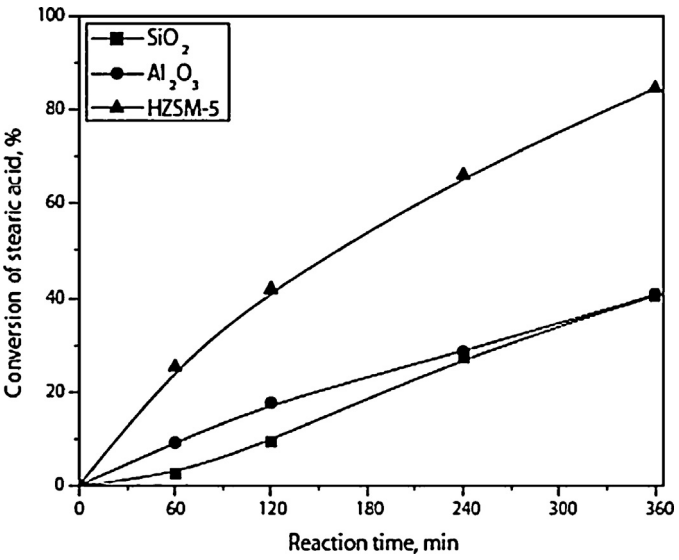

Fig. 11. Effect of support on stearic acid conversion. Conditions: concentration of stearic acid = 0.18 kmol/m^3, *n*-dodecane = 100 mL, catalyst loading = 0.5(w/v)%, temperature = 270 °C, initial hydrogen pressure = 8 bars. Source: Ref. [119].

way for biodiesel upgrading is the removal of oxygen-containing functional groups, namely the transformation of methyl esters into hydrocarbons.

A full conversion of biodiesel was obtained in reaction temperatures exceeding 300 °C over all catalysts studied [95]. The products obtained were linear liquid hydrocarbons C_6–C_{19} and methane. The experiments carried out at different temperatures showed that the heptadecane yield (main product) decreases as the temperature rises, whereas the yield of light hydrocarbons becomes higher. This indicates that at higher temperatures hydrocracking occurs along with SDO, leading to the formation of CH_4 and hydrocarbons with a lower molecular weight. However, as far as heptadecane was obtained as the main reaction product, it can be concluded that the SDO of bio-diesel over the Ni and Ni-Cu catalysts involves deCO_x steps. The absence of CO and CO_2 in the gas products shows that full methanation takes place. It is well known that Ni-based catalysts are able to perform the carbon oxides methanation under the given reaction conditions [121]. However, the analysis of the reaction products indicated that the hydrocarbons chain shortening occurred predominantly by the end —CH_3 group removal [95]. Thus the formation of methane should be related to the hydrocracking.

Concerning the monometallic catalysts it was demonstrated the critical role of the support for determining the selectivity of the hydrocarbons involved in the liquid product. High content of light hydrocarbons C_6–C_{12} in the reaction products was obtained over the Ni/ZrO_2 catalyst. The highest selectivity towards the heptadecane formation was attained over the Ni/CeO_2–ZrO_2 catalyst. This indicates that the presence of ceria in the mixed support favors deCO_x and suppress hydrocracking. The use of ceria single support (Ni/CeO_2) also suppresses hydrocracking but results to relatively high selectivity towards C_{18} and C_{19} hydrocarbons formation.

However, the monometallic Ni/CeO_2, Ni/ZrO_2 and Ni/CeO_2–ZrO_2 catalysts were proved to be unsuitable for production of considerable amounts of liquid alkanes at temperatures above 300 °C. In fact, biodiesel was almost quantitatively converted to methane over these catalysts even at 320 °C under the relatively low hydrogen pressure adopted (10 bar). In contrast, the bimetallic Ni–Cu/CeO_2, Ni–Cu/ZrO_2 and Ni–Cu/CeO_2–ZrO_2 catalysts were proved to be more attractive due to their ability to prevent the methane formation over wide temperature range (280–340 °C) [95]. Taking into account that one of the weaknesses of the nickel metallic catalysts is the high extent of methanation reactions at relatively high temperatures and relatively low hydrogen pressures the development of cooper promoted nickel catalysts or the development of copper–nickel bimetallic catalysts on various high surface area supports (e.g., alumina, zeolites or mesoporous Al modified ordered silica) would be a quite promising perspective.

The same group reported again on the hydrodeoxygenation of fatty acid esters (biodiesel) over the aforementioned catalytic systems adopting mild reaction conditions (290–320 °C, 1.0 bar) [96]. In this case, the Ni–Cu/CeO_2–ZrO_2 catalyst exhibited the highest activity allowing the quantitative conversion of biodiesel into linear alkanes with selectivity for heptadecane of about 70–80%. The characterization of the samples allowed the emergence of "structure–activity" relationships indicating that the high activity of the Ni–Cu/CeO_2–ZrO_2 catalyst can be partly explained by the presence of a $Ni_{1-x}Cu_x$ (x = 0.2–0.3) solid solution as a constituent of the active component of the catalyst and partly by the occurrence of a mixed phase of cerium and zirconium oxides. It is remarkable that the introduction of copper makes it possible to decrease the reduction temperature of a nickel oxide phase, on the average, by 100 °C presumably. This is because copper metal, formed at lower reduction temperature, activates adsorbed molecular hydrogen, which, in turn, is responsible for the reduction of nickel oxide at lower temperatures.

To summarize, the study of the influence of non-reducible (HZSM-5, HBeta, HY, SAPO-11, SBA-15, Al-SBA-15, γ-Al_2O_3, SiO_2) and slightly reducible (ZrO_2, TiO_2, CeO_2, ZrO_2–CeO_2) carrier oxides on the nickel SDO activity revealed the critical role of the support. The most promising supports among the non-reducible oxides (HBeta, SAPO-11, Al-SBA-15 and γ-Al_2O_3) exhibit high specific surface area and mild acidity for promoting SDO and preventing extending cracking. In contrast, supports with high acidity (HZSM-5, HY), though they provide very active catalysts, favor extended cracking. Silica and SBA-15 are not so suitable supports due to their low acidity though the latter ensures high nickel dispersion own to its very high specific surface area. The Ni catalysts supported on slightly reducible supports (zirconia, titania and ceria) exhibit high activity for SDO reaction which is attributed to the participation of the support surface on the reaction mechanism. Among the reducible oxides ZrO_2 seems to be quite attractive especially combined with CeO_2 as a mixed support. Systematic studies concerning nickel catalysts supported on TiO_2 are scarce although it is well known that TiO_2 is quite stable under the hydrothermal conditions predominating during the HDO reactions [122]. As the nickel loading one can conclude that the SDO activity of Ni catalysts increases with this parameter in good correlation to the increase of the active surface developed. The beneficial action of copper for hindering extended methanation at relatively high temperatures and low hydrogen pressures calls for future contributions relevant to other promoters or bimetallic catalysts (e.g., Ni–Co, Ni–Zn etc.).

3.3. SDO pathways over the nickel metallic catalysts

The group of Lercher studied the SDO pathways over nickel metallic catalysts, in parallel to the influence of the support on catalytic performance described in the previous sub-section. In the first paper of the series [110] the kinetic study was mainly done over the 10 wt% Ni/HBeta zeolite (Si/Al = 180) under the conditions illustrated in Table 2, entry 1. Concerning the kinetics of the transformation of the microalgae oil it was found that the yield of stearic acid exceeded 70 wt% within 1 h. Then, it gradually decreased accompanied with an increase in alkane yields of octadecane and heptadecane as a function of time (Fig. 12).

Taking into account the above kinetic results and the composition of the microalgae oil [unsaturated C_{18} fatty acids (88.4 wt%),

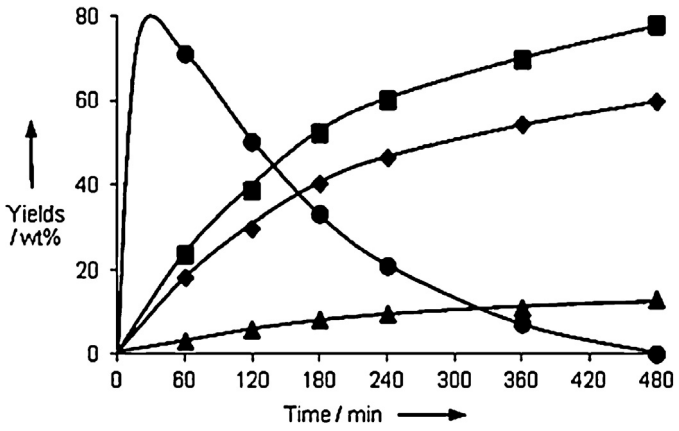

Fig. 12. Product distributions for the transformation of microalgae oil over 10 wt% Ni/HBeta at 260 °C as a function of time. Total liquid alkanes yield (■), octadecane yield (♦), heptadecane yield (▲) and stearic acid yield (●). Source: Ref. [110].

saturated C_{18} fatty acids (4.4 wt%)] they concluded that the hydrogenation of double bonds in the alkyl chain occurs very fast. The subsequent, slower, hydrogenolysis of saturated triglycerides produces fatty acids and propane as initial primary products. It follows the SDO of fatty acids to alkanes. Based on the distribution of alkanes, the identification of trace of intermediates [octadecanal and 1-octadecanol] and the detailed kinetics of probe molecules they moreover concluded that the subsequent hydrogenation of the carboxylic group of fatty acid leading to the corresponding aldehyde is the rate-determining step. This is followed by either decarbonylation of octadecanal to *n*-heptadecane and carbon monoxide (minor route) or hydrogenation of octadecanal to 1-octadecanol (major route). Subsequently, the produced 1-octadecanol undergoes sequential acid-catalyzed dehydration and metal-catalyzed hydrogenation leading to the final n-octadecane. An abundance of acidic sites in the zeolite leads to hydroisomerization and hydrocracking of the alkanes. Finally, CO may react with H_2 over the supported nickel nanoparticles to produce methane and water.

In the second paper of the series [111] the group of Lercher extended its studies on the SDO pathways by investigating in details the reaction mechanism over a 10% Ni/ZrO_2 catalyst (Table 2, entry 2). One of the purposes of the study was to explain the higher activities obtained over the nickel catalysts supported on zirconia, titania and ceria with respect to ones supported on alumina and silica presented in the Section 3.2. Like in the previous contribution [110] the work concerned the SDO of stearic acid and of micro-algae oil as well. The study of the mechanism was based on the SDO kinetics of stearic acid and 1-octadecanol at 260 °C and various pressures. Moreover, it taken into account the intermediate and side products detected [1-octadecanol, traces of octadecanal, stearyl stearate (formed via esterification of stearic acid with the 1- octadecanol intermediate on acid–base sites) and stearone (obtained from ketonization of stearic acid over pure zirconia)].

It was concluded that SDO is mainly realized above the nickel supported nanoparticles following the sequence illustrated in Fig. 13 (route 1).

Similarly to the nickel catalysts supported on zeolites [110], the reduction of stearic acid to octadecanal is the rate determining step. The octadecanal produced, being in equilibrium with the 1-octadecanol (produced by further reduction), is rapidly decarbonylated producing n-heptadecane. The equilibrium between octadecanal and 1-octadecanol favors the later under the reaction conditions. It was moreover concluded that the SDO is also realized through another parallel route (Route 2 in Fig. 13) taking place partly over the support and partly over the nickel supported nanoparticles. The stearic acid is adsorbed dissociatively on the defect oxygen sites of the support resulting to carboxylate and dihydrogen. This step is corroborated by previous results relevant to the selective hydrogenation of carboxylic acids to aldehydes over the reducible oxides (zirconia, titania and ceria) [123–125]. The reaction proceeds through a ketene intermediate which is hydrogenated to octadecanal over the nickel supported nanoparticles. The authors propose that the function of this parallel route may explain the higher activities obtained over the nickel catalysts supported on zirconia, titania and ceria with respect to the ones supported on alumina and silica (Section 3.2). The production of the small amounts of n-octadecane takes place through the HDO of 1-octadecanol which proceeds via two successive steps (dehydration and hydrogenation). This mechanism may explain why the increase in the hydrogen pressure, which shifts the octadecanal ↔ 1-octadecanol equilibrium to the 1-octadecanol, favors the HDO with respect deCO.

Based on the overall kinetics of the SDO of micro-algae oil and the kinetics of the SDO of stearic acid and 1-octadecanol the following main pathway was proposed for the SDO of the former: (a) hydrogenation of the C=C bonds in the alkyl chains of the triglycerides, (b) selective hydrogenolysis of the C—O bonds of the formed saturated triglycerides to fatty acids and propane, (c) hydrogenation of the carboxylic group of the fatty acids to the corresponding aldehyde (rate-determining step) either catalyzed solely by metallic Ni or synergistically by Ni and ZrO_2 through a ketene as intermediate, (d) deCO of octadecanal to *n*-heptadecane and carbon monoxide. The octadecanal is in equilibrium with the 1-octadecanol. This may hydro-deoxygenated resulting to n-octadecane (minor product) through dehydration and subsequent hydrogenation of the resulting olefin. The direct $deCO_2$ of the fatty acids formed in the step (b) is another minor route. It was inferred that the rate of reaction for each one of the steps of

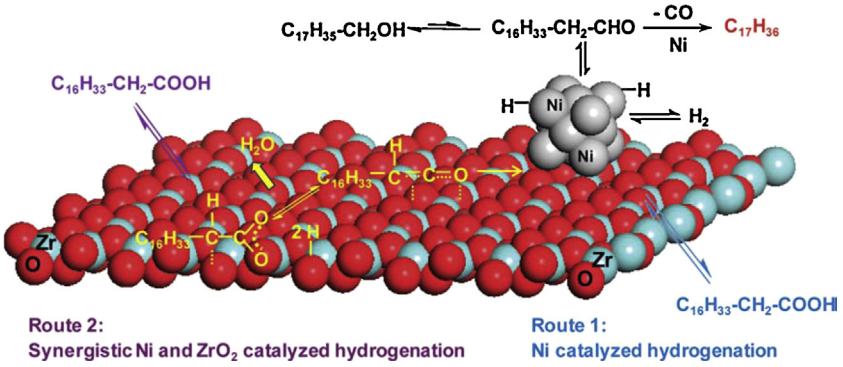

Fig. 13. Mechanism of transformation of stearic acid to n-heptadecane via synergistic catalysis over Ni/ZrO_2. Source: Ref. [111].

the main pathway follows the order: hydrogenation of the C=C bonds > hydrogenolysis of saturated triglycerides > deCO of octadecanal > hydrogenation of the carboxylic group of the fatty acids to the octadecanal.

A strict difference concerning the mechanism of the SDO inferred over the zirconia and zeolites supported nickel catalysts is that in the first case the deCO of octadecanal is the major SDO route whereas in the second case the major route is the HDO of 1-octadecanol. This clearly shows the critical role of the support in determining the SDO pathways. Besides this difference the main features of the SDO mechanism over the nickel supported catalysts remains the same irrespectively of the kind of the support.

The Lercher group continued its work devoted to the elucidation of the reaction pathways relevant to SDO [112] (Table 2, entry 3). They studied the kinetics and mechanism of the catalytic conversion of palmitic acid (instead of stearic acid used in the previous two works [110,111]) and intermediate products (1-hexadecanol and palmityl palmitate) over a 5%wt Ni/ZrO_2 catalyst. They also studied the change obtained in the catalytic pathway by altering the active element (Pd, Pt) and the support (C, ZrO_2, Al_2O_3, SiO_2, HBEA, or HZSM-5). The role of hydrogen was also investigated. Thus this work completes the previous two works [110,111] from the viewpoint of elucidating the various factors eventually affecting the SDO pathways including the reactant used.

A similar reaction scheme was proposed for the SDO of palmitic acid over the 5% Ni/ZrO_2 catalyst to that mentioned before for the SDO of stearic acid over the 10% Ni/ZrO_2 catalyst [112]. In fact, the mechanism proposed involves the initial hydrogenation of palmitic acid to hexadecanal which is rapidly transformed/equilibrated with 1-hexadecanol. Under the reaction conditions applied (12 bar of hydrogen) the equilibrium favors the later. The hexadecanal is subsequently decarbonylated rapidly to n-pentadecane and carbon monoxide (major route). The small amount of the hexadecane observed in the products was formed by sequential dehydration and hydrogenation reactions of 1-hexadecanol (minor route). The weak acidic sites of the support catalyze a slight cracking and isomerization of the straight-chain alkanes. In parallel to the aforementioned major and minor routes, the acid sites of the support catalyze the esterification of the 1-hexadecanol with palmitic acid to form palmityl palmitate. This can be dissociated by metal-catalyzed hydrogenolysis, leading to 1-hexadecanol and hexadecanal. The later is decarbonylated to form *n*-pentadecane. The produced CO_2/CO may further react with H_2 to produce water and methane observed in the gas phase. The same mechanism seems to be followed over all Ni/ZrO_2 catalysts studied (Table 2, entry 3). In the frame of this mechanism the ratio of support sites to nickel sites, regulated by the nickel content, seems to affect the product distribution. The increase of the nickel loading accelerates both decarbonylation of the hexadecanal and the hydrocracking, both catalyzed by nickel sites. It is remarkable that over the pure ZrO_2 support the main product was palmitone, derived from the ketonization of palmitic acid (see below). Pure support also showed some hydrogenation activity, converting palmitic acid with selectivities of 18, 7.6 and 4% to 1-hexadecanol, palmityl palmitate, and C_{15} and C_{16} hydrocarbons, respectively.

Taking into account the above and the mechanism mentioned before for the SDO of stearic acid over the same Ni/ZrO_2 catalysts [111] it is moreover inferred that the SDO of palmitic acid is also realized through a parallel route taking place partly over the support and partly over the nickel supported nanoparticles (Fig 14a, left) [112]. According to this route the palmitic acid is adsorbed dissociatively on the defect oxygen sites of the support resulting to palmitate. One of the α-H of the palmitate can subsequently be abstracted to produce a ketene intermediate which is hydrogenated to hexadecanal on supported Ni particles. The remaining two protons, one generated upon the adsorption of palmitic acid and the other derived from abstraction of the α-H, are recombined with the oxygen bound on the ZrO_2 defect site and are desorbed as H_2O. The authors attributed to this parallel route the higher activities obtained over the nickel catalysts supported on zirconia with respect to the ones supported on alumina and silica presented in the section 3.2. The SDO kinetics of the palmitic acid indicated also direct deCO$_x$ but at very low conversion.

The above indicate that the main characteristics of the SDO mechanism over nickel supported catalysts do not practically depend on the kind of the fatty acid used as probe molecule.

The critical role of the support for determining the relative extent of SDO pathways in the frame of the above mechanism is illustrated by studying the nickel catalysts supported on ZrO_2, Al_2O_3, SiO_2, HBEA, or HZSM-5 [112]. The effect of the support is related to the acid centers developed on their surfaces which can catalyze the dehydration of the 1-hexadecanol and thus facilitate the formation of the *n*-hexadecane through the hydrogenation of the resulting alkene on the nickel metallic active sites. In fact, the major product at complete conversion of palmitic acid was *n*-hexadecane (65–72% yield) over the two H-zeolite-supported Ni catalysts due to the Bronsted acid sites developed on their surfaces. Moreover, these sites catalyzed hydroisomerization giving *iso*-C_{15} and *iso*-C_{16} (yields of up to 20.8%) and hydrocracking products (4.9–6.0% yields). In contrast, the nickel catalysts supported on Lewis acidic oxides (ZrO_2 and Al_2O_3) did not catalyzed the formation *n*-C_{16} and *iso*-C_{16} indicating that Lewis acid sites are much less active than Bronsted acid sites for dehydration of the 1-hexadecanol. The dehydration of the 1-hexadecanol catalyzed by the Bronsted acid sites is also favored over the nickel catalysts supported on HBEA, or HZSM-5 due to the very high specific surface area of these catalysts (565 and 304 $m^2\,g^{-1}$, respectively [110]) which allow being exposed a large portion of bare support surface containing the Bronsted acid sites.

A drastic change of the mechanism is concluded going from nickel supported catalysts to Raney Ni ones which favor direct deCO$_x$ with respect the aforementioned multi step route described above [112]. The influence of the support on the SDO mechanism is also pronounced for the palladium and platinum catalysts. Carbon supported and unsupported Pd and Pt favor direct deCO$_x$ whereas the Pd and Pt catalysts supported on zirconia follow the aforementioned multi step route concluded for the nickel catalysts [112].

The influence of gas composition (H_2, N_2 and mixtures H_2–N_2 from 0 to 100% in hydrogen) on the SDO pathway concerning nickel catalysts supported on zirconia is very important. It was inferred that in the absence of hydrogen the mechanism is quite different. The ketene intermediate produced on the zirconia surface cannot be hydrogenated on the supported nickel particles and thus it forms palmitone through interaction with a neighboring palmitate moiety adsorbed on the ZrO_2 support under elimination of CO_2 (Fig. 14b). In situ IR spectroscopy strongly supports the mechanisms illustrated in Fig. 14 through capturing the ketene intermediates.

Experiments in nitrogen atmosphere indicated that direct deCO$_2$ of palmitic acid (resulting to the formation of carbon dioxide) was the dominant pathway over the Pd black, whereas the direct deCO (resulting to the formation of carbon monoxide) was more prevalent on Pt black and Raney Ni. This difference could be related to the different intermediate species formed upon the direct deCO$_x$. Previous studies devoted to the adsorption of acetic acid on Pd (1 1 1) and Pt (1 1 1) had shown formation of CH_3COO^* and CH_3CO^* corresponding, respectively, to deCO$_2$ and deCO [126,127].

As already mentioned in a previous Section, Zuo et al. [113,114] (Table 2, entry 4) studied the SDO of methylpalmitate over nickel metallic catalysts supported on various carriers (SiO_2, γ-Al_2O_3, SAPO-11, HZSM-5, and HY) for recovering a promising support. In the same study they proposed the following reaction

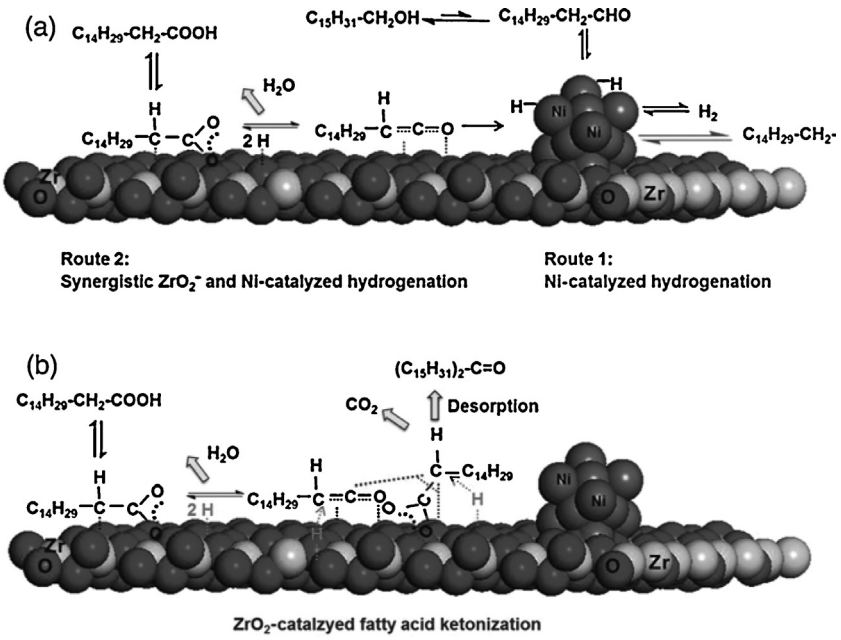

Fig. 14. Reaction mechanism for (a) the hydrogenation of palmitic acid to hexadecanal by synergistic catalysis over Ni/ZrO_2 in the presence of H_2 and (b) for the ketonization of palmitic acid to palmitone over ZrO_2 in nitrogen atmosphere. Source: Ref. [112].

scheme (Fig. 15) which was simply based on the reaction products (methane, CO_2, CO, dimethyl ether and alkanes) and intermediates (hexadecanoic acid as well as traces of methanol, hexadecanal, hexadecanol and hexadecene).

Inspection of this scheme shows that it involves all the pathways proposed by the Lercher group which were discussed previously, that is the main route for the production of C_{15} (methyl palmitate => palmitic acid => hexadecanal => pentadecane) and the minor route (methyl palmitate => palmitic acid => hexadecanal => 1-hexadecanol => hexadecene => hexadecane). Moreover, it involves the less probable pathways of the direct $deCO_x$ of the palmitic acid resulting to pentadecane. The authors note that although the $deCO_x$ approach proposed is based on palmitic acid and hexadecanal intermediates, $deCO_2$ might also occur directly for methyl palmitate because of their similar molecular structure. The detection of methanol and dimethyl ether in the products enforced the authors proposing an alternative route for the production of the hexadecanal intermediate by hydrogenolysis of methyl palmitate resulting to the production of methanol which may in turn dehydrated producing dimethyl ether. In this respect this work provides more alternative pathways for SDO. However, the relatively large amounts of palmitic acid detected for small reaction time [114] clearly shows that SDO mainly proceeds through the formation of palmitic acid. Moreover, the proposed scheme indicates that besides the direct production of pentadecane via $deCO_x$ of palmitic acid/hexadecanal, it may be first produced pentadecene which in turn is hydrogenated resulting to pentadecane. Finally, the authors note that considering H_2O formed from methanol and hexadecanol dehydration, hexadecanoic acid intermediate could be also produced by methyl palmitate hydrolysis.

As already mentioned in the previous sub-section the nickel supported catalysts on γ-Al_2O_3 and SAPO-11 exhibiting weak and medium acidity are proved to be the most promising ones for obtaining high conversion and low cracking [113,114]. Taking into account the above mechanism the author assumed that the electrophilic acidic sites activate the carbonyl and/or bridge oxygen atoms of methyl palmitate, weakening the acyl and/or ether bond, which is favorable to be attacked by the over spilled H atoms activated from the adjacent Ni atoms. These result, respectively, to the formation of 1-hexadecanal and methanol or hexadecanoic acid and methane. Thus, the above catalysts were proved to be more active than that supported on silica which exhibits much less acidity Fig. 15.

A fundamental insight for the SDO reaction pathways that arise when different catalysts [Pd, Ni, CoMoS*x*, and NiMoS*x*] are used under different reaction conditions has been obtained in a recent work reported by Kim et al. [128] (Table 2, entry 12). The achievement of this goal was based on the comprehensive analysis of the composition of renewable diesel produced from soybean oil. This analysis was obtained by developing a novel four-dimensional gas chromatography approach combined with time-of-flight mass spectrometry. The contribution is interesting because allows comparing the SDO pathways favored over a nickel catalyst (57.6% Ni/SiO_2–Al_2O_3) with those favored over Pd, CoMoS*x* and NiMoS*x* catalysts (4.29% Pd/γ-Al_2O_3, 2.8% Co 7.6% Mo/γ-Al_2O_3, and 2.4% Ni 11.8% Mo/γ-Al_2O_3) under a wide range of reaction conditions (temperature: 300–440 °C, initial H_2 pressure: 45-120 bar (mainly 92 bar)). A batch reactor has been used for this study loaded with 2.5 g of commercial catalysts and 28.1 g of soybean oil. Upon reaction the temperature was increased for 1 h up to the desired temperature and then it is remained constant for 1 h (Table 2, entry 12).

This study showed that the composition of the liquid product (green diesel) depends on the catalyst used and the reaction conditions. Typical compositions obtained at 440 °C and 92 bar are illustrated in Fig. 16. Moreover, carbon dioxide, carbon monoxide, and C_1–C_3 alkanes are detected in the gas phase.

Based on the liquid and gas phase compositions obtained over the catalysts studied under various reaction conditions they proposed the following quite general scheme for the SDO pathways (Fig. 17). The first difference in the SDO pathways between the metallic and the sulphided catalysts at the initial stage of SDO is related to the high ability of metallic catalysts to hydrogenate the C=C bond resulting in the production of saturated triglycerides (1″). Therefore, the main SDO route over the metallic catalysts is illustrated in the right side of the reaction scheme. In contrast, the sulphided catalysts, mainly CoMoS*x*, do not fully saturate the C=C bonds. This manifested by quite large amounts of C_{17} and C_{18} olefins

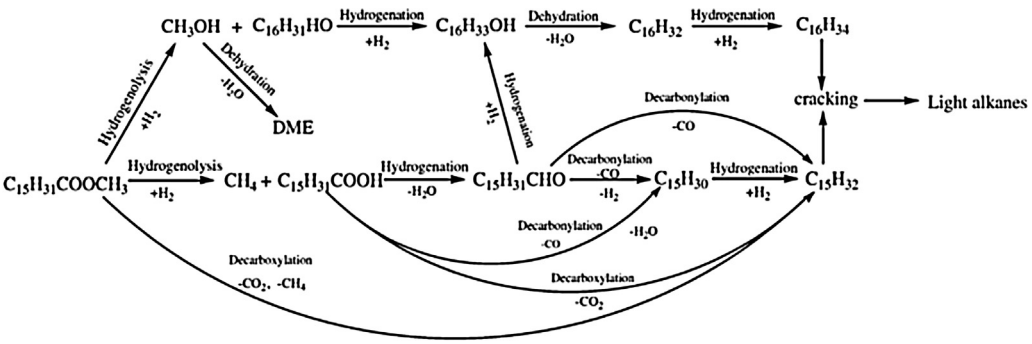

Fig. 15. Pathways for the SDO of methyl palmitate. Source: Ref. [114].

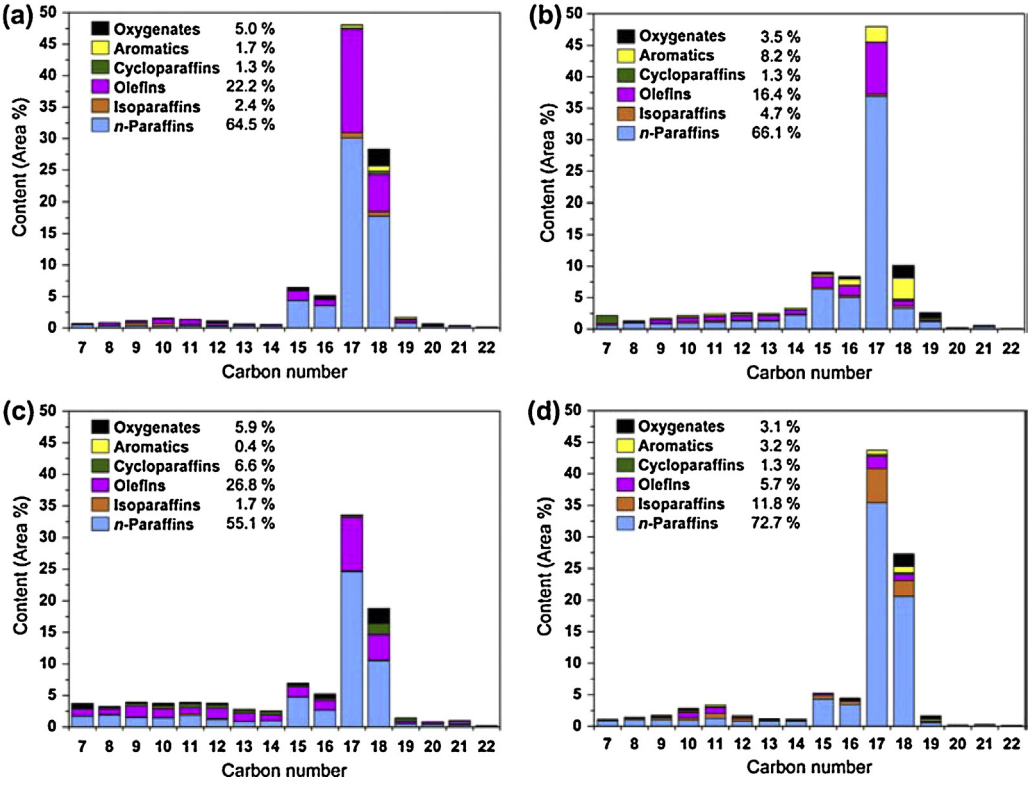

Fig. 16. Liquid product distribution for the SDO of soybean oil over the catalysts studied: (a) CoMoS*x*, (b) Ni, (c) Pd, and (d) NiMoS*x* catalysts. Conditions: 400 °C and 92 bar of H_2. Oxygenates include acids, esters, alcohols, aldehydes, and ketones. Source: Ref. [128].

detected in the end products for the CoMoS*x* catalysts (Fig. 16a). Thus, the main SDO route over the sulphided catalysts is illustrated in the left side of the reaction scheme.

The second difference in the SDO pathways between the two types of catalysts studied is manifested by the decomposition of the glycerol backbone of the triglyceride upon the initial stage of SDO (1′ or 2″). Relatively large amount of propane is observed over the CoMoSx and NiMoSx catalysts resulting from the higher C–O cleavage rate (1′) while the metallic catalysts produce larger volumes of C_1–C_3 alkanes because of the higher rates of C–C bond scission (2″). This difference originates from the difference between the reactions rates of C–C and C–O bond scission over each type of catalyst. Functional theory calculations had indicated that C–C cleavage is favored on metal surfaces [129], whereas C–O cleavage is activated by the sulfhydryl species present on the edges of transition metal sulfides [130].

However, in both cases a fatty acid is the intermediate product produced through the step 1′ or 3″. The SDO of the intermediate fatty acid may proceed following two different routes, namely direct deCO$_2$ (3′, 5″) and hydrogenation-dehydration to produce aldehyde (2′, 4″) which is rapidly equilibrated with the corresponding alcohol (2′a or 4″a). The very high C_{17}/C_{18} ratios obtained over the Ni and Pd catalysts (Fig. 16b and c) suggest that the SDO over these catalysts proceeds at large extent via the direct deCO$_2$ of the fatty acid (5″) and / or the deCO of the aldehyde (6″). This can be also attributed to that the C–C cleavage is favored on metal surfaces [129]. Moreover, based on the values obtained for the ratio CO/CO$_2$ and the negligible methanation and water gas shift reaction in the gas phase over palladium catalyst it was concluded that the deCO of aldehyde is favored with respect to direct deCO$_2$ of the fatty acid over this catalyst. The same main route has been proposed for nickel supported catalysts [111,112] though relative reaction rates of deCO$_2$/deCO cannot be easily estimated over this catalyst because of the extensive methanation in the gas phase [128]. Thus, the main route over the metallic catalysts up to the production of n-heptadecane involves the steps (1″, 2″, 3″, 4″, and 6″). A minor route responsible for the relatively low amounts of the n-octadecane in the liquid products involves the steps (1″, 2″, 3″, 4″, 4a″, 7″).

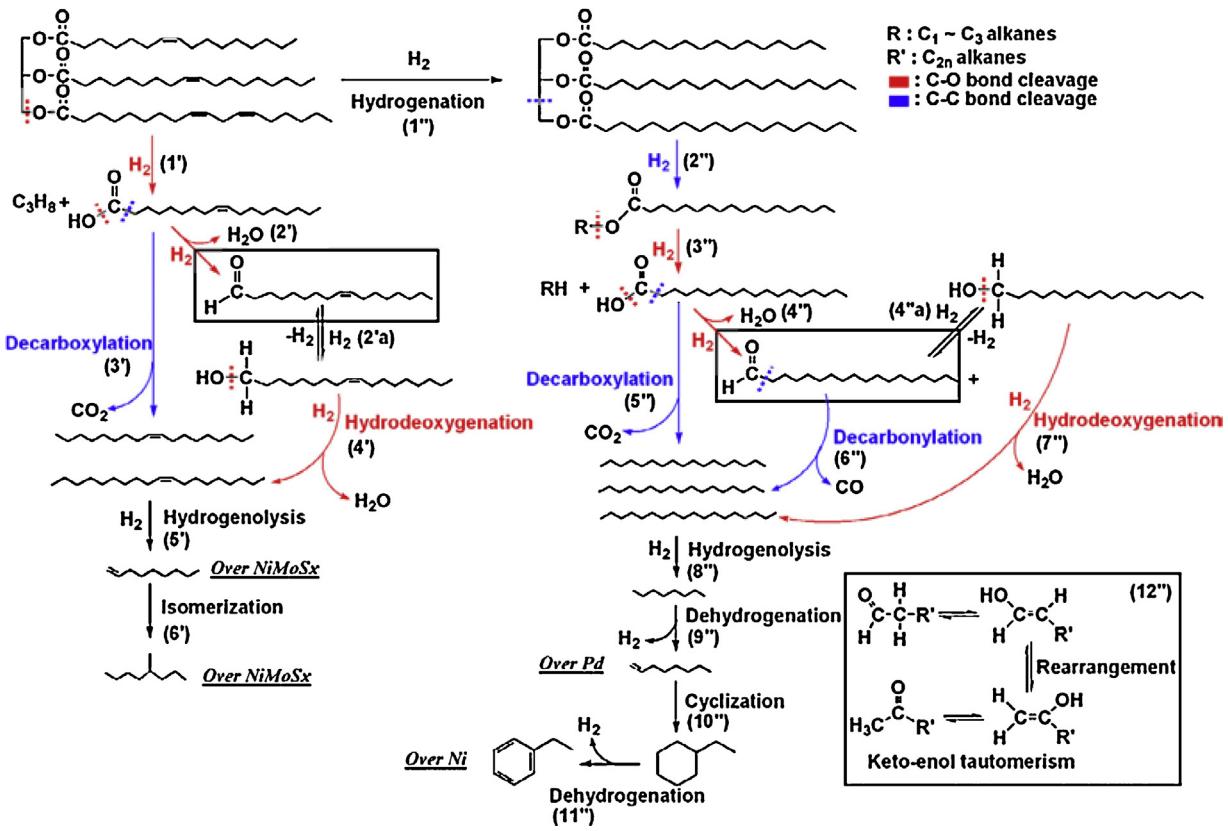

Fig. 17. SDO pathways for the catalytic deoxygenation of a triglyceride over Ni, Pd, CoMoS*x* and NiMoS*x* catalysts studied. Broken lines represent bond scission. The end-product characteristics corresponding to each catalyst are emphasized by the underlined labels. Source: Ref. [128].

The above picture is similar if not identical to those described in the previous paragraphs of this section for the SDO pathways over nickel and palladium metallic catalysts supported on oxidic supports.

The picture is different over the sulphided catalysts. The ability of these catalysts to cleavage the C–O bond [130] facilitates the HDO of alcohol to produce C_{18} hydrocarbons which are detected in considerable amounts in the end-products (Fig. 16a and d). Moreover, the low values obtained for the ratio CO/CO_2 under negligible methanation and water gas shift reaction indicates direct $deCO_2$ of the fatty acid to produce C_{17} hydrocarbons. Therefore, the SDO of triglycerides over the sulphided catalysts follows two routes involving the steps (1′, 3′) or (1′, 2′, 2′a, 4′).

The produced C_{17} and C_{18} linear hydrocarbons may undergo small extent transformations including hydrogenolysis (5′, 8″), isomerization (6′), dehydrogenation (9″, 11″), cyclization (10″) and transformation of the intermediate aldehydes into ketones (12″).

The effect of increase of the hydrogen pressure was studied over the CoMoSx and nickel catalysts. It was found that this increase favors the HDO pathway and the saturation of the C=C bonds. These effects are rather expectable taking into account the stoichiometry of these reactions. In contrast, the increase in the reaction temperature increases the relative amount of olefins produced by the endothermic dehydrogenation of hydrocarbons.

A slightly different SDO pathway has been proposed by Kumar et al. [119] (Table 2, entry 9) studying the SDO of stearic acid in a high pressure batch reactor over nickel metal catalysts supported on SiO_2, γ-Al_2O_3, and HZSM-5 in the temperature range of 260–290 °C. More precisely, they propose the reduction of stearic acid into octadecanol which is then dehydrogenated into octadecanal. The later is decarbonylated producing heptadecane. Moreover, they propose that the intermediate octadecanol can undergo HDO (into octadecane) and/or hydrocracking (into smaller hydrocarbons).

Recently, Kaewmeesri et al. [131] studied the effect of water and free fatty acid content on the SDO of waste chicken fats to green diesel over a Ni/γ-Al_2O_3 catalyst in a trickle-bed reactor (Table 2, entry 13). They found that the major reaction pathway was $deCO_x$, whereas HDO was minor. Methane, produced from the methanation of the resultant CO/CO_2 and the propane cracking, was the major gaseous product. The FFA and water content improved the green diesel yield. In particular, water accelerated the breakdown of the triglyceride molecules into FFAs. Therefore, waste chicken fat from food industries containing a high degree of FFAs and water content can be used as a low-cost feedstock for renewable diesel production without the requirement of a pretreatment process.

To summarize, the SDO over the supported nickel metallic catalysts is realized by various routes related to the catalysts formulation and the reaction conditions. To be specific:

(a) The main route involves: (i) the very rapid hydrogenation of the C—C double bonds of the unsaturated fatty acids, (ii) the rapid hydrogenolysis of the C—O bonds to form propane and saturated fatty acids, (iii) the reduction of the saturated fatty acids to form aldehydes, which are in equilibrium to the corresponding alcohols, (iv) the rapid deCO of aldehydes to produce saturated hydrocarbons (mainly with 17 carbon atoms). In this mechanism the step (iii) is the rate determining one. The formation of the intermediate aldehydes over nickel catalysts supported on reducible oxides can be also realized but in smaller extent following a parallel mechanism partly realized on the defect

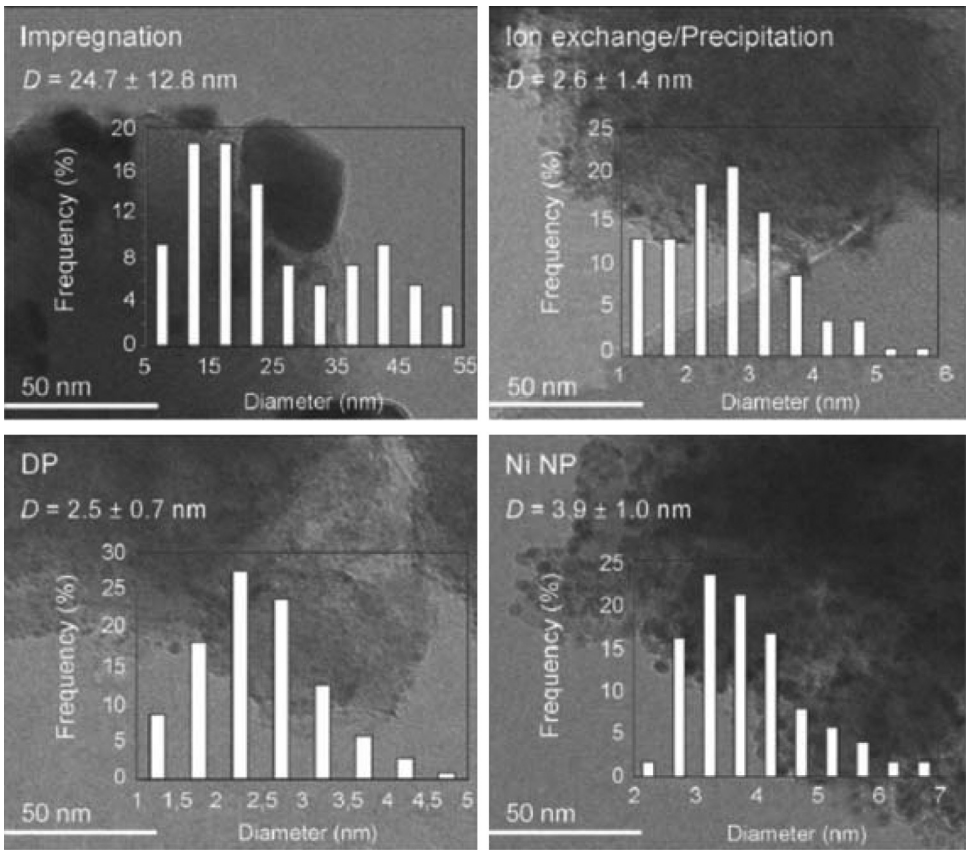

Fig. 18. TEM images of Ni/HBEA samples prepared by different methods; the respective insets are the histograms of Ni particle size distribution after counting 300 particles. Source: Ref. [132].

oxygen sites of the support and partly on the nickel supported particles.

(b) A minor but also important route involves the steps (i)–(iii) which are followed by HDO of the alcohols realized in two steps, (iv)′ dehydration of the alcohol over the Bronsted acid sites of the support followed by (v)′ hydrogenation of the resulting alkenes to produce saturated hydrocarbons (mainly with 18 carbon atoms). The use of high surface area supports with Bronsted acid sites (e.g., zeolites) favors the route (b) with respect to route (a).

(c) Some other SDO routes/steps taken place but in very small extent are: (i)" the direct deCO_2 of the intermediate fatty acids or the triglycerides, (ii)" the indirect deCO of the intermediate aldehydes resulting first to alkenes which are then hydrogenated to alkanes, (iii)" the hydrogenolysis of triglycerides resulting to the formation of aldehydes and alcohols, (iv)" the formation of ethers by etherification of the intermediate alcohols over the Bronsted acid sites of the supports, (v)" the acid esterification of the intermediate fatty acids and alcohols resulting to intermediate esters which then undergo SDO, (vi)" the transformation of the resulting alkanes into alkenes, aromatics and/or naphthenes under relatively high temperatures and (vii)" the cleavage of the C—C bonds of the propane formed by hydrogenolysis of the C—O bonds of the triglycerides (step ii) to form C_1–C_2 hydrocarbons.

(d) More fundamental studies would be very useful, devoted to the elucidation of the structure of the nickel active sites and their interactions with the carboxylic acids upon the critical (rate determining) hydrogenation step to form the intermediate aldehydes.

3.4. The effect of preparation method on the catalytic performance of nickel metallic catalysts

In the previous two sections we have seen that concerning the nickel metallic catalysts the research is focused on the influence of the support and nickel loading on catalytic performance and SDO pathways. A very little attention has been directed so far to the preparation methods. Actually, there is only one important contribution dealing systematically with the influence of preparation method, limited in the context of impregnation techniques, on the catalytic performance of nickel metallic catalysts. This was reported by the Lercher group [132]. Continuing their work on the nickel catalysts supported on zeolites [110] they prepared four 5%Ni/HBEA catalysts using conventional incipient wetness impregnation, ion-exchange/precipitation (actually "equilibrium deposition filtration" at relatively high pH favoring deposition by surface precipitation [133]), deposition precipitation (DP) using ammonia as precipitating agent [134] and grafting of as-synthesized Ni nanoparticles (Ni NP) [135]. The catalysts were characterized using various techniques and tested in the SDO of stearic acid and microalgae oil using a BR (Table 2, entry 14).

In order to study the catalyst stability four recycling runs were performed over each catalyst. TEM, TPR and IR spectra of adsorbed CO showed that ion-exchange/precipitation, DP and grafting of Ni NP lead to catalysts with smaller supported nanocrystals compared to that prepared by impregnation (Fig. 18). This justifies the considerably higher SDO activity of these catalysts (in first and recycling runs) with respect to the catalyst prepared by conventional impregnation (Fig. 19). Thus, the size of the supported crystallites is a critical factor determining catalytic activity.

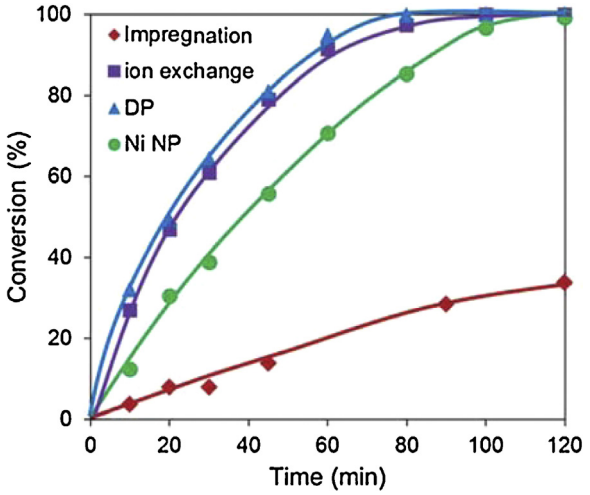

Fig. 19. Conversion of stearic acid as a function of time over fresh Ni/HBEA catalysts prepared by four different methods. Source: Ref. [132].

Among the catalyst exhibited the highest activity more stable were proved to be the DP and Ni NP ones whereas the activity of the catalyst prepared by ion-exchange/precipitation decreased considerably after the second recycling run. This was attributed to the wider size distribution of the supported nickel particles on this catalyst (Fig 18) which facilitates the increase of their size through the Ostwald ripening. Thus, the good size uniformity ensures high catalyst stability for longer utilization. The preparation method does not affect considerably the ratio n-C_{18}/n-C_{17} hydrocarbon ratio which was found to be about 2.0 over all catalysts studied.

To summarize, the first systematic study dealing with the influence of preparation method on the catalytic performance indicated that this may influence considerably the size and uniformity of the nickel supported nanoparticles and thus the catalytic behavior of the resulting catalysts. We believe that the subject is open for further contributions on other supports and preparation techniques (e.g., catalysts prepared by co-precipitation or co-gelation). Therefore, new studies would be welcomed in the field of SDO catalysts. We note that relevant theoretical [136] and experimental studies [137–143] concerning the preparation of supported Ni catalysts are abundant in the literature but they mainly addressed to hydrogenation.

3.5. *Comparison of a nickel metallic catalyst with other metallic and sulphided catalysts and the effect of reaction parameters on catalytic behaviour of the nickel metallic catalyst*

In the previous sections we reviewed the works dealing with various aspects of metallic nickel catalysts. In the present section we are dealing with a small number of recent works focusing on the comparison of the nickel metallic catalysts with other types of candidate catalysts for commercial applications and the effect of reaction parameters on catalytic behaviour of the nickel metallic catalysts.

In this context Onyestyak et al. [144] compared the activity of two nickel catalysts, namely an impregnated catalyst (27% Ni/γ-Al_2O_3) and a non-pyrophoric Raney nickel catalyst (NPR 27% Ni/γ-Al_2O_3) prepared by partial leaching with sodium hydroxide of an Al–Ni alloy and modified with various amounts of Pb or Sn with the activity of a commercial 9% Mo2.5% Ni/γ-Al_2O_3 catalyst doped with P and Si. The later is used as reference in its reduced form. The catalysts were characterized using various techniques and the SDO of sunflower oil and octanoic acid into hydrocarbons were used as probe reactions (Table 3, entry 1).

The same (very high) sunflower conversion was obtained over the nickel-molybdenum catalyst with the ten times higher nickel content monometallic catalysts. The relatively high activity of the nickel–molybdenum catalyst should be attributed to the fact that the Mo supported phase is also active to SDO and to the some kind of synergy between the supported phases as well. It was observed once again that the nickel–molybdenum catalyst favors HDO whereas the monometallic catalysts favor deCO_x, as it was inferred by the number of carbon atoms of the principal hydrocarbon produced in each case (Fig. 20). Moreover, methane is produced in the monometallic catalysts as a result of the complete hydrogenation of the evolved CO_2/CO. Finally, an extended cracking of the aliphatic chains, manifested by the appearance of hydrocarbons with 11–16 carbon atoms in the products, was observed over the monometallic catalysts, mainly over the NPR 27%Ni/γ-Al_2O_3 catalyst (Fig. 20). Obviously, the extensive hydrogen consumption in the hydrocracking and the production of methane is undesirable. The aforementioned undesired cracking over the monometallic catalysts should be related with the relatively high reaction temperature (340 °C).

Similar conversions were obtained over the monometallic catalysts for the transformation of octanoic acid into heptane and methane but at 40 °C lower reaction temperature and at doubled space velocity as for sunflower oil. This probably indicates the relatively high reactivity of the probe molecule with respect to sunflower oil. The non-pyrophoric Raney nickel catalyst is proved to be more active than the impregnated one especially in the undesirable hydrocracking. This could be related to the observation that the nickel phase was found mainly in metallic state in the non-pyrophoric Raney nickel in contrary to supported Ni-catalyst where the oxide phase was dominant in spite of the same reduction treatment. An effort to increase the selectivity of the non-pyrophoric Raney nickel catalyst by poisoning it with Sn or Pb was not successful. In contrast, addition of large amount of In_2O_3 was found to be completely effective in suppressing side reactions though it directed the process to the production of alcohols. Decreasing the amount of In_2O_3 the original reaction pathway is gradually restored producing mainly heptane beside octanol whereas paraffin hydrogenolysis is effectively eliminated.

The group of Kim reported two interesting contributions devoted to the transformation of soybean oil into green diesel. In the first one, [145] (Table 3, entry 2), they compared the catalytic activity and selectivity of one supported nickel catalyst with other metallic and sulphided supported catalysts in the hydrotreatment of soybean oil for producing liquid hydrocarbons, mainly in the diesel range. It is important to note that the comparison of the active phases in this study concerned commercial catalysts supported on the same or nearly the same support (γ-alumina, silica-alumina). This renders the comparison of the active phases more valuable. In contrast, the comparison concerns catalysts with different amounts of the active phase. In the second contribution, [146] (Table 3, entry 3), they studied the effect of reaction conditions on the hydrotreatment of soybean oil using two commercial catalysts selected from the first study.

Concerning the first contribution [145], the monometallic catalysts were studied in their reduced form whereas the bimetallic ones in their sulphided form (Table 3, entry 2). Several parameters were taken into account when evaluating the catalysts studied (oil conversion, naphtha, kero/jet and diesel selectivity, free-fatty acid content, oxygen removal, saturation of double bonds).

Unexpectedly, it was reported that the order of oil conversion depends on the catalyst/oil weight ratio. Thus, at a catalyst/oil weight ratio equal to 0.044, the following order was obtained: sulfided NiMo/γ-Al_2O_3 (92.9%) > 5% Pd/γ-Al_2O_3 (91.9%) > sulfided CoMo/γ-Al_2O_3 (78.9%) > 66%Ni/SiO_2–Al_2O_3 (60.8%) > 5%Pt/γ-Al_2O_3

Table 3
An overview of the reactant, catalysts, preparation, characterization and reaction conditions for the SDO of soybean oil over metallic and sulphided catalysts.

Entry/Refs.	Reactant	Catalyst/preparation	Characterization	Reaction conditions
1/[144]	Refined sunflower oil (SO) Octanoic acid (OA)	Commercial 9% Mo2.5% Ni/γ-Al_2O_3 doped with (P, Si), used as reference 27% Ni/γ-Al_2O_3, w.i. Non-pyrophoric Raney nickel (NPR 27% Ni/γ-Al_2O_3) prepared by partial leaching with sodium hydroxide of an Al–Ni alloy modified with various amounts of Pb or Sn.	BET XRD TPR	FBR, 340 °C, SO/H_2 or OA/H_2/He mixtures at 21 bar. WHSV for the SO = 1, 2 and 3 h^{-1}. Hydrogen in excess (H_2/triglycerides = 140 mol/mol).
2/[145]	Soybean oil	66% Ni/SiO_2–Al_2O_3 5% Pd/γ–Al_2O_3 5% Pt/γ–Al_2O_3 5% Ru/Al_2O_3 sulphided NiMo/γ–Al_2O_3 sulfided CoMo/γ–Al_2O_3 [3.5% (CoO)/14.0% (MoO_3)] all catalysts used were commercial samples	N_2-physisorption ICP-ES AAS TEM	BR, 28.1 g of soybean oil, catalyst/oil weight ratio: 0.044 or 0.088 Temperature: 400 °C Initial H_2 pressure 92 bar. (Upon reaction the temperature was increased for 1 h up to 400 °C; then it is remained constant for 1 h),
3/[146]	Soybean oil	57.6% Ni/SiO_2–Al_2O_3 2.8% Co7.6% Mo/γ-Al_2O_3 the catalysts used were commercial samples	N_2-physisorption ICP-ES AAS TEM	BR, mass of catalyst: 2.5 g, mass of oil; 28.1 g H_2 pressure: 25–150 bar Temperature: 300–440 °C (see entry 2 for temperature rump) FBR, mass of catalyst: 20.0 g H_2 pressure: 150 bar Temperature: 400 °C LHSV = 0.5 h^{-1}, H_2/oil molar ratio of either 30.1 or 46.3.
4/[147]	Commercial tristearin (stearic acid 87.5%, palmitic acid 10.6%) in dodecane stearic acid in dodecane	20% Ni/C w.i. 5% Pd/C commercial	N_2-physisorption CO-chemisorption XRD TPR H_2-chemisorption CO_2-TPD NH_3-TPD	SBR, mass of catalyst: 0.5 g, mass of reactant: 1.75 g, mass of solvent: 25 g Reaction atmosphere: N_2, 10% H_2/N_2 or H_2 Conditions for stearic acid: temperature: 300 °C, pressure: 9.2 bar, time: 1.5 h, Conditions for tristearin: temperature: 360 °C, pressure:39.5 bar, time: 6 h
5/[148]	Palm oil Oleic acid	5CoAl 10CoAl 5NiAl 10NiAl 2PdAl 5PdAl 2PtAl 5PtAl		FBR, mass of catalyst: 2.8 g Conditions for palm oil: H_2 pressure: 50 bar, Temperature: 330 °C, LHSV: 1 h^{-1}, H_2/oil feed ratio: 1000 (Ncm^3/cm^3). Conditions for oleic acid: LHSV: 2 and 8 h^{-1}, the rest were the same with the aforementioned

(50.8%) > 5% Ru/Al_2O_3 (39.7%). With the exception of less active platinum and ruthenium catalysts the free fatty acid content obtained was lower than 8%. At a catalyst/oil weight ratio equal to 0.088 the following order was obtained 66% Ni/SiO_2–Al_2O_3 (95.9%) > sulfided NiMo/γ-Al_2O_3 (91.9%) > 5% Pd/γ-Al_2O_3 (90.9%) > sulfided CoMo/γ-Al_2O_3 (79.9%). The less active Pt and the Ru catalysts were not studied at the later catalyst/oil weight ratio. One may observe that the increase in the catalyst/oil weight ratio affects principally the performance of the monometallic nickel catalyst studied. In fact, the conversion over this catalyst was increased drastically from 60.8% to 95.9% whereas the free fatty acid content was decreased from 7.96 to 0.55 wt%.

Hydrocarbons in the diesel range (principally *n*-C_{17}, *n*-C_{18} and *n*-C_{15}) were mainly produced in almost all cases. Considerable amounts of naphtha and kero/jet oil are also produced using the sulphided CoMo/γ-Al_2O_3 catalyst (Fig. 21).

Over the nickel, palladium and ruthenium catalysts *n*-C_{17} and *n*-C_{15} alkanes were mainly produced indicating that the SDO proceeds via deCO_x. On the other hand significant amounts of *n*-C_{18} alkane are also produced over the platinum and the bimetallic catalysts studied indicating the considerable contribution of the HDO pathway in the triglyceride transformation.

The gaseous phase formed after accomplished the SDO reactions contains H_2, CO, CO_2, CH_4 and C_2–C_4 alkanes. The composition of this phase depends on the catalyst used (Fig. 22).

We may observe that the gaseous phase is rich in CH_4 over the nickel catalyst. This observation in conjunction with the very low portion of CO and the relatively low portion of hydrogen indicate that high extent methanation takes place over this catalyst under the quite high reaction temperature used. In contrast, the gaseous phase is rich in CO over the palladium catalyst. Finally, the gaseous phase formed over the bimetallic sulfided catalysts is very rich in hydrogen and shows that the use of these catalysts in SDO of oils is related with the consumption of relatively small amount of hydrogen compared to the monometallic catalysts tested. The above are in line with the findings reported from the same group concerning the influence of the catalyst on the SDO pathways mentioned before (Fig. 17).

From the above study one may conclude that the nickel monometallic and the sulphided NiMo and CoMo bimetallic catalysts are presumably proved to be the most promising catalytic formulations for the industrial SDO of the soybean oil for producing liquid hydrocarbons; the nickel catalyst due to its low cost and high catalytic performance and the sulphided catalysts due the relatively small consumption of hydrogen. The main weakness of this

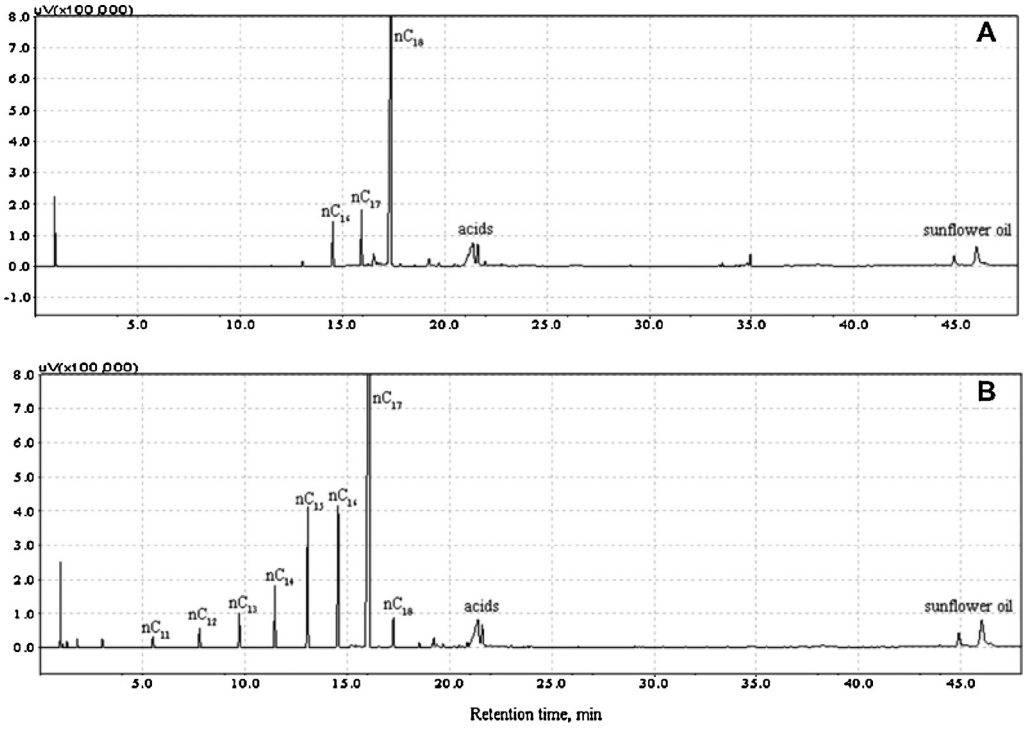

Fig. 20. The chromatograms for the products obtained from the SDO of sunflower oil over 9Mo 2.5Ni/Al_2O_3 (P, Si) (A) and NPR 27%Ni/γ-Al_2O_3 (B) catalysts. Source: Ref. [144].

nickel catalyst is the consumption of quite large amounts of hydrogen in methanation reactions taking place in the gaseous phase upon the SDO of triglycerides.

In view of the above the group of Kim selected two promising formulations (57.6 wt% Ni/SiO_2–Al_2O_3 and CoMo/Al_2O_3 with 2.8 wt% of Co and 7.6 wt% of Mo) and studied the effect of reaction conditions on the hydrotreatment of soybean oil [146] (Table 3, entry 3). The first catalyst is used in its reduced form whereas the second one in its sulphided form. Taking into account the subject of the present review we limit ourselves to the presentation of the main findings concerning the influence of the reaction conditions for the nickel metallic catalyst.

The reactions were carried out in a batch reactor at wide ranges of reaction temperatures and hydrogen pressures (300–440 °C, and of 25–150 bar) and in a flow reactor at 400 °C and 150 bar. The effects of reaction parameters on oil conversion, gasoline/jet/diesel selectivity and the degree of oxygen removal have been investigated to optimize the hydrotreatment conditions. HDO, deCO and $deCO_2$ occurred competitively. As expected from the thermodynamics, each process pathway is related to different optimal conditions.

The batch reactor experiments showed that both oil conversion and diesel yield increased with increasing reaction temperature, exhibiting maximum values at 400 °C, most likely because the endothermic deCO and $deCO_2$ reactions were the dominant reaction pathways for the SDO of triglycerides. The gasoline and the jet yields are negligible compared to that obtained for diesel in this region (300–400 °C). Further Increase in the temperature up to 440 °C causes a slight decrease in the oil conversion, attributed to the inverse water gas-shift reaction which needs hydrogen, and a considerable increase in the gasoline and the jet fractions in the products at expense of the diesel fraction, presumably due to the enhancement of cracking. Very high values in the range 0.93–0.96 were obtained for the ratio n-C_{17}/(n-C_{17} + n-C_{18}) suggesting SDO mainly via $deCO_x$. Increase in the hydrogen pressure in the range 2.5–120 bar, at 400 °C, showed increase in the yields of liquid n-paraffins, mainly those of n-C_{17} and n-C_{18}.

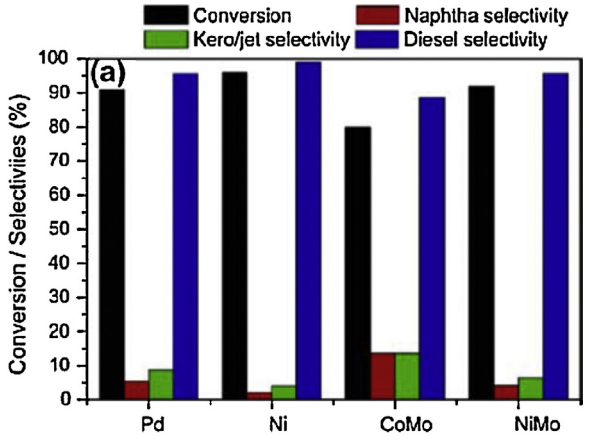

Fig. 21. Conversion and selectivities to various oil fractions obtained over the most active of the catalysts studied in a catalyst/oil weight ratio equal to 0.088, reaction temperature: 400 °C, initial H_2 pressure: 92 bar. Source: Ref. [145].

Under the batch reactor conditions the product gas phase was rich in methane, indicating remarkable methanation. A decrease in CH_4 content with increasing reaction temperature was attributed to the exothermic formation of CH_4 from CO and H_2.

The flow reactor experiments showed considerable gasoline and jet yields fractions in the liquid products and a very high fraction of methane in the gaseous phase.

The above study revealed that concerning the nickel metallic catalyst a temperature at about 400 °C and a relatively high pressure in the range of 120 bar are the optimum reaction conditions for transforming soybean oil into n-C_{17} alkane.

The comparison between the nickel and palladium metallic catalysts mentioned before (Figs. 21 and 22) concerned catalysts supported on oxidic supports. Santillan-Jimenez et al. [147] attempted a similar comparison for catalysts supported on carbon (Table 3, entry 4). Specifically, they studied the catalytic SDO of commercial tristearin and stearic acid over a carbon supported

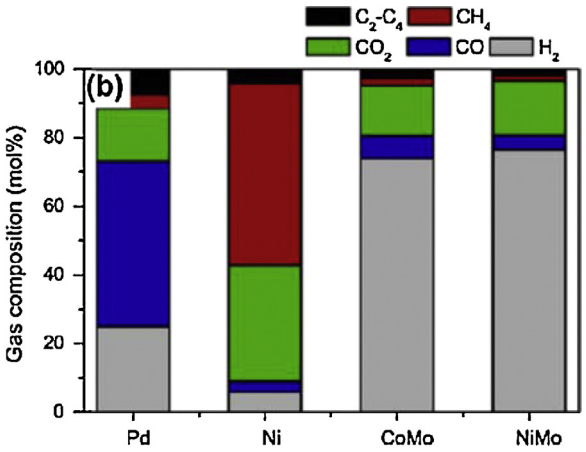

Fig. 22. Composition of the gaseous phase obtained over the most active of the catalysts studied in a catalyst/oil weight ratio equal to 0.088, reaction temperature: 400 °C, initial H_2 pressure: 92 bar. Source: Ref. [145].

nickel catalyst (20 wt% Ni/C) and compared its catalytic behavior with that of the more expensive 5 wt% Pd/C commercial catalyst.

The catalytic experiments were performed in a semi-batch reactor. It was found that both catalysts provided quite good yields of fuel-like hydrocarbons. The conversion and selectivity values obtained depend on the gas atmosphere (N_2, 10% H_2/N_2 or H_2). While the presence of hydrogen resulted in improved catalytic performance, the optimum hydrogen partial pressure was found to depend on the catalyst used. Higher conversion values and selectivity to C_{17} were obtained over the palladium catalyst, though the differences in the conversion of tristearin, if any, are very small. The nickel catalyst provided lighter products in the C_{10}–C_{17} range than the 5 wt% Pd/C one. It was attributed to observation that the nickel catalyst was more acidic both in terms of the strength and the amount of its acid sites. This relatively high acidity is suggested to decrease both the conversion and the selectivity to long chain hydrocarbons because it favors respectively the strong adsorption of carbonaceous species on the catalyst surface and the cracking reactions. Finally, it was confirmed once again that SDO proceeds through deCO$_x$ over the nickel and palladium catalysts. The authors concluded that the inexpensive Ni/C represents an interesting alternative to costly Pd-based formulations as a catalyst for the conversion of fatty acids and triglycerides to drop-in hydrocarbon fuels. In this case the affordance for lighter products in the C_{10}–C_{17} range could be exploited for fuel blending purposes.

Recently Srifa et al. [148] (Table 3, entry 5) published an interesting work in which a direct comparison of catalytic performance of four γ-Al_2O_3-supported monometallic catalysts (Co, Ni, Pd, and Pt) concerning the deoxygenation of palm oil to green diesel has been attempted. The catalysts with metal loadings of 2, 5, and 10 wt% were labeled as 5CoAl, 10CoAl, 5NiAl, 10NiAl, 2PdAl, 5PdAl, 2PtAl, and 5PtAl, where the prefix numbers represent the %metal loadings. They were prepared by the incipient wetness impregnation method and were characterized using various techniques.

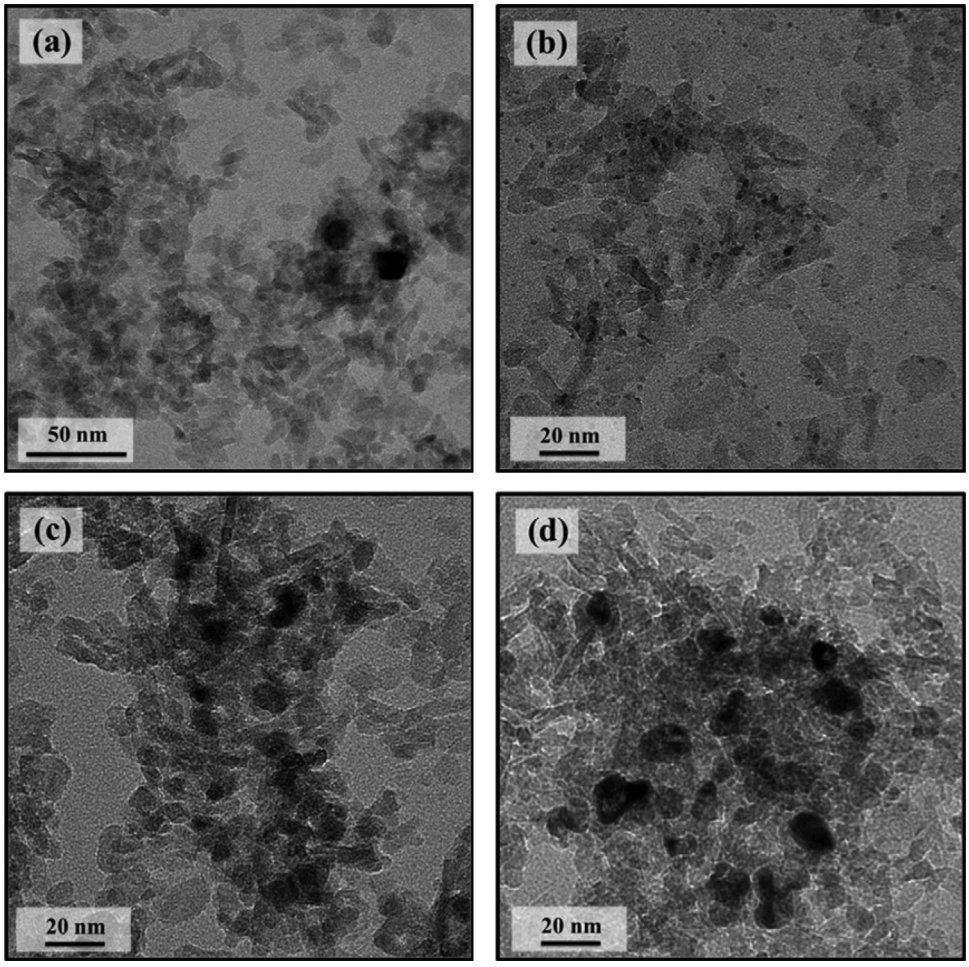

Fig. 23. TEM images of the reduced (a) 5CoAl, (b) 5PtAl, (c) 5NiAl, and (d) 5PdAl catalysts. Source: Ref. [148].

The characterization results revealed that reduced catalysts in H_2 exhibit different metal particle sizes and metal dispersions on γ-Al_2O_3. This is evident in Fig. 23 where TEM images of reduced catalysts with 5% metal loading are presented. Inspection of this figure shows that the average metal particle size follows the order Co > Pd > Ni > Pt. In fact, it seems that the Pt catalysts exhibited the highest metal dispersion.

The catalytic performance of the aforementioned catalysts for the deoxygenation of palm oil was investigated in a continuous-flow trickle-bed reactor. These experiments realized over pure γ-Al_2O_3 resulted in 56% conversion of triglyceride into free fatty acids and propane without green diesel production. It should be concluded that γ-Al_2O_3 possessed no catalytic activity in the deoxygenation of triglycerides.

Green diesel production was achieved when the reaction was catalyzed by the metal catalysts, confirming the deoxygenation activity of the metal species. As demonstrated in Fig. 24a, complete conversion of triglycerides was achieved over the 5NiAl, 10NiAl, 5CoAl, 10CoAl, 5PdAl, and 5PtAl catalysts, whereas it reached approximately 95% over the 2PdAl and 2PtAl catalysts. The higher metal loading in the Ni, Pd, and Pt catalysts resulted to higher product yields. Nonetheless, the increase in the Co loading from 5 to 10 wt% did not significantly affect the product yield and triglyceride conversion. By comparing the catalysts at the same metal loading, the deoxygenation activity in terms of product yield decreased in the order of 5CoAl (88.5%) > 5PdAl (85.2%) > 5PtAl (79.5%) > 5NiAl (69.7%), whereas the turnover frequency (TOF) increased with increments of the metal particle size.

As represented in Fig. 24b, deCO_x is the dominant reaction pathway over Ni, Pd, and Pt catalysts. In fact, the liquid product is mainly composed from the n-C_{15} and n-C_{17} alkanes. These results are in line with previous studies showing that deCO_x was favored over HDO in the aforementioned catalysts [76,107,117,145–147,149–152]. On the contrary, both deCO_x (35.4–37.8%) and HDO (45.5–52.3%) are important reaction pathways over the Co catalyst. In this case the liquid product was mainly composed from the n-C_{15}, n-C_{16}, n-C_{17}, and n-C_{18} alkanes. A small amount of hydrocarbons in the range n-C_8 to n-C_{14} was also observed in the products over the Ni and Co catalysts indicating a non negligible cracking activity. The effects of monometallic catalysts on the gas product composition are represented in Fig. 24c. The most important observation is the high extent methanation over the Ni and Co catalysts as it compared to that over the Pd and Pt catalysts.

Closing this section one can stress that the direct comparison of commercial nickel metallic catalysts with other metallic (Pd, Pt and Ru) or sulphided catalysts (NiMo, CoMo) supported on similar supports reveals that the Ni, Pd, CoMo and NiMo catalysts are very active and selective for SDO of vegetable oils but this is not the case for the Pt and Ru catalysts. The Ni monometallic and the sulphided NiMo and CoMo bimetallic catalysts are presumably most promising; the nickel catalyst due to its low cost and high catalytic performance and the sulphided catalysts due the relatively small consumption of hydrogen. A temperature at about 400 °C and a relatively high pressure in the range 25–120 bar are the optimum reaction conditions for the nickel catalyst. The main weakness of this catalyst is the consumption of quite large amounts of hydrogen in methanation reactions taking place in the gaseous phase upon SDO of triglycerides. The Raney nickel catalyst though active is related to extending cracking of the hydrocarbon chains. The direct comparison of nickel and palladium catalysts supported on active carbon showed similar values for the conversion of tristearin which indicates that the inexpensive nickel catalyst represents an interesting alternative to costly Pd-based formulations for the conversion of triglycerides into hydrocarbons, though the nickel catalyst provides lighter products in the C_{10}–C_{17} range than the palladium catalyst. Further contribution to this subject would involve the comparison of the optimum nickel catalyst to the other types of catalysts. This requires more effort for optimizing nickel loading, kind of the support, preparation, and activation method/conditions.

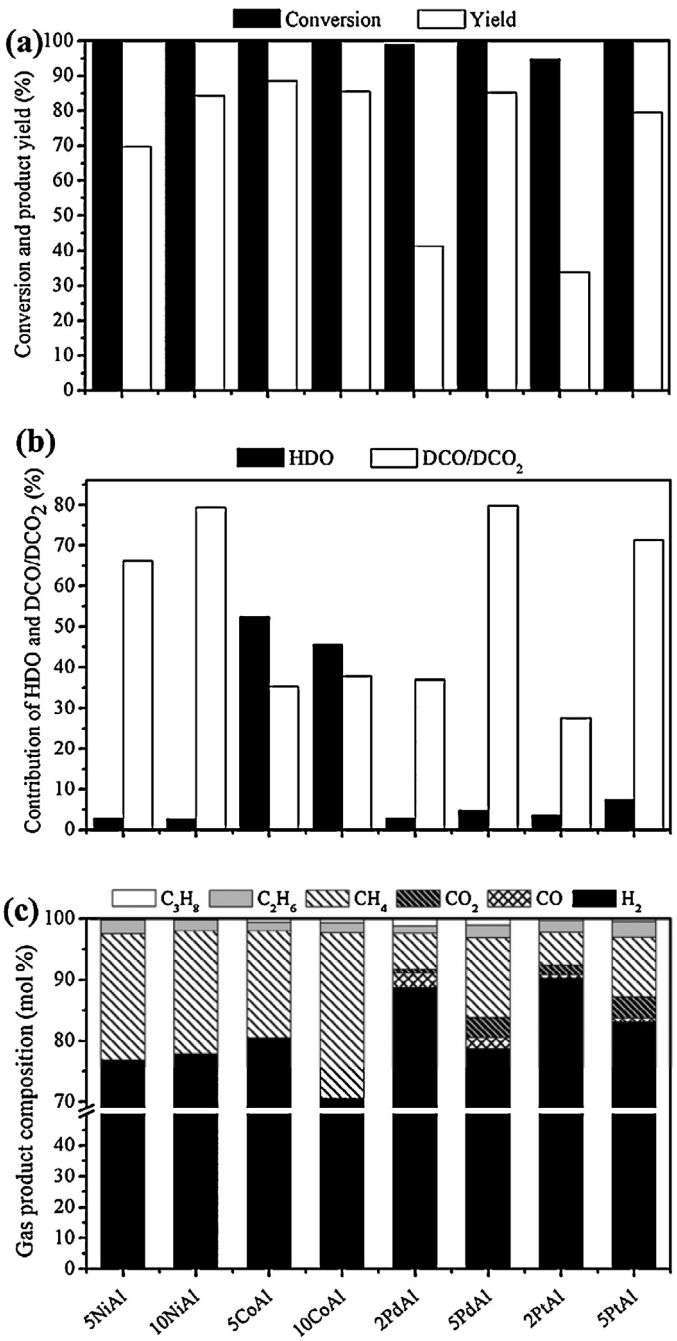

Fig. 24. Catalytic performance of the Co, Ni, Pd, and Pt monometallic catalysts with different metal loadings upon SDO of palm oil: (a) conversion and green diesel yield, (b) % contribution of HDO and deCO_x, and (c) gas product composition. All experiments were performed in a FBR at a temperature: 330 °C, H_2 pressure: 50 bar, LHSV: 1 h^{-1}, and H_2/oil ratio: 1000 (Ncm^3/cm^3). Source: Ref. [148].

3.6. Development of nickel phosphide catalysts

In the previous sections we reviewed works dealing with nickel supported catalysts in their reduced state. The main disadvantage of these catalysts is their high methanation activity. Taking into

Table 4
An overview of the reactant, catalysts, preparation, characterization and reaction conditions for the SDO of methyl oleate and methyl laurate over nickel phosphide catalysts.

Entry/Refs.	Reactant	Catalyst/preparation	Characterization	Reaction conditions
1/[168]	Methyl oleate in heptane	HT-Ni_2P unsupported Ni_2P, prepared by nanocasting using SBA-15 as hard template Ni_2P conventional unsupported sample Ni_2P/SBA-15 supported sample, prepared by wet impregnation	N_2-sorption XRD H_2-TPR TEM	FBR, mass of catalyst: 90 mg (40–60 mesh mixed with silicon carbide) Reaction conditions: 30 bar of H_2, 340 °C, hydrogen flow rate: 30 mL min^{-1}, organic phase flow rate: 6 mL min^{-1}(s.v: 45.3 h^{-1}), total ester content in the solution feeding: 10%.
2/[169]	Methyl oleate in heptane	Ni_2P/SBA-15 (18.8%wt Ni). Wet co-impregnation for depositing Ni and P phases. Ni/SBA-15 (19.6%wt Ni). Wet impregnation for depositing the Ni phase. Laboratory prepared SBA-15. A H_2-TPR procedure was followed for transforming the oxidic precursors into the final catalysts.	ICP-AES N_2-sorption XRD TEM	FBR, mass of catalyst: 200 mg blended with silicon carbide. Various hydrogen pressures (3–40 bar) and temperatures (250–340 °C). H_2 flow rate: 30mL/min. Organic phase flow rate: 6 mL/h (WHSV = 20.4 h^{-1}). For some experiments, the WHSV was increased up to 81.6 h^{-1}. Total ester content in the solution feeding: 10%.
3/[170]	Methyl laurate	12%wt Ni: (Ni_2P/SBA-15 Ni_2P/MCM-41 Ni_2P/SiO_2–H Ni_2P/SiO_2-L s-Ni_2P/SiO_2) Ni/SiO_2-H (15%wt Ni) Pd/SiO_2-H (5%wt Pd) H,L: high, low SSA of SiO_2 Dry co-impregnation for depositing Ni and P phases on commercial supports followed by H_2-TPR to obtain nickel phosphides. s-Ni/SiO_2 was obtained by sol-gel, then impregnated with P and transformed to the s-Ni_2P/SiO_2 by H_2-TPR.	ICP–AES XRD TEM N_2-sorption CO chemisorption NH_3-TPD H_2-TPR H_2-TPD	FBR, mass of catalyst: 0.4 g blended with 3.2 g quartz sand. 300–340 °C, 20 bar of H_2 WHSV of methyl laurate: 10 h^{-1} H_2/ methyl laurate ratio = 50
4/[171]	Methyl laurate	Ni_2P/SiO_2 Ni_3P–$Ni_{12}P_5$/Al_2O_3 Ni_2P/TiO_2 Ni_2P/SAPO-11 Ni_2P–$Ni_{12}P_5$/HY Ni_2P/CeO_2 Nickel content = 15%wt. Dry co-impregnation for depositing Ni and P phases on commercial supports (CeO_2 was lab made) followed by H_2-TPR to obtain nickel phosphides.	N_2-sorption XRD CO chemisorption XPS NH_3-TPD H_2-TPR	FBR, mass of catalyst: 0.4 g blended with 3.2 g quartz sand. 300–340 °C, 20 bar of H_2 WHSV of methyl laurate: 10 h^{-1} H_2/methyl laurate ratio: 50.
5/[176]	Methyl laurate	Ni_2P/SAPO-11 Ni/SAPO-11 Nickel content = 3%wt. Preparation as in entry 4	N_2-sorption TGA XRD TEM SEM Raman	FBR, mass of catalyst: 0.4 g blended with 3.2 g quartz sand. 320–380 °C, 10–50 bar of H_2 WHSV of methyl laurate: 2–8 h^{-1} H_2/methyl laurate ratio: 25.
6/[177]	Methyl laurate, lauric acid, dodecanal, dodecanol	Metal content 15%: (Ni_3P–Ni/SiO_2 Ni_3P–$Ni_{12}P_5$/SiO_2 $Ni_{12}P_5$/SiO_2 Ni_2P/SiO_2 Ni_2P(1:2)/SiO_2 CoP–Co_2P/SiO_2 Fe_2P–FeP/SiO_2 MoP/SiO_2 WP/SiO_2) Preparation as in entry 4 Ni/SiO_2, MoO_2/$SiO_2$and PO_x/SiO_2 were prepared by i.w.i. for comparison	N_2-sorption H_2-TPR NH_3-TPD CO chemisorption H_2 chemisorption H_2-TPD XRD XPS DRIFTS/pyridine	FBR, 300 °C, 20 bar of H_2 WHSV: 5.2 h^{-1} H_2/methyl laurate ratio: 25.
7/[178]	Soybean oil	Ni_2P/silica Ni_2P/HY Ni_2P content: ~25% Preparation as in entry 4	N_2-sorption H_2-TPR NH_3-TPD XRD FTIR	FBR, 340–370 °C, 30 bar, LHSV = 1 h^{-1}, H_2 flow rate: 300 N mL/min.

account the above, the idea to test other nickel supported phases seems to be plausible. In this context, significant contributions have been reported very recently which concern nickel phosphide catalysts supported on various carriers.

The driving force for the development of nickel phosphide catalysts for the SDO of triglycerides is that the transition metal—phosphide catalysts had been proved quite promising in many hydroprocessing reactions. The hydrodesul-

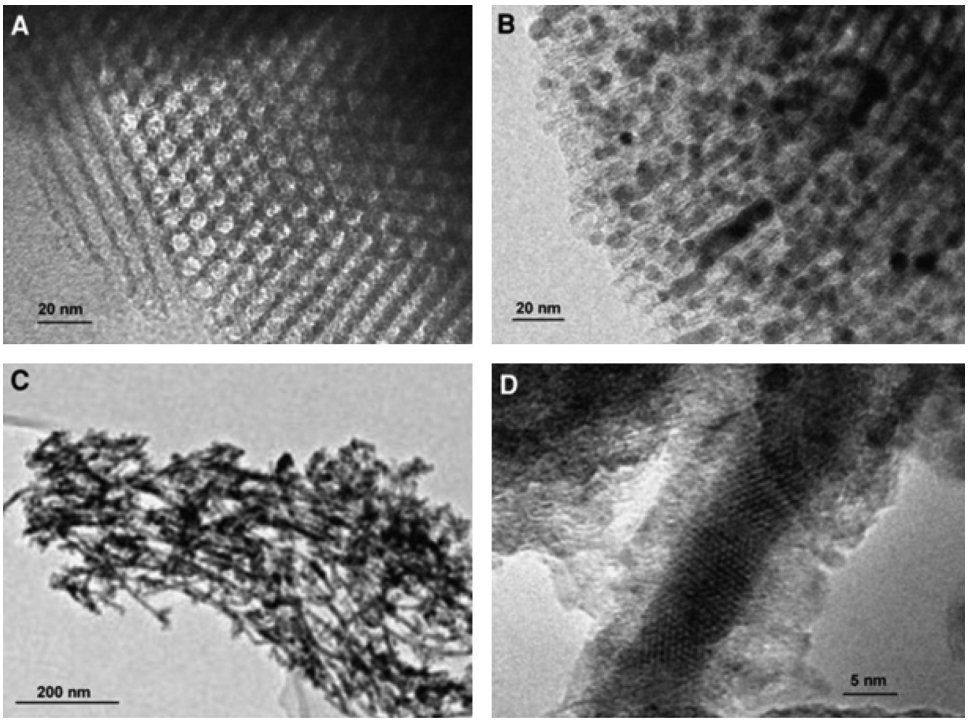

Fig. 25. TEM images of the SBA-15 (A), the Ni_2P/SBA15(B) supported sample and the Ni_2P nanorods (HT-Ni_2P sample, C and D). Source: Ref. [168].

phurization/hydrodenitrification [153,154], hydrodechlorination [155,156], synthesis gas conversion [157,158], hydrazine decomposition [159] and water gas-shift reaction [160] should be mentioned. Moreover, it has been reported that the metal—phosphide catalysts may catalyze the removal of oxygen from molecules present in bio-oils [161–164]. Their special catalytic property has been attributed to the ensemble and/or ligand effects of phosphorus [165–167]. Two groups have reported on the catalytic behavior of nickel phosphide catalysts with respect the SDO of methyl oleate, methyl laurate and lauric acid, used as model compounds, and soybean oil as well.

The first group (Yang et al. [168]) synthesized nickel phosphide nanorods by nanocasting, using SBA-15 as a hard template (HT-Ni_2P) and tested in the SDO of methyl oleate (Table 4, entry 1). The wet impregnation of the template with an aqueous solution of nickel nitrate and ammonium phosphate was followed by drying, calcination and temperature-programmed reduction. After reduction of the phosphate precursor infiltrated within the pore walls of SBA-15, the matrix was removed with diluted HF and the unsupported material was obtained. Fig. 25 illustrates the TEM images of the SBA-15, the Ni_2P/SBA-15 supported sample and the HT-Ni_2P sample.

The pore channel of the SBA-15 dictated an elongated morphology in the HT-Ni_2P sample. In fact, TEM shows that the catalyst is mainly constituted by agglomerates of nanorods and the only crystalline phase revealed by XRD was Ni_2P. The HT-Ni_2P nanostructured sample exhibited a significantly higher surface area ($135\ m^2\ g^{-1}$) than the reference sample synthesized in the absence of template (Ni_2P, $1\ m^2\ g^{-1}$).

The activity of the samples were studied in a fixed-bed lab scale reactor operated at 30 bar and 340 °C, with a feedstock containing methyl oleate reagent (70% in methyl oleate) in heptane (total ester content: 10 wt%). A fourfold enhancement in the conversion of methyl oleate was obtained over the nano-structured sample with respect to the conventionally synthesized sample in absence of hard template, but it does not exceed that obtained over the Ni_2P/SBA-15 composite sample ($206\ m^2\ g^{-1}$). Nevertheless, when these data are normalized to surface area, the activity of the nano-structured sample is significantly lower than that of the conventional. The main product of the reaction over the nano-structured sample is n-heptadecane indicating high $deCO_x$ activity. However, a significant amount of n-octadecane is also produced. Different selectivity was obtained in the conventional sample (production of approximately equal amounts of *n*-heptadecane and *n*-octadecane).

In the second paper of the group, Yang et al. [169] attempted to compare directly the activity and selectivity of a phosphide nickel catalyst with a metallic one (Table 4, entry 2). Specifically, they studied the SDO of methyl oleate ($C_{17}H_{33}$—COO—CH_3) over one nickel metallic and one nickel phosphide catalyst supported on SBA-15; the latter had been proved to be very active in the previous study [168]. The mesostructured support was prepared following the standard methodology and using TEOS and Pluronic 123 as silica source and structure directing agent, respectively. The SBA-15 supported nickel phosphide catalyst [Ni_2P/SBA-15(Ni: 18.8%wt)] was prepared by wet impregnation of aqueous solutions of nickel nitrate and ammonium phosphate in a Ni/P molar ratio of 1:1 followed by drying, calcination and temperature-programmed reduction in hydrogen. A similar procedure was followed for the preparation of the SBA-15 supported nickel metallic catalyst [Ni/SBA-15 (Ni: 19.6%wt)]. The catalysts were characterized using various methods and evaluated at a various temperatures and pressures using a fixed bed reactor.

It was found that the Ni_2P particles with an average diameter of 7 nm are well-dispersed within the mesopores of SBA-15. In addition, a much lower proportion of larger Ni_2P particles (at about 25 nm) is formed outside of SBA-15 channels (Fig. 26).

In contrast, the nickel metallic sample revealed the formation of larger Ni metallic particles over the SBA-15 external surface. These particles present a rather wide size distribution (25–60 nm) and a more irregular morphology as compared to the Ni_2P nanocrystals (Fig. 27).

Both catalysts achieve more than 80% ester conversion at $20\ h^{-1}$ WHSV in the whole range of pressures studied and for temperatures higher than 290 °C. For example, nearly complete conversion

achieved over both catalysts at temperature higher than 290 °C and pressure equal to 30 bar. However, Ni/SBA-15 is slightly more active than Ni_2P/SBA in the whole range of temperatures, pressures and space velocities.

The analysis in the gas phase revealed the formation of methane and minor amounts of CO and CO_2 suggesting that methanation of CO and CO_2 is significant under these operation conditions.

In the liquid phase, linear paraffins in the C_{15}–C_{18} range are the main products detected from a feedstock composed mainly of C_{18} (80%) and C_{16} (9%) fatty acids. In the most of the reaction conditions studied the ratio $C_{18}/(C_{17}+C_{18})$ is lower than 0.5 indicating once again that nickel favors $deCO_x$ with respect to HDO. The increase of pressure and the decrease of temperature and space velocity cause an increase of this ratio. More importantly, it was found that the n-C_{18}/n-C_{17} ratio was remarkably higher for Ni_2P/SBA-15 than for Ni/SBA-15 catalysts under all the assayed conditions. For example, this ratio takes the value of 0.55 and 0.03 over the Ni_2P/SBA-15 and Ni/SBA-15 catalyst, respectively, at 250 °C and 30 bar. Another very important difference between the catalysts studied concerns the cracking activity which is significantly higher in the Ni/SBA-15 catalyst, mainly at relatively high temperatures. An example is illustrated in Fig. 28.

Taking into account that the extensive cracking is actually undesirable and that HDO favors carbon atom economy, the authors concluded that the Ni_2P/SBA-15 is superior with respect to the Ni/SBA-15 catalyst and very promising for the production of green diesel.

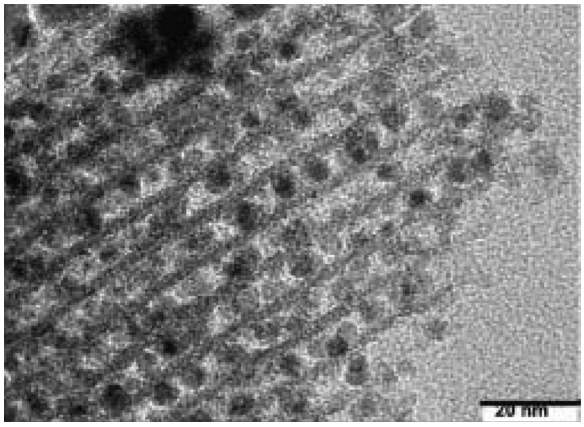

Fig. 26. TEM image of the sample Ni_2P/SBA-15. The black spots on the image denote the Ni_2P supported particles. Source: Ref. [169].

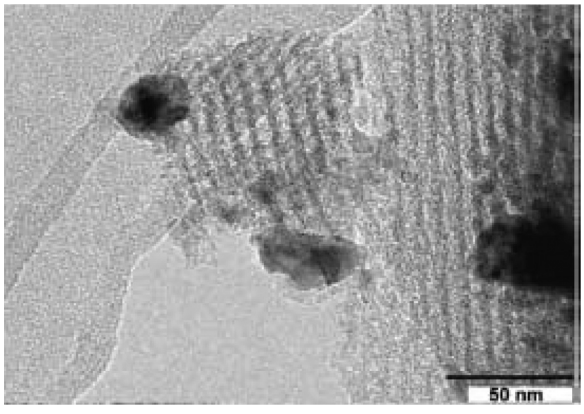

Fig. 27. TEM image of the sample Ni/SBA-15. The black spots on the image denote the nickel supported particles. Source: Ref. [169].

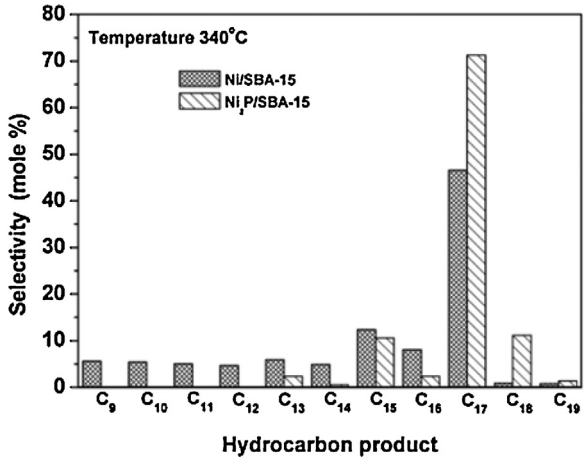

Fig. 28. Hydrocarbon product distribution over Ni_2P/SBA-15 and Ni/SBA-15 catalysts. Reaction conditions: 340 °C; 30 bar; WHSV = 20.4 h^{-1}; H_2/feedstock ratio = 300 N m^3 m^{-3}; time on-stream = 6 h. Source: Ref. [169].

The second group {Chen group} studied the SDO of methyl laurate over nickel phosphide catalysts also supported on ordered and non-ordered mesoporous silica [170]. The samples studied, their preparation method and the characterization techniques used are illustrated in Table 4, entry 3. In all cases the catalysts prepared have exposed very small Ni_2P supported crystallites with mean (XRD) values ranging between 3 and 12 nm and surplus P species non-associated with nickel.

Although the initial Ni/P molar ratio was adjusted to be equal to 1, this ratio is larger in the final catalysts (ranging from 1/0.76–1/0.58) due to partial elimination of phosphorous in the form of P_xH_y upon the hydrogenation of the samples. The formation of the supported crystallites is related to the significant decrease of the BET specific surface area initially exposed by the carriers. This is ranged from 411 to 163 m^2 g^{-1} in the final catalysts. The decrease in the specific surface area was attributed to the blockage/wall collapse of the pores which in the case of the Ni_2P/MCM-41 destroyed completely its ordered hexagonal pore structure. This is not the case for the Ni_2P/ SBA-15, in agreement with the findings of Yang et al. [169] mentioned above (Fig. 26).

For the Ni_2P supported catalysts studied, CO and CH_4 were found in the gaseous products. We note the absence of CO_2 in the gaseous products, in disagreement to the results of Yang et al. [169] mentioned just before. This difference could be related to different model compound used. The detected liquid products include n-C_{11} and n-C_{12} alkanes, oxygenated intermediates (lauryl alcohol, lauraldehyde, lauric acid, and lauryl laurate), methanol, and cracked hydrocarbons. In addition, there was some light yellow insoluble substance in the liquid at low conversion. Presumably these are polymers with high boiling points not detectable by GC. The reaction mechanism on the most active s-Ni_2P/SiO_2 sample was kinetically investigated. The following scheme (Fig. 29) seems to explain the most important results.

According to this scheme the production of the lauric acid, the most important intermediate, mainly occurs by hydrogenolysis (a) and/or hydrolysis (b) of the reactant while the lauraldehyde can be produced via reduction of the lauric acid and /or direct hydrogenolysis of the methyl laurate (c). The production of the $C_{11}H_{24}$, which is the main product, takes place through the pathway assumed over the nickel metallic catalysts {methyl laurate → laurate acid → lauraldehyde → $[C_{11}H_{22}]$ → n-$C_{11}H_{24}$} and/or directly (d). This is also the case for the production of the n-$C_{12}H_{26}$ {methyl laurate → laurate acid → lauraldehyde → lauryl alcohol → $C_{12}H_{24}$ → n-$C_{12}H_{26}$}. Because the ratio n-$C_{11}H_{24}/n$-$C_{12}H_{26}$ is always greater than 1 and CO_2 was not detected in the

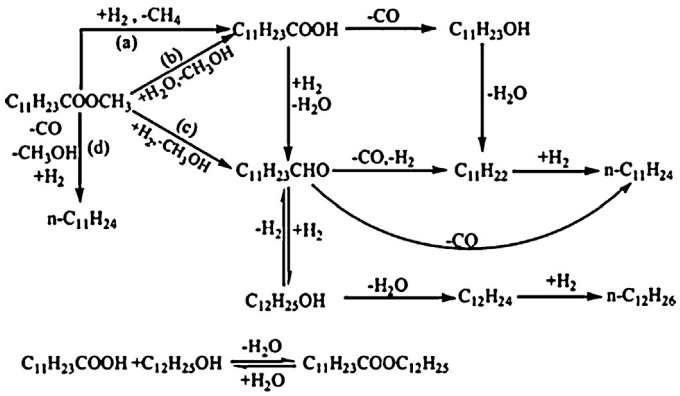

Fig. 29. Proposed reaction pathways of methyl laurate on the s-Ni_2P/SiO_2 sample. Source: Ref. [170].

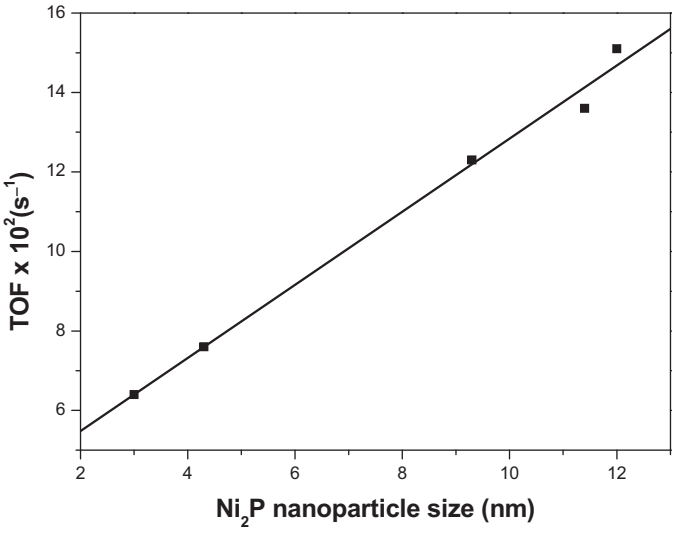

Fig. 30. Linear increase of TOF calculated at 300 °C with the particle size of N_2P determined from TEM images (the values have been taken from Table 1 of Ref. [170]).

product, the deCO route seems to take place in larger extent than the HDO route. In fact, this ratio is between 2.4 and 4.0 at 300 °C. However, this ratio is much smaller than that obtained over the Ni/SiO_2–H (23.7) and Pd/ SiO_2–H (10.8) at the same temperature. This corroborates previous studies mentioned above [169] that the supported nickel phosphides inhibit (favor) $deCO_x$ (HDO) with respect to the metallic catalysts. Finally, the intermediate laurate acid and lauryl alcohol may react to produce the corresponding ester. It is reasonable to assume that lauryl laurate was deoxygenated via a similar mechanism to methyl laurate.

Comparing the proposed mechanism to those proposed over the nickel metallic catalysts (Section 3.3) we observe that the former includes several additional steps (b, c and d as well as the direct production of the lauryl alcohol from the laurate acid and the transformation of the lauraldehyde into $C_{11}H_{22}$). We note that the steps b and c are postulated to take into account the presence of methyl alcohol in the products. The absence of the CO_2 in the products and the very low activity of the catalyst studied for the hydrogenation of CO_2 even at 340 °C indicates that $deCO_2$ does not takes place and this points out another important difference with respect to nickel metallic catalysts.

The activity of the catalysts studied depends on three main factors: the intrinsic activity, the dispersion of the supported nickel, estimated by the CO sorption, and the acidity of the catalysts. The intrinsic activity is well correlated to the size of the supported Ni_2P crystallites. In fact, as it can be seen from Fig. 30, the TOF determined increased linearly with this size. The stronger interaction between Ni and P may account for the lower TOF on smaller Ni_2P crystallites. In contrast, the Ni sites having less interaction with P are more active concerning the main deCO route. This route is also favored by the increase of the Bronsted acidity due to the P–OH groups. The combination of the aforementioned factors provided the following activity order at 300 °C for the catalysts studied: s-Ni_2P/SiO_2 > Ni_2P/SiO_2–H > Ni_2P/SiO_2–L > Ni_2P/SBA-15 > Ni_2P/MCM-41. In agreement to those mentioned for the nickel metallic catalysts an increasing reaction temperature, causes increase in the conversion, the selectivity to n-C_{11} and n-C_{12} and in the n-C_{11}/n-C_{12} ratio. Moreover, in comparison to the nickel catalyst supported on silica, the nickel phosphide catalysts studied exhibited lower activities for methanation and cracking reaction because of the electronic and geometrical effects of phosphorous. This behavior is similar to that of the palladium supported on silica bringing about a decrease in the hydrogen consumption and increase in the SDO product yield. Finally, considering the cost of the catalyst and the aforementioned activity order it seems that silica is a quite suitable support for the phosphide catalysts.

Chen group [171] continued its work by studying the SDO of methyl laurate over nickel phosphide catalysts supported on various supports, among which the silica with the high surface area used in the previous paper [170]. The initial Ni/P molar ratio is equal to 1.0 in all precursors. The supported solid phases indentified by XRD are illustrated in Table 4, entry 4. For comparison nickel and phosphorus catalysts supported on silica and bulk unsupported nickel phosphate were also synthesized. The samples studied, their preparation method, the characterization techniques used and the evaluation conditions for determining the percentage conversion of methyl laurate and the percentage selectivity for each product are illustrated in Table 4, entry 4.

It was found that the main products obtained are n-C_{11} and n-C_{12} alkanes. With the exception of Ni_2P/CeO_2, the selectivity to minor products [dodecene, undecene, isododecane, isoundecane and cracked hydrocarbons (n-C_6–n-C_{10})] was lower than 1%. Moreover, oxygenated intermediates (lauryl alcohol, lauraldehyde, lauric acid and lauryl laurate), methanol, heavy compounds, CO and CH_4 and traces of the C_2–C_4 hydrocarbons were also detected. Taking into account the aforementioned products and the relevant literature [114,170,172] they arrived at a SDO scheme identical with that proposed in the first study of the group (Fig. 29).

At every temperature, Ni_2P/SiO_2 provided the highest conversion and the Ni_3P–$Ni_{12}P_5/Al_2O_3$ took the second place. The following order was obtained at 340 °C: Ni_2P/SiO_2 > Ni_3P–$Ni_{12}P_5/Al_2O_3$ > Ni_2P/TiO_2 > Ni_2P/SAPO-11 > Ni_2P–$Ni_{12}P_5$/HY > Ni_2P/CeO_2. The total percentage selectivity for C_{11} and C_{12} hydrocarbons exhibited a very similar trend. The activity and the aforementioned total selectivity per gram of the catalyst studied were correlated with the nickel sites surface density estimated by the CO uptake.

However, although Ni_2P/CeO_2 exhibited larger CO uptake than Ni_2P/TiO_2 and Ni_2P/SAPO-11, it exhibited lower conversion. Therefore, the activity per Ni site expressed by the turnover frequency of methyl laurate is another important factor. The following trend was obtained for the TOF values: Ni_2P/SAPO-11 > Ni_2P/TiO_2 > Ni_3P-$Ni_{12}P5/Al_2O_3$ > Ni_2P/CeO_2 > Ni_2P/SiO_2. It is remarkable that Ni_2P/SiO_2 had the lowest TOF though it exhibited the highest conversion. This was correlated to the weak support effects due to the low acidity and reducibility of the silica with respect to other supports, for example to titania and SAPO-11. In fact, the relatively high acidity and reducibility of the support seems to favor the manifestation of a synergy between the nickel site and the acid sites or oxygen vacancies. Bronsted or Lewis acid sites can convert carboxylic ester to carboxylic acid via hydrolysis

or hydrogenolysis while the oxygen vacancies may activate ester group via oxygen adsorption [95,173,174]. Moreover, the oxygen vacancy and the acid site could catalyze the hydrodeoxygenation and decarbonylation to produce hydrocarbons. Although the above sites exhibit very low activity, they would cooperate with the Ni sites. Thus, the C=O group activated by the oxygen vacancy of titania surface may interact with hydrogen adsorbed on nickel site. On Ni_2P/SAPO-11, the Bronsted acid site can provide hydrogen species to attack the C=O group adsorbed on the Ni site. The electron density of nickel and the Ni_2P crystallite size seem also to affect the catalytic activity.

An important observation is that the total selectivity to cracked products was lower than that determined over the metallic nickel catalysts supported on silica. The relatively low activity for cracking of nickel phosphide catalysts was ascribed to the ligand (electronic) and ensemble (geometrical) effects of P [175]. These results are in full agreement to those obtained by the same group [170] and by Yang et al. [169] presented before. The only exception is the Ni_2P/CeO_2 catalyst. The higher cracking activity of this catalyst was mainly attributed to its higher electron density of Ni sites.

Moreover, comparison of the catalytic activity and total selectivity to C_{11} and C_{12} hydrocarbons obtained over the most active nickel phosphide catalyst (Ni_2P/SiO_2) with the corresponding metallic nickel catalyst (Ni/SiO_2) does not indicate different behavior. In contrast, the transition from the nickel metallic crystallites to the supported Ni_2P ones affects considerably the selectivity between the deCO and HDO pathways expressed by the C_{11}/C_{12} molar ratio, indicating that the nickel phosphide catalysts are less active with respect to deCO. It was mainly attributed to the P electronic effect which leads to the electron deficiency of Ni via the electron transfer from Ni to P and to geometrical effect which alter the Ni–Ni distance. The higher electrophilicity of deficient Ni site is more favorable for the adsorption and activation of oxygen of C=O bond in ester group, favoring HDO. The electronic density of the supported nickel phosphide depends on the support and the kind of the nickel phosphide formed. Taken into account the above the authors were able to explain the following order for the C_{11}/C_{12} molar ratio obtained at all temperature studied: $Ni_2P/CeO_2 > Ni_3P–Ni_{12}P_5/Al_2O_3 > Ni_2P/SiO_2 > Ni_2P$/SAPO-11 > $Ni_2P/TiO_2 > Ni_2P–Ni_{12}P_5$/HY.

In a recent article, Zhao et al. [176] compared the performance of Ni_2P/SAPO-11 to that of the Ni/SAPO-11 catalyst for the SDO of methyl laurate (Table 4, entry 5). It was found that the increase of temperature and the decease of WHSV and H_2 pressure increased the conversion of methyl laurate and promoted the decarbonylation, hydroisomerization and cracking reactions. A catalytic test of about 101 h on stream showed that Ni_2P/SAPO-11 is more stable than Ni/SAPO-11 for the SOD of methyl laurate. In contrast, both catalysts were deactivated with respect to hydroisomerization. To explore catalyst deactivation, the fresh and the used catalysts were characterized by the methods presented in Table 4, entry 5. The characterization results revealed that the sintering of Ni particles and carbonaceous deposit contribute to inferior stability of Ni/SAPO-11 for both SDO and hydroisomerization, while no obvious sintering of Ni_2P particles took place and the carbonaceous deposit mainly led to the loss of the activity for hydroisomerization on Ni_2P/SAPO-11. It was proposed that carbonaceous deposits are mostly formed on acid sites which are indispensible for hydroisomerization [176].

The same group [177] compared the SDO performance of nickel phosphide catalysts to that of other metal phosphides (Table 4, entry 6). In the frame of this investigation a series of silica-supported metal (Ni, Co, Fe, Mo and W) phosphides were prepared and evaluated for the SDO of methyl laurate. To insight into the mechanism, the SDO of the intermediates

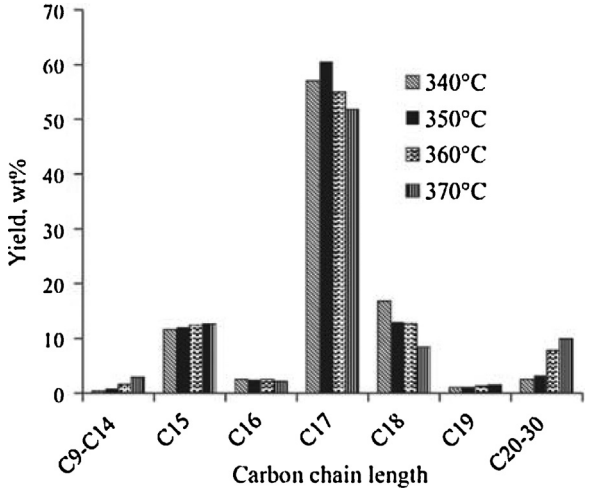

Fig. 31. Carbon distribution of the liquid organic product obtained by hydroprocessing of soybean oil over Ni_2P/silica catalyst measured at LHSV = 1 h^{-1}, 30 bar, H_2 300 N mL/min. Source: Ref. [178].

(lauric acid, dodecanal and dodecanol) were also evaluated. For comparison, Ni/SiO_2 MoO_2/SiO_2 and PO_x/SiO_2 were also studied. It was found that the catalyst activity followed the order: Ni_2P > MoP > CoP–Co_2P > WP > Fe_2P–FeP. The metallic Ni proved to be equally active to $Ni_2P > Ni_{12}P_5 > Ni_3P$. The main products on the metallic Ni and the Ni, Co and Fe phosphides were *n*-C_{11} alkanes, whereas the predominating products over the MoP and WP catalysts were *n*-C_{12} alkanes. In addition, alkenes and iso-hydrocarbons are formed over the Fe, Mo and W phosphides which are attributed to their lower hydrogenation ability and higher Brönsted acidity. The nickel phosphides exhibited much lower activities for methanation and cracking reaction than the metallic nickel and this was again attributed to the electronic and geometrical effects of P. In general, the different catalytic behavior of the catalysts studied and the relative contribution of each reaction pathway to the whole reaction mechanism was interpreted in terms of the electron property of metal site, Brönsted acidity and its synergy.

Zarchin et al. [178] have recently reported on the conversion of soybean oil into green fuels over Ni_2P catalysts supported on silica (an inert support) and Ultrastable zeolite HY (a highly acidic support). Both catalysts were tested at similar operating conditions (Table 4, entry 7). The main goal was to investigate the critical role of the support acidity on the catalytic behavior of nickel phosphide catalysts. They found similar yields in both cases. The yield of the organic liquid product was lower as it compared to that obtained over a Pt/Al_2O_3-SAPO-11 catalyst [179]. Concerning the Ni2P/silica catalyst, the distribution of hydrocarbons inside the organic liquid displayed a slight change (Fig. 31). Specifically, the heavy paraffins fraction (C_{20}–C_{30}) increased with temperature, probably due to oligomerization of intermediate olefinic products of triglycerides decomposition.

No considerable hydrocracking and isomerization activity was recorded over the Ni_2P/silica catalyst, in full agreement to the studies mentioned previously concerning the effect of phosphorous. But this is not the case for the Ni_2P/HY catalyst which displayed high hydrocracking and isomerization activity (see Fig. 32). This is diminished with time on stream. Characterization of the fresh and spent Ni_2P/HY indicated that exposing the catalyst to water vapors generated upon soybean oil hydrotreatment decreased the acidity of the catalyst reducing thus its hydrocracking activity [178].

A completely different stability of the two catalysts was recorded. Ni_2P/silica was very stable for >600 h on stream providing essentially a constant performance. It indicates that the

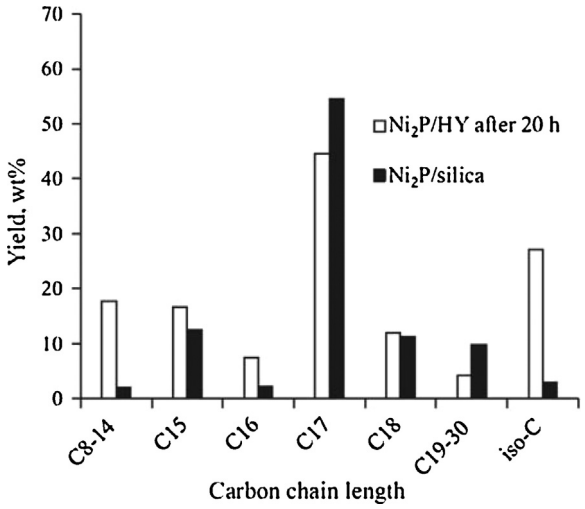

Fig. 32. Product yields obtained by hydroprocessing of soybean oil over Ni_2P/silica and Ni_2P/HY catalysts measured at 370 °C, 30 bar, LHSV = 1 h^{-1}, H_2 300 N mL/min, and 20 h on stream. Source: Ref. [178].

catalyst experienced no significant changes and negligible coke was generated during the run. On the other hand, a dramatic change in performance was measured with Ni_2P/HY. The performance of Ni_2P/HY after >150 h on stream approached that of Ni_2P/silica, namely the zeolite-related hydrocracking activity diminished while the SDO activity of Ni2P was maintained [178].

The main findings concerning the development of nickel phosphide catalysts can be summarized as follows: the aforementioned studies showed that Ni_2P supported nanocrystals of various sizes are formed in the most cases. The conversion of the reactant and the total yield to the diesel range hydrocarbons over phosphide catalysts are similar to those obtained over the corresponding nickel metallic catalysts. However, the nickel phosphides exhibit relatively low activities for methanation and cracking reactions. Moreover, they seem to be more tolerant to the deactivation. Their catalytic behavior is attributed mainly to the electronic and geometrical effects of the phosphorous inhibiting deCO and favoring HDO. The P electronic effect leads to the electron deficiency of Ni via the electron transfer from Ni to P whereas the geometrical effect alters the Ni–Ni distance. The higher electrophilicity of deficient Ni site is more favorable for the adsorption and activation of oxygen of C=O bond in ester group, favoring HDO and inhibiting deCO. These effects are probably responsible for the low cracking and the methanation activity exhibited by the phosphide catalysts compared to those exhibited by the corresponding nickel metallic ones. The magnitude of the P effects decreases with the size of the supported Ni_2P nanocrystals. The SDO pathways over the phosphide catalysts are similar but not identical to those followed over the nickel metallic catalysts. Several additional steps are involved. A strict difference is the absence of decarboxylation over nickel phosphide catalysts.

The effect of the support is important in the nickel phosphide catalysts. This is manifested by various ways. It seems that the support which leads to a catalyst with high specific surface area and thus to high dispersion of the active phase results to high conversion of the reactant and total yield of the diesel range hydrocarbons. This is perhaps the most important factor. As already mentioned the SSA is also a critical factor in the nickel metallic catalysts. The relatively high acidity and reducibility of the support seems to favor the manifestation of a synergy between the nickel site and the acid sites or oxygen vacancies. The C=O group activated by the oxygen vacancy may interact with hydrogen adsorbed on nickel site whereas the Brönsted acid site can provide hydrogen species to attack the C=O group adsorbed on the Ni site. These explain respectively the high intrinsic activity exhibited by Ni_2P/TiO_2 and Ni_2P/SAPO-11 catalysts as well as the low intrinsic activity expressed by the Ni_2P/SiO_2 catalysts. The support acidity influences also the isomerization activity of these catalysts. However, the use of support with very high acidity leads to high hydrocracking and isomerization activity.

Overall, the efforts done for the development of phosphide catalysts supported on various carriers are very promising, mainly in the frame of producing very active catalysts based on nickel with low activity with respect to the cracking and methanation. Silica, alumina and SBA-15 provided the most active catalysts per gram. Studies aiming to the development of additional high surface area nickel phosphide catalysts supported on carriers with medium acidity and reducibility would be welcomed.

3.7. Development of NiMo and NiW reduced catalysts

As already mentioned the NiMo, CoMo or NiW sulfide catalysts supported on γ-alumina may be used effectively for the simultaneous HDS/SDO of petrol fractions/natural triglycerides in the frame of a co-processing industrial approach. However, these commercial catalysts in their sulfided form are not so suitable in the frame of a stand-alone strategy though they are very active. This is because they require the addition of sulfur-containing compounds, such as hydrogen sulfide, to keep the catalysts in their sulphided form. It was reported that the sulfur could leach out from the catalysts under long-term conditions [180]. Moreover, as the plant oil does not contain sulfur the quality of the biofuels might be affected by sulfur residues contained in the SDO products. Finally, the toxic and corrosive hydrogen sulfide could bring great harm to the environment, human health and instruments. In view of the above the effort to develop NiMo, CoMo or NiW non-sulfided catalysts supported on γ-alumina with an activity similar to the corresponding sulfided catalysts seems to be plausible. In this context interesting contributions devoted to the improvement of the catalytic behavior of the reduced form of the aforementioned catalysts have been recently reported mainly by Professor Rong group [181–183,185–188]. This is mainly attempted by introducing additional phases in the catalyst formulations (Table 5).

More specifically, Liu et al. [181] studied the transformation of Jatropha oil into green diesel over lanthana free and lanthana doped NiMo catalysts supported on high surface area alumina (Table 5, entry 1). Five samples were studied: one 5%Ni15%Mo/γ-Al_2O_3 catalyst in both sulfided and non-sulfided state and three non-sulfided lanthanum doped catalysts (5% Ni 15% Mo 0.5% La/γ-Al_2O_3, 5% Ni 15% Mo 5% La/γ-Al_2O_3, 5% Ni 15% Mo 15% La/γ-Al_2O_3). The samples were characterized using various techniques and tested using a fixed bed reactor (Table 5, entry 1). Among the lanthanum doped samples the 5% Ni 15% Mo 5% La/γ-Al_2O_3 one was studied more extensively.

The conversion over the catalysts increases with temperature in the range 280–400 °C. The sulfided catalyst has been proved to be the most active within this temperature range. However, the activity of the 5% Ni 15% Mo/γ-Al_2O_3 sulfided catalyst was not very different compared to the 5% Ni 15% Mo 5% La/γ-Al_2O_3 non-sulfided one. This is illustrated in Fig. 33. Therefore, among the non-sulfided catalysts the 5% lanthanum doped one is the most promising.

The maximum yield of the C_{15}–C_{18} fraction was observed over the most promising 5% Ni 15% Mo 5% La/γ-Al_2O_3 non-sulfided catalyst. This yield greatly increased from 280 °C to 370 °C. There was no significant effect on this yield in the temperature range 370–400 °C. As it is illustrated in Fig. 34, the yield remains practically constant at least for 180 h on stream.

Heptadecane and octadecane are the main products indicating SDO via HDO and deCO_x. It seems that the HDO is favored

Table 5
An overview of the reactant, catalysts, preparation, characterization and reaction conditions for the SDO over NiMo or NiW reduced catalysts.

Entry/ Refs.	Reactant	Catalyst/preparation	Characterization	Reaction conditions
1/[181,182]	Jatropha oil	5% Ni 15% Mo*x*La/γ-Al_2O_3 non-sulfided (x = 0, 0.5, 5, 15%) 5% Ni 15% Mo/γ-Al_2O_3 sulfided Co-w.i. for Mo and Ni, i.w.i. for La. Powder metallurgy was also used for preparing non sulfided catalysts.	N_2-sorption XRD XPS H_2-TPD CO_2-TPD TGA	FBR, mass of the non-activated catalyst = 10 g Reaction conditions: 280–400 °C, 35 bar, LHSV: 0.9 h^{-1}, H_2 to feed ratio = 1000 mL H_2 gas/mL liquid feed.
2/[183]	Jatropha oil	5% Ni 15% Mo*x*Ce /γ-Al_2O_3 non-sulfided (x = 0, 1, 5, 25%) 5% Ni 15% Mo/γ-Al_2O_3 sulfided Co-w.i for Mo and Ni, i.w.i for Ce.	N_2-sorption SEM XRD H_2-TPD	FBR, mass of the non-activated catalyst = 10 g Reaction conditions: the same as in entry 1
3/[184]	Coconut oil	Mo–Ni/γ-Al_2O_3 Mo: 5.0 wt% and Ni: 9.1 wt% Co-i.w.i.		FBR, catalyst volume: 1 mL, Reaction conditions: 350 °C, pressure 8 bar, LHSV 1–20 h^{-1}, H_2 to feed ratio of 15.
4/[185,186]	Jatropha oil	Ni-HPW/Al_2O_3 5.54 wt% Ni, 28.49 wt% W, 0.38 wt% P w.i. for phosphotungstic acid and then w.i. for Ni	N_2-sorption SEM XRD TGA NH_3-TPD	FBR, mass of catalyst: 10 g Reaction conditions: 300–380 °C, H_2/oil v/v ratio 600 (Nm^3)/m^3, pressure 33 bar, LHSV 1 h^{-1}
5/[187]	Jatropha oil	NiW-nHA Ni/W loading: 73.24% and 65.99% co-precipitation	XRD FTIR TEM EDX	FBR, mass of catalyst: 10 g Reaction conditions: 340–400 °C, pressure 30 bar, LHSV 2 h^{-1}, H_2 to feed ratio of 600 mL H_2 gas/mL liquid feed.
6/[188]	Jatropha oil	Ni/nHA (5% Ni) co-precipitation Ni-HPW/nHA impregnation of $H_3O_{40}PW_{12}$ (10, 20, 30 and 40% HPW in the final catalyst) nHA precipitation HPW/nHA co-precipitation (10% HPW)	N_2-sorption XRD FTIR XPS TGA TPD-NH_3	FBR, mass of catalyst: 10 g Reaction conditions: 340–400 °C, pressure 30 bar, LHSV: 2 h^{-1}, H_2 to feed ratio of 600 mL H_2 gas/mL liquid feed.

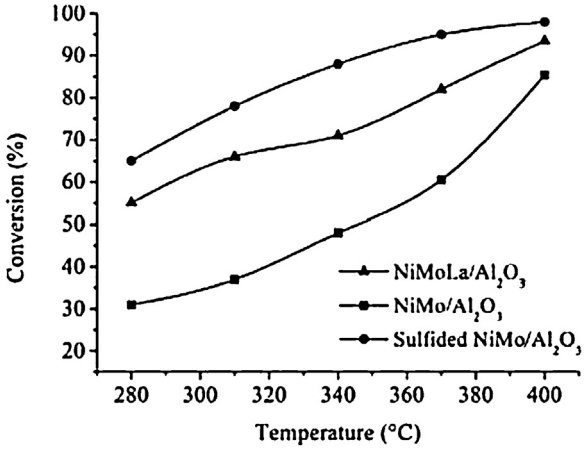

Fig. 33. Conversion of Jatropha oil at various temperatures over the 5% Ni 15% Mo/γ-Al_2O_3 sulfided catalyst, the 5% Ni 15% Mo 5% La/γ-Al_2O_3 and the 5% Ni 15% Mo/γ-Al_2O_3 non-sulfided catalysts. Source: Ref. [181].

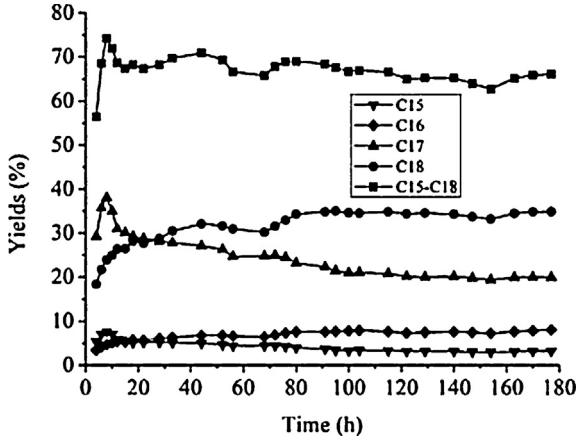

Fig. 34. Yields of *n*-alkanes in the green diesel range (C_{15}–C_{18}) as a function of time on the stream over the 5% Ni 15% Mo 5% La/γ-Al_2O_3 catalyst (370 °C, 0.9 h^{-1}). Source: Ref. [181].

with respect to the nickel monometallic catalysts. Over the same catalyst the heavy fraction (>C_{18}) yield gradually decreased as temperature increased. Finally, the light fraction (<C_{15}) yield increased with temperature, as higher temperatures favored cracking and the consequent production of smaller molecule hydrocarbons.

The beneficial action of the well dispersed lanthanum oxide on the catalyst surface was attributed to its ability for promoting the reduction of the Ni^{2+} into metallic nickel and the oxidation of Mo^{4+} into Mo^{6+}. The metallic nickel centers are responsible for the easier hydrogen adsorption observed in the lanthanum oxide doped samples. Moreover, lanthanum oxide increased the basicity of the catalyst.

Recently Liu et al. [182] proposed a novel method (powder metallurgy) for preparing Ni–Mo–La/γ-alumina non-sulfided catalysts (Table 5, entry 1). These were used in the green diesel production from the SDO of Jatropha oil. A selectivity of 77% was obtained for the straight-chain C_{11}–C_{20} alkanes at 370 °C, 30 bar, and 0.9 h^{-1}. The conversion of Jatropha oil under these conditions was equal to 80%.

Liu et al. [183] continued their studies on the transformation of Jatropha oil into green diesel examining the effect of cerium doping on the NiMo/γ-Al_2O_3 catalysts (Table 5, entry 2). They studied five catalysts: one 5% Ni 15% Mo/γ-Al_2O_3 catalyst in both sulfided and non-sulfided state and three non-sulfided cerium doped catalysts (5% Ni 15% Mo 1% Ce/γ-Al_2O_3, 5% Ni 15% Mo 5% Ce/γ-Al_2O_3, 5% Ni

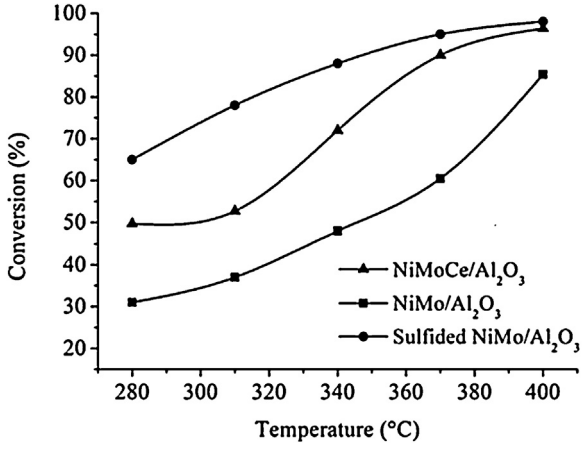

Fig. 35. Conversion of Jatropha oil at various temperatures over the 5% Ni 15% Mo/γ-Al_2O_3 sulfided catalyst, the 5% Ni 15% Mo 5% Ce/γ-Al_2O_3 and the 5% Ni 15% Mo/γ-Al_2O_3 non-sulfided catalysts. Source: Ref. [183].

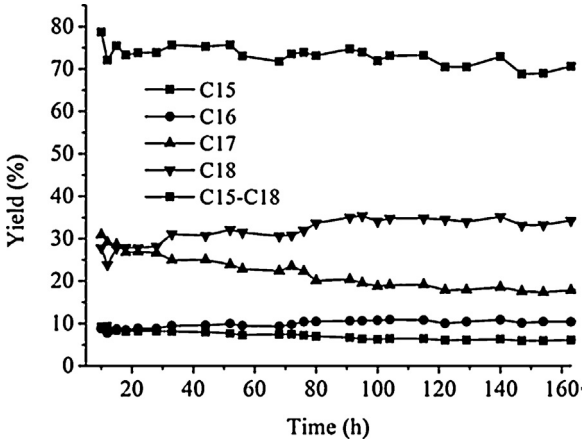

Fig. 36. Yields of *n*-alkanes in the green diesel range (C_{15}–C_{18}) as a function of time on stream over the 5% Ni 15% Mo 5% La/γ-Al_2O_3 catalyst (370 °C, 35 bar, 0.9 h^{-1}). Source: Ref. [183].

15% Mo 25% Ce/γ-Al_2O_3). Among the cerium doped samples the 5% Ni 15% Mo 5% Ce/γ-Al_2O_3 one was studied more extensively.

The conversion over the catalysts increased with temperature. Although the sulfided catalyst has been proved to be the most active its activity was similar to that of the 5% Ni 15% Mo 5% Ce/γ-Al_2O_3 non-sulfided catalyst. In contrast, the non-sulfided 5% Ni 15% Mo/γ-Al_2O_3 presented considerably lower activity. Therefore, among the non-sulfided catalysts the 5% cerium doped one has been proved to be the most active (Fig 35).

The maximum yield of the C_{15}–C_{18} alkanes was obtained over the 5% Ni 15% Mo 5% Ce/γ-Al_2O_3 non-sulfided catalyst. As it can be seen in Fig. 36 the C_{15}–C_{18} yield over this catalyst remains practically constant at least for 160 h on stream.

Heptadecane and octadecane are the main products indicating that SDO proceeds via both HDO and deCO$_x$. It seems that the HDO is favored with respect to the nickel monometallic catalysts. The yield concerning the <C_{15} hydrocarbons was ranged between 6 and 10% whereas that of the heavier hydrocarbons and esters between 13 and 38%. The concentration of the smaller hydrocarbons increases with the reaction temperature. The favorable action of doping was attributed to the well dispersed CeO_2 which increases the dispersion of the supported nickel and molybdenum species, leading to the formation of more active centers, and enhances H_2 uptake.

The aforementioned three contributions [181–183] indicate that lanthanum and cerium doping have very similar favorable effects on the catalytic behavior of NiMo non-sulfided catalysts supported on γ-Al_2O_3. This doping can eliminate the necessity of working over sulfided NiMo catalysts supported on γ-Al_2O_3.

Kimura et al. [184] studied the hydroconversion of coconut oil into saturated hydrocarbons under relatively low hydrogen pressure (8 bar) using a sulfur-free (reduced) Mo–Ni/γ-Al_2O_3 catalyst (Mo: 5.0 wt% and Ni: 9.1 wt%) prepared by co-impregnation of Ni and Mo species (Table 5, entry 3). This catalyst exhibited remarkably high conversion of coconut oil as well as high selectivity to hydrocarbons associated with jet fuel. Examining variations in product distributions with contact time they showed that the hydrocarbons were primarily produced through deCO$_x$. Increase in the contact time favored HDO.

According to the proposed reaction pathways (Fig. 37) the hydrogenolysis of the C—O bond between the fatty acid and the glycerol backbone (1) yields to fatty acids and propane or lighter hydrocarbons. The fatty acids thus formed are readily transformed into hydrocarbons with odd carbon numbers through subsequent deCO$_x$. Hydrocarbons with even carbon numbers are generated by stepwise reduction of the fatty acids (HDO). Under low hydrogen pressure, the rate of fatty acid deCO$_x$ is predominant relative to the rate of the HDO, leading to the selective formation of the odd numbered hydrocarbons. The deCO$_x$ and the HDO routes are well established and have presented in details in Section 3.3. Here the authors proposed and additional pathway for the production of odd numbered hydrocarbons (2), namely through direct cracking of the bond between the ester carbonyl carbon and the α carbon of the triglycerides. However, they noted that it likely requires a prolonged residence time on the catalyst. Morgan et al. [106] had proposed that the observed formation of significant amounts of ethene during the deoxygenation of tristearin in the absence of hydrogen involves bond scission between the β and **γ** carbons of the fatty acid structure. Since Kimura et al. [184] have observed ethane in the product mixture at higher yields than the C_4–C_6 hydrocarbons, they also assumed scission of the C—C bond between the β and **γ** carbon atoms (3) leading to the formation of hydrocarbons with three carbon number less than that of the parent fatty acid together with ethene and CO_x. These reactions are then followed by the hydrogenation of ethene and CO_x to ethane and methane, respectively. In our opinion the ethane observed in the reaction mixture can be partly attributed to the dissociation of the propane produced in the first hydrogenolysis step.

Liu et al. [185,186] extended their efforts to improve, by doping, the catalytic behavior of the reduced form of the conventional hydrotreatment catalysts concerning SDO. They synthesized a nickel, phosphorous, tungsten catalyst supported on γ-alumina (Ni-HPW/Al_2O_3) and tested in the SDO of Jatropha oil to produce green diesel (Table 5, entry 4).

This catalyst was tested for the SDO of Jatropha oil using a fixed bed reactor in the temperature range 300–380 °C. Its catalytic activity for the conversion of Jatropha oil was compared to that exhibited by a commercial NiW/γ-alumina hydrotreatment catalyst, with the latter both in the reduced and sulphided form. For all the catalysts tested the conversion increases with temperature. The reduced form of the Ni-HPW/Al_2O_3 catalyst was proved to be considerably more active than the reduced form of the NiW/γ-alumina hydrotreatment catalyst and almost equally active with the sulphided form of the latter (Fig. 38).

Figs. 38 and 39 indicate that a conversion equal to 99.85% was obtained at 360 °C over the synthesized Ni-HPW/Al_2O_3 catalyst. This catalyst is also very selective in the production of hydrocarbons in the range *n*-C_{15}–*n*-C_{18} (Fig. 39). One may observe that the selectivity for hydrocarbons in this range is maximized also at 360 °C attaining a value equal to ~85%. Moreover, we may observe that the increase of reaction temperature increases the selectivity to

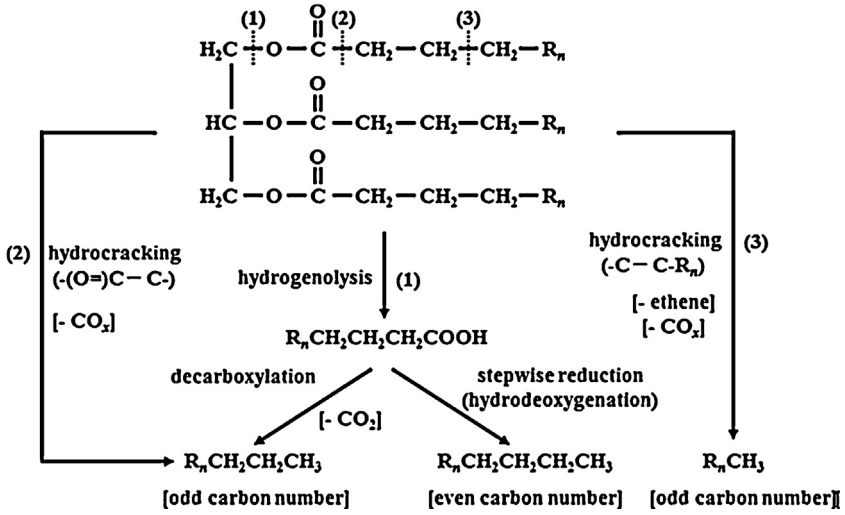

Fig. 37. Proposed pathways for the reaction of triglycerides over Mo–Ni/γ-Al_2O_3 under low hydrogen pressure. Source: Ref. [184].

hydrocarbons with carbon atoms less than 15 and decreases the selectivity to hydrocarbons with carbon atoms more than 18.

Recently, the Rong research group experienced with NiW and Ni-HPW catalysts supported on nano-hydroxyapatite [187,188]. First, a NiW-nano-hydroxyapatite (NiW-nHA) catalyst was prepared by a co-precipitation (Table 5, entry 5). High conversion of Jatropha oil was achieved over this catalyst mainly to straight chain alkanes ranging from C_{15} to C_{18}. The reaction pathway involved hydrocracking of the C=C bonds of the Jatropha oil triglycerides [187].

The aforementioned group studied a new series of catalysts [188], in an effort to improve the quality of the Jatropha oil hydroconversion product by increasing its iso-paraffins content and thus decreasing the cold filter plugging point (CFPP) [189–193]. The main idea was the exploitation of isomerization ability of heteropoly acids [194–197]. A series of Ni-HPW/nHA catalysts was prepared containing 10 wt%, 20 wt%, 30 wt% and 40 wt% HPW. The effect of HPW content on the liquid products yield, light ($<C_{10}$) and middle (C_{10}–C_{22}) hydrocarbons selectivities, iso-paraffins to normal paraffins ratio (iso/n) and pour point of product oil was investigated in a fixed-bed reactor (Table 5, entry 6).

The influence of HPW loading on the yield of liquid product as well as on the distribution of hydrocarbons in the liquid product is depicted in Fig. 40. Inspection of this figure reveals that the light paraffins were increased as the HPW loading increased, but the yield of liquid product was decreased. Moreover, it was found that the $(C_{15}+C_{17})/(C_{16}+C_{18})$ ratio increased with HPW-loading. It can be deduced that $deCO_x$ enhanced with HPW-loading much more than HDO.

Although the product oil obtained over Ni/nHA contained the highest amount (95%) of C_{10}–C_{22} hydrocarbons, the (iso/n) ratio was low (0.2) and thus the pour point of the product too high (12 °C). The properties of the liquid product were improved considerably using the Ni-HPW(30%)/nHA sample. In fact, the (iso/*n*) ratio obtained is equal to 1.64 and the pour point was dropped to -28 °C. A Jatropha oil conversion equal to 100% and a yield of the liquid product equal to 83.4% were obtained over this sample. Further increase in the HPW loading to 40% brings about a decrease in the Jatropha oil conversion (76.4%) and (iso/*n*) ratio (0.86). This behavior has been attributed to the decrease of specific surface area and pore blockage observed for HPW-loading higher than 30%.

It is well known that the isomerization reaction mechanism of paraffins involves carbenium ion intermediates the formation of which is related to the catalyst acidity [198,199]. The *n*-paraffins are

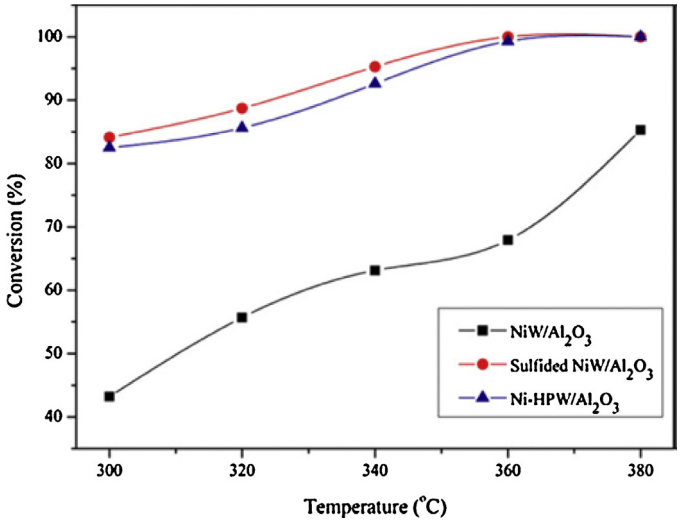

Fig. 38. Conversion of Jatropha oil at various temperatures over the synthesized Ni-HPW/Al_2O_3 and commercial NiW/γ-Al_2O_3 catalysts, the latter in both reduced and sulphided form. Source: Ref. [185].

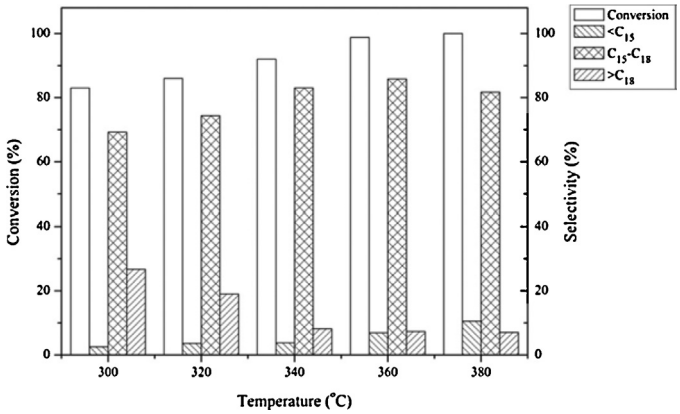

Fig. 39. Conversion and selectivities to various hydrocarbon fractions obtained for the SDO of Jatropha oil over the synthesized Ni-HPW/Al_2O_3 catalyst. Source: Ref. [185].

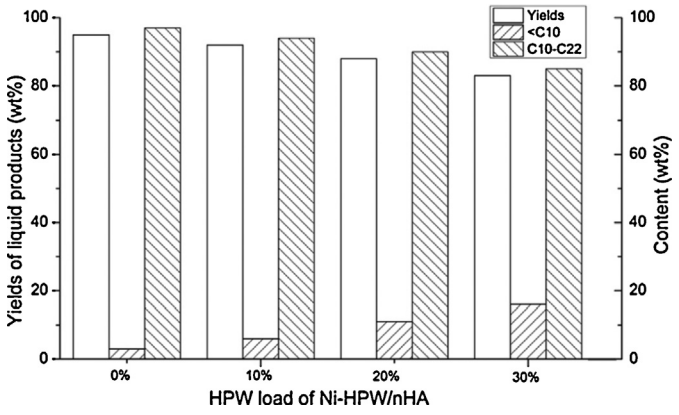

Fig. 40. Yield of liquid product and distribution of hydrocarbons in the liquid product obtained over Ni-HPW/nHA catalysts with various HPW-loadings at 360 °C, 30 bar, H_2/oil (v/v) = 600, LHSV = 2 h^{-1}. Source: Ref. [188].

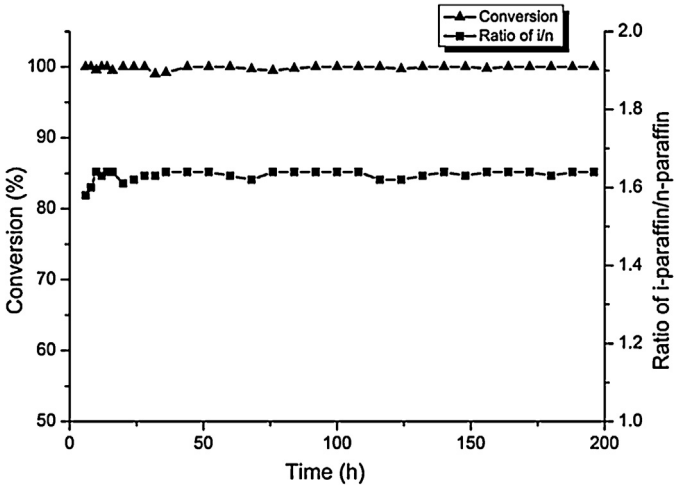

Fig. 41. Conversion of Jatropha oil and (iso/n) ratio in the liquid product obtained over Ni-HPW(30%)/nHA catalyst as a function of time on stream at 360 °C, 30 bar, H_2/oil (v/v) = 600, LHSV = 2 h^{-1}. Source: Ref. [188].

transformed into iso-paraffins at the acid sites. The NH_3-TPD profiles obtained over the Ni-HPW/nHA catalysts had revealed that the amount of acid sites increased proportionally to the HPW loading [188]. This explains very well the increase of (iso/*n*) ratio with HPW-loading. However, because of the carbenium ion formation the cracking reactions are also facilitated following the β-elimination principle, which led to even more light paraffins (<C10).

The conversion of Jatropha oil and (iso/*n*) ratio in the liquid product obtained over the most promising catalyst (Ni-HPW(30%)/nHA) of this series are showed in Fig. 41 as a function of time on stream. It is observed that both, conversion and (iso/n) ratio remain nearly constant for at least 200 h on stream.

The most important findings concerned the development of NiMo and NiW reduced catalysts can be summarized as follows: The introduction of additional phases (lanthana, ceria) in the NiMo/γ-Al_2O_3 and phosphorous in the NiWP/γ-Al_2O_3, Ni-HPW/Al_2O_3 and Ni-HPW/nHA catalysts, investigated in the hydrotreatment of petrol fractions, improves the catalytic behavior of their reduced forms for the SDO of triglycerides. This allows avoiding the problems arising from the use of the sulfided forms of the catalysts in the frame of the stand-alone approach. The majority of the above studies improved the catalytic behavior of catalysts with the optimum Ni/Mo or Ni/W ratio relevant to their sulfided form and the hydrotreatment of petrol oils. However, the last reviewed study [188] shows that presumably this is not the same for the reduced form of these catalysts and the SDO of triglycerides. Searching for this ratio in the latter case will probably be another way for improving the catalytic behavior of the reduced state.

3.8. Development of bimetallic (NiMo, NiW) carbide, nitride and phosphide catalysts

In previous sections we have mentioned the reasons compelling the use of non-sulfided NiMo, CoMo and NiW supported catalysts in the SDO of vegetable oils and animal fats to produce hydrocarbons in the diesel range. We have seen that the improvement of the catalytic behavior of their reduced state by introducing another phase in the catalyst formulation is a very interesting alternative. Another alternative is the use of carbides, nitrides and phosphides of the aforementioned metals instead of the sulfides. It is well known that the supported carbides, nitrides and phosphides of the early transition metals, exhibiting an activity similar to noble metals, are quite promising catalysts for the hydrotreatment of petroleum fractions and may substitute the conventional NiMo, CoMo and NiW sulfided catalysts [200–204]. Their high intrinsic activity is due to the introduction of nitrogen, carbon or phosphorus into the lattice of the metal resulting to an increase in the d-electron density and of the lattice parameter a_0 as well [205]. Thus, transition metal mono- and bimetallic carbide, nitride and phosphide catalysts have been tested successfully in the HDS, HDN and HDO of oil and bio-oils [206–211]. Specifying on natural triglycerides and fatty acids few contributions suggest that this kind of catalysts is indeed promising. Thus, nitrides of molybdenum, tungsten, and vanadium supported on γ-Al_2O_3 have been used successfully in the SDO of oleic acid and canola oil [212]. More importantly, molybdenum carbide supported on multi-walled carbon nanotubes exhibits high activity and selectivity for one-step conversion of vegetable oils into branched diesel-like hydrocarbons [213] and the molybdenum carbide supported on ordered mesoporous carbon [214] exhibits also excellent performance. The catalytic performance of nickel phosphide catalysts for SDO of natural triglycerides has been already discussed in Section 3.6 while the optimizing action of phosphorous on bimetallic catalysts became evident in Section 3.7. The above encouraging results motivated recent studies on bimetallic carbide, nitride and phosphide catalysts which are generally considered to be more active and stable than the monometallic ones [215].

Wang et al. [216] studied NiMo carbides and nitrides supported on ZSM-5 (Table 6, entry 1). The precursor (oxidic) catalysts were synthesized and were carburized in a stream of 20 vol% CH_4/H_2 or nitridated following a TPR procedure [217–220].

Although the procedures used for the catalysts preparation brought about structural rearrangements/pore blockage of the support leading to considerable decrease of its initial specific surface area the resulted catalysts still exhibited quite high specific surface areas. The XRD patterns of the catalysts studied (Fig. 42) indicated the presence of a mixed Ni/Mo phase ($NiMoO_4$) together with single Ni and Mo carbides (Mo_2C and NiC) and nitrides (Mo_2N and Ni_3N).

The kinetic experiments were carried out using soybean oil in a fixed bed reactor. Due to the high acidity of the support and the relatively high reaction temperatures a liquid organic product was produced instead of green diesel together with gaseous products (CO, CO_2, C_2H_6, C_3H_8 and C_4H_{10}) and water. Therefore, for this point of view this work does not belong rigorously to the works devoted to SDO. The reactor was considered to be in a steady state when the OLP yield and the selectivity for gasoline to diesel range hydrocarbons were maintained relatively constant on a daily basis, usually after 4–5 days on stream. In addition to hydrocarbons the OLP contained several side products (partially converted triglycerides, oxygenates, monomers, dimmers and tars). Complete conversion of the reactant and up to 50 wt% yield of hydrocarbon fuels was

Table 6
An overview of the reactant, catalysts, preparation, characterization and reaction conditions for the SDO over NiMo and NiW carbide, nitride and phosphide catalysts.

Entry/Refs.	Reactant	Catalyst/preparation	Characterization	Reaction conditions
1/[216]	Soybean oil	Four NiMoC/ZSM-5 catalysts with varying Ni/Mo molar ratio (0.0, 0.5, 1.0 and 1.5) and one NiMoN/ZSM-5 catalyst. Total metal loading: 10%. Dry co-impregnation for depositing Ni and Mo phases on commercial ZSM-5 Drying, calcination and TPR carburization or nitrification of the oxidic precursors	N_2 Physisorption XRD	FBR, catalyst mass: 2 g. Reaction temperature and pressure: 360,400, 450 °C, 44.2 bar LHSV = 1.5 h^{-1} Quartz beads were used to dilute the catalyst bed and optimize heat transfer.
2/[221]	Soybean oil	NiMoC/Al-SBA-15 NiMoC/γ-Al_2O_3 NiMoC/USY zeolite NiMoC/ZSM-5 NiMoC/Zeolite β Total metal loading: 10%. Preparation as is described in entry 1	N_2 Physisorption XRD TEM	FBR, catalyst mass: 2 g. Temperature: 400 °C, Pressure: 44.2 bar LHSV= 1 h^{-1} H_2 flow rate: 50 mL/min. Quartz beads were used to dilute the catalyst bed and optimize heat transfer.
3/[224]	Distillers dried grains with soluble corn oil	Four NiWC/Al-SBA-15 catalysts with varying Ni/Mo ratio (1/9, 1/1, 2/1, 9/1) following dry co-impregnation for depositing Ni and Mo phases. Three NiWC/Al-SBA-15 catalysts (Ni/W = 1/9, 2/1 and 1/1) prepared by dendrimer-encapsulated nanoparticles method. Drying and calcination TPR carburization of the oxidic precursors Total metal loading: 10%.	N_2 Physisorption SEM-EDS TEM ICP	FBR, catalyst mass: 2 g. Temperature: 400 °C Pressure: 44.2 bar LHSV = 1 h^{-1} H_2 flow rate: 30 mL/min. Quartz beads were used to dilute the catalyst bed and optimize heat transfer.
4/[226]	Methyl laurate	Ni_2P/SiO_2 (12% Ni – 0% Mo) NiMo3/1 (12% Ni – 6.5% Mo) NiMo3/2 (12% Ni – 13% Mo) NiMo3/3 (12% Ni – 19.6% Mo) NiMo2/3 (8% Ni – 19.6% Mo) NiMo1/3 (4% Ni – 19.6% Mo) MoP/SiO_2 (0% Ni – 19% Mo) co-i.w.i. of Ni and Mo phases, successive i.w.i. with $NH_4H_2PO_4$ solution [nominal P/metal(Ni and/or Mo) molar ratio:1] and H_2-TPR	N_2-Physisorption XRD TEM CO-chemisorptions XPS NH_3-TPD	FBR, 0.35 g passivated catalyst blended with 2.8 g quartz sand Temperature: 300–340 °C H_2 pressure 30 bar WHSV: 14 h^{-1} H_2/methyl laurate: 50
5/[227]	Methyl laurate	Five Ni_2PMoP/SiO_2 catalysts whose the precursors were calcined at 400, 500, 600, 700 and 800 °C co-i.w.i. of Ni, Mo and P phase, [nominal P/metal(Ni and Mo) molar ratio: 1] and H_2-TPR	UV–vis DRS H_2-TPR XRD TEM CO-chemisorptions H_2-TPD NH_3-TPD	FBR, 0.5 g passivated catalyst blended with 4 g quartz sand Temperature: 300–340 °C H_2 pressure 30 bar WHSV: 10 h^{-1} H_2/methyl laurate: 25

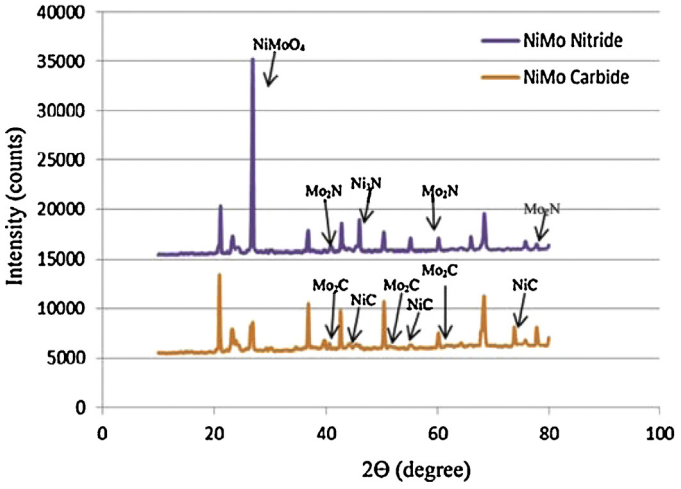

Fig. 42. XRD spectra of NiMoC/ZSM-5 and NiMoN/ZSM-5 catalysts. Source: Ref. [216].

obtained. The deactivation effect of temperature was important. Both catalysts at low reaction temperature (360 °C) proved to be not resistant to water poisoning produced via HDO. A little amount of hydrocarbons was produced after reaction time equal to four days and the OLP was rich to the intermediate carboxylic acids. The authors attributed the deactivation to the disturbance of the support acidity by the adsorbed water and thus to the disturbance of metal/acid balance of the catalysts. Increase of temperature at 450 °C enhanced the water desorption and thus diminished deactivation. The carbide catalyst has an advantage with respect the nitride catalyst because it exhibited lower methanation activity. For this catalyst it was found that increase in the contact time enhances further the hydrocarbons content in the OLP.

Finally, four carbide catalysts (NiMoC/ZSM-5) were synthesized of varying Ni/Mo molar ratio (0, 0.5, 1.0, 1.5) to investigate the effect of this ratio on the catalytic performance. A full conversion of the natural triglycerides was obtained at 400 °C and 44.2 bar. However, the composition of the OLP was strongly depended on the presence of nickel in the catalyst which enhances hydrogen activation and transferring. Thus, polymerization might be

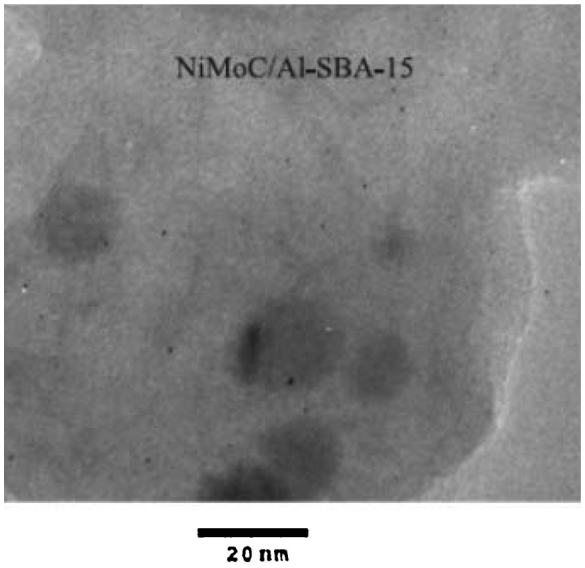

Fig. 43. TEM image of the NiMoC/Al-SBA-15. The black spots on the image denote the supported particles (NiMo carbides and/or oxides). Source: Ref. [221].

the predominant reaction over Mo/ZSM-5 carbide catalyst causing plugging in the catalyst bed after three days. A large amount of C_{23} < hydrocarbons were produced but almost no hydrocarbons in the gasoline, kerosene and green diesel range. The catalysts with Ni/Mo molar ratios equal to 0.5, 1.0, and 1.5 showed similar selectivity to kerosene and diesel hydrocarbons, but the increase of this ratio decreased the selectivity to gasoline hydrocarbons. It would be interesting in a future study comparing the catalytic behavior of the above catalyst with one containing only nickel carbide.

In a subsequent work Wang et al. [221] studied the most promising NiMo carbide by changing the support (Table 6, entry 2). Again the catalysts were evaluated in the transformation of soybean oil into hydrocarbons in the gasoline to diesel range. Since the support could affect the cracking and isomerization activity [222], the main goal of the work was to investigate the effects of support on catalyst behavior. Presumably the underline idea of this work was to investigate whether a shift could be achieved from the production of OLP through hydrocracking into green diesel through SDO by altering the support. Three different types of materials were examined: a mesoporous material [Al-SBA-15 synthesized using commercial SBA-15 and following a standard procedure [223], γ-alumina (commercial) and three types of commercial zeolites (ZSM-5, Zeolite β, USY zeolite)]. The catalysts were prepared following the procedure described in the previous work of the group [216].

The catalysts exhibited high values of specific surface areas and very small supported nanoparticles (carbides or oxides presumably lower than 5 nm) non-detectable by XRD were obtained in all cases with the best dispersion obtained in the case of the high surface area and pore volume NiMoC/Al-SBA-15 material (Fig. 43).

The evaluation of the catalysts was carried out using a bench scale FBR. An experiment was considered to be at steady state when yield and selectivity remained constant on a daily basis, usually after 4–5 days on stream. A percentage conversion of triglycerides equal to 100 was obtained under these conditions over all catalysts studied. The product was composed from an organic liquid product, OLP, containing mainly *n*-alkanes C_{15}–C_{18} and only minor amounts of iso-alkanes and olefins, partially converted triglycerides, oxygenates, monomers, dimmers and tars, gaseous products containing un-reacted hydrogen, carbon monoxide, carbon dioxide, and C_1–C_4 hydrocarbons and water. The maximum yield of OLP was obtained over the NiMoC/Al-SBA-15 (96%) and NiMoC/γ-Al_2O_3 (90%) catalysts. The yield of the OLP was limited to the 60-80% for

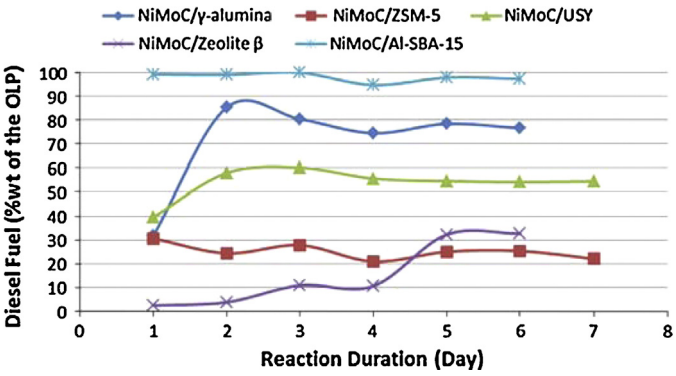

Fig. 44. Diesel fuel selectivity in OLP. Source: Ref. [221].

the zeolite based catalysts which favor the formation of lighter gas hydrocarbons. Moreover, the maximum selectivity of diesel fraction of OLD was also obtained over the NiMoC/Al-SBA-15 (97%) and NiMoC/γ-Al_2O_3 (80%) catalysts whereas the zeolite based catalysts favored the production of a considerable gasoline fraction (about 15–40%, Fig. 44).

The authors explained their results in terms of the support texture. In this context it is remarkable to note that triglyceride molecules have a longitudinal section diameter around 5.3–7.4 Å and chain length of about 30–45 Å. According to the authors the mesoporous structure of NiMoC/Al-SBA-15 and NiMoC/γ-Al_2O_3 catalysts may provide a larger diffusion space for the large triglyceride molecules than the microporous zeolites. Therefore, the diffusion of the triglyceride molecule within the mesoporous is much easier than that within the micro-pores and therefore secondary cracking is limited. In contrast, the zeolite micro-pores favor more secondary cracking leading to lower (higher) diesel (gasoline, gaseous) fraction. The better behavior of NiMoC/Al-SBA-15 compared to NiMoC/γ-Al_2O_3 formulation was mainly attributed to its regular pore structure and larger pore volume. The above explanation visualizes an additional aspect related to the support effect on the catalytic performance with respect to SDO, besides support acidity which is not considered in this work. This aspect could be refined in the future on the base of more detailed structural information (e.g., pore size distributions etc.). On the other hand the support acidity should be also taken into account to explain the catalytic behavior. The authors correctly concluded that the NiMoC/Al-SBA-15 is a promising catalytic system for hydrotreating vegetable oil into green diesel. One could also claim that the easier prepared NiMoC/γ-Al_2O_3 catalyst is also a promising material. Again, It would be interesting in a future study comparing the catalytic behavior of the above two catalysts with the corresponding ones containing only nickel carbides.

In a third paper [224] published by the same group a new NiWC/Al-SBA-15 catalyst series was studied for the hydrocracking of distillers dried grains with solubles (DDGS) corn oil (Table 6, entry 3). The effect of the Ni/W ratio and the catalyst preparation method on activity, selectivity, and durability of the catalyst for green diesel production was investigated under relatively mild reaction conditions. The metal dispersion on the support and the alloy formation were studied to elucidate their effects on the catalyst performance and provide a better understanding of the hydrocracking process. Four NiWC/ Al-SBA-15 catalysts with varying Ni/W ratio (1/9, 1/1, 2/1, 9/1) were prepared by incipient wetness impregnation to study the effect of metal ratio on the catalyst structure, activity, and selectivity. In addition, three NiWC/Al-SBA-15 catalysts (Ni/W = 1/9, 2/1 and 1/1) have been studied which were prepared by a dendrimer-encapsulated nanoparticles (DENP) method in order to minimize alloy formation and increase the metal dispersion on the support (Table 6, entry 3).

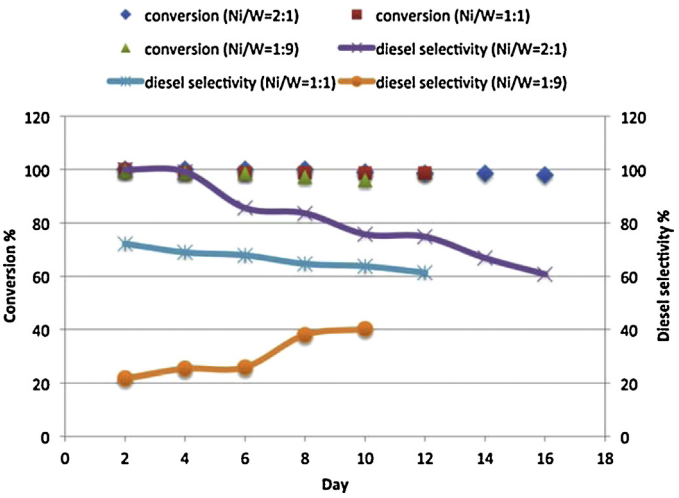

Fig. 45. Conversion of DDGS corn oil and the diesel selectivity over a DENP NiWC/Al-SBA-15 catalyst. Source: Ref. [224].

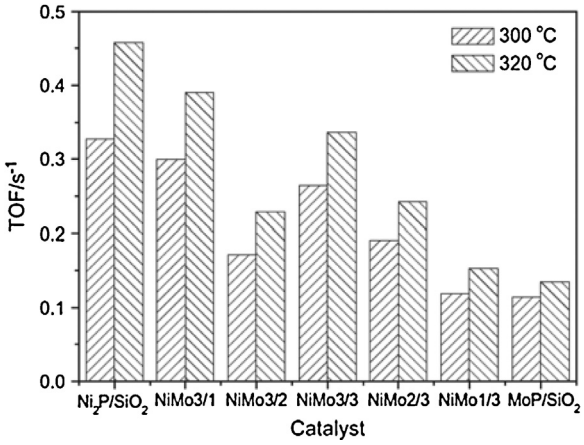

Fig. 46. TOF of methyl laurate achieved over Ni–Mo phosphide catalysts with various Ni/Mo molar ratios. Source: Ref. [226].

The preparation of the impregnated samples and the carburization of all samples were obtained following the method mentioned in the previous two works of the group [216,221]. The protocol for preparing the catalysts by the DENP was adapted and modified in a previous study [225]. The samples were characterized using various methods and evaluated in the SDO of DDGS corn oil (instead of soybean oil) in order to meet the need of using low-quality vegetable oils for avoiding food competition. The kinetic experiments were performed at 400 °C and 44.2 bar using a fixed bed reactor.

The change of the Ni/W ratio of the impregnated samples and the change of the preparation method affect several surface characteristics. It seems that the best dispersion of the W phase and the lack of Ni_4W is obtained in the impregnated sample with Ni/W = 9/1 and in all DENP samples. As we shall see these justify the better catalytic performance of these samples with respect to the remainder impregnated samples.

The above predictions were confirmed by the evaluation results. In fact, the evaluation of the impregnated catalysts showed that the catalyst with the Ni/W ratio equal to 9/1 exhibits the best activity, significant resistance against deactivation and high selectivity for hydrocarbons in the diesel range. This catalyst was also proved to be the more stable as it is demonstrated by comparing its XRD spectra before and after usage. Moreover, almost complete conversion of the reactant was obtained over the catalysts prepared by the DENP method (Fig. 45). These catalysts are more active than the catalysts prepared by impregnation, in agreement to the characterization results. On the other hand, although all the DENP catalysts showed high metal dispersion and no formation of Ni_4W they exhibited different selectivities for hydrocarbons in the diesel range (Fig. 45). The catalyst riche in nickel exhibits the highest selectivity. However, even in this catalyst the selectivity to diesel starts to decrease after five days (Fig. 45). This is due to the formation of other compounds, mainly esters and alcohols detected in the liquid product. The authors proposed two alternative mechanisms for alcohol production, besides those already stated for other types of nickel based catalysts. According to the first mechanism the long saturated hydrocarbons are cracked forming smaller saturated and unsaturated hydrocarbons and then the unsaturated hydrocarbons are hydrated to produce alcohols. According to the second mechanism the alkane produces a radical at the surface of metal active sites which then reacts with the dissolved oxygen to make a peroxo radical species that leads to alcohol. In our opinion the second mechanism is not very probable due to the presence of hydrogen.

This very interesting work revealed the importance of the Ni/W ratio and the preparation method for controlling the physicochemical characteristics and thus catalytic behavior of NiW carbide catalysts for the SDO of natural triglycerides. Taking into account that the impregnated catalysts are less expensive than the DENP ones, the evaluation of the promising impregnated catalysts with Ni/W = 1/9 for more than two days would be welcomed. Moreover, the preparation, characterization and evaluation of an impregnated nickel carbide catalyst without tungsten it is needful in order to investigate whether a synergy between the nickel and the tungsten phase is actually exist.

Lets' now review two interesting papers reported by the same group which are dealing with bimetallic phosphide catalysts. In the first contribution Chen et al. [226] studied Ni–Mo phosphide catalysts in the SDO of methyl laurate. Specifically, they prepared SiO_2-supported Ni_2P, MoP and Ni-Mo bimetallic phosphides with different Ni/Mo molar ratios (3/1, 3/2, 3/3, 2/3, 1/3). The catalysts were characterized by various physicochemical methods and evaluated in a fixed bed reactor (Table 6, entry 4).

A slightly higher conversion of methyl laurate has been achieved over the Ni–Mo bimetallic phosphide catalysts than Ni_2P/SiO_2 and MoP/SiO_2. However, TOF calculated on the base of the surface density of metal sites (i.e., CO uptake) displayed a very different variation trend. Ni_2P/SiO_2 and MoP/SiO_2 exhibited the highest and the lowest TOF, respectively. As it can be seen in Fig. 46, the TOF of methyl laurate generally increases with the Ni/Mo ratio.

Methyl laurate was not completely converted into hydrocarbons (C_{11} and C_{12}) because oxygenated intermediates (lauric acid, dodecanal, dodecanol and lauryl laurate) are also present in the product. Thus, the site time yield (STY) of the C_{11} and C_{12} hydrocarbons presented in Fig. 47 was always smaller than TOF at each temperature. STY is defined as the number of molecules of both C_{11} and C_{12} hydrocarbons produced per metal site and unit time. As the reaction temperature increased, the difference between STY and TOF decreased, indicating that the high temperature favors the SDO reactions.

The C_{11}/C_{12} ratio, reflecting the deCO vs. HDO selectivity, can be tuned by altering the Ni/Mo ratio in the bimetallic phosphides (Fig. 48). Therefore, by using a bimetallic NiMo phosphide catalyst instead of monometallic Ni phosphide one, we may decrease considerably the participation of deCO pathway in the whole SDO process. This could be a quite useful tool for confronting the methanation problem related to the nickel catalysts.

In the second contribution [227] the same group studied the effect of calcination temperature of the precursor of a SiO_2-supported Ni–Mo phosphide catalyst, selected from the first study,

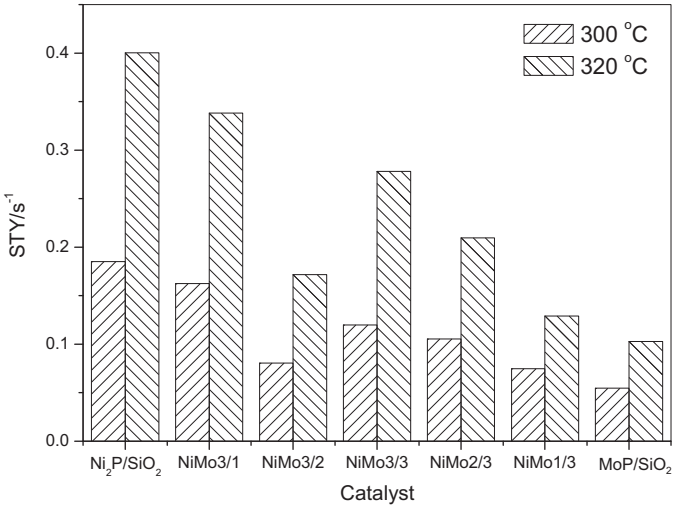

Fig. 47. Site time yield of the C_{11} and C_{12} hydrocarbons upon SDO of methyl laurate over Ni–Mo phosphide catalysts with various Ni/Mo molar ratios. Source: Ref. [226].

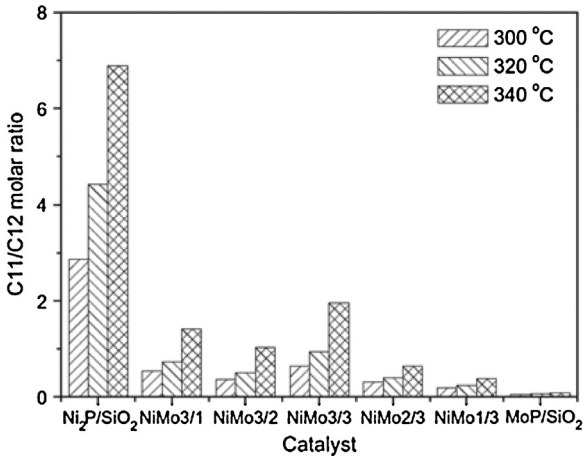

Fig. 48. C_{11}/C_{12} molar ratios in the SDO product of methyl laurate obtained over Ni–Mo phosphide catalysts with various Ni/Mo molar ratios at various reaction temperatures. Source: Ref. [226].

on the catalyst structure and catalytic performance for the SDO of methyl laurate (Table 6, entry 5). The phosphide catalysts prepared from the precursors calcined at 400, 500, 600, 700 and 800 °C were denoted as C400, C500, C600, C700 and C800, respectively.

Extensive characterization showed that the $NiMoP_2$ phase is formed in the samples C400 and C500 besides the Ni_2P and MoP phases, whereas only the Ni_2P and MoP phases are detected in the C600, C700 and C800 samples. Moreover, it was found that the Mo atoms are penetrated in the lattice of the Ni_2P phase in the C400, C500 and C600 samples but the extent of penetration decreases with the calcination temperature. In general, as the calcination temperature increases the interaction between Ni and Mo decreases and the phosphide crystallite size tended to increase, subsequently leading to the decrease in the surface metal site density.

Inspection of Fig. 49 shows that the highest activity is exhibited by the C600 catalyst over all temperatures studied. The samples calcined at 700 and 800 °C exhibited relatively low activity and total selectivity to C_{11} and C_{12} hydrocarbons (Fig. 50).

Inspection of Fig. 50 shows, moreover, that the C_{11}/C_{12} molar ratio increases with the calcination temperature suggesting that deCO is favored over HDO [177,180]. This behavior has been mainly attributed to the decreased Ni-Mo interaction and the increased phosphide particle size with calcination temperature.

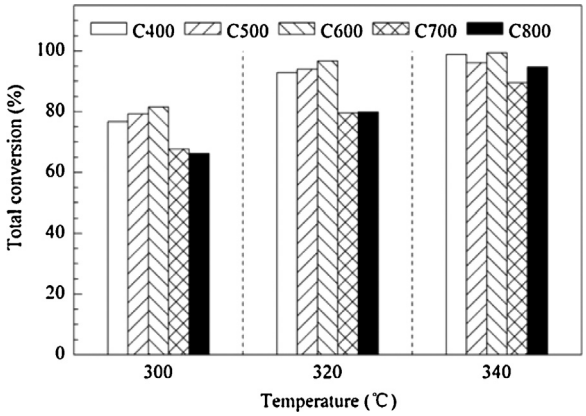

Fig. 49. Methyl laurate conversion over SiO_2-supported Ni–Mo phosphide catalysts determined at various reaction temperatures. Source: Ref. [227].

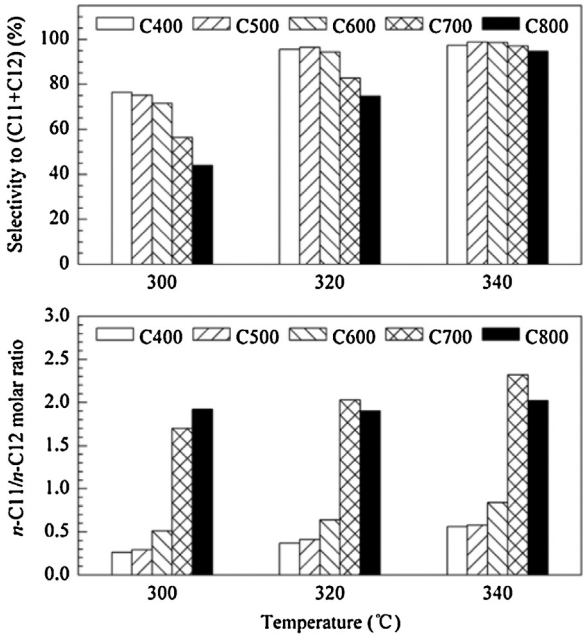

Fig. 50. Variation of $(C_{11}+C_{12})$ selectivity and C_{11}/C_{12} molar ratio with calcination temperature at various reaction temperatures. Source: Ref. [227].

The above shows that the structure and performance of Ni-Mo bimetallic phosphide catalyst can be further tuned by regulating the calcination temperature of the precursor. The calcination at 600 °C seems to be quite attractive leading to a catalyst with the highest activity, quite high total selectivity to C_{11} and C_{12} hydrocarbons and relatively small C_{11}/C_{12} ratio suppressing deCO and facing thus the methanation problem.

Closing this subsection we have to stress that the NiMo carbides and nitrides supported on the acidic ZSM-5 catalyze the production of OLP instead of green diesel upon hydrotreatment of soybean oil. This is mainly due to the high acidity of the support. The carbides are in advantage with respect to the nitrides due to their relatively low methanation activity. The Ni/Mo molar ratio is also critical for the carbide catalysts revealing the beneficial action of nickel. In fact, in the absence of nickel, polymerization might be the predominant reaction causing plugging in the catalyst bed whereas a large amount of $>C_{23}$ hydrocarbons was produced but almost no hydrocarbons in the gasoline, kerosene and green diesel range. The change of the support in the Ni/Mo carbide catalysts from the acidic microporous zeolites (ZSM-5, zeolite β, USY zeolite) to the mesoporous support (Al-SBA-15, γ-alumina) shifts the process from the

cracking/hydrocracking to the SDO and thus increases considerably the selectivity to green diesel. It was mainly attributed to the mesoporous structure which facilitates the diffusion of large triglyceride molecules, limiting thus the secondary cracking which is not the case for the microporous zeolites. This reveals the importance of the support texture on the selectivity to green diesel besides the effect of acidity. The study of NiW catalysts supported on the most promising support (Al-SBA-15) revealed the influence of the preparation method and the Ni/W ratio on the activity and selectivity for the transformation of natural triglycerides into green diesel. Concerning the less sophisticated impregnated catalysts it was found that the highest Ni/W molar ratio (9/1) results to the best physicochemical and catalytic behavior, again pointing out the beneficial role of nickel. The direct comparison of the NiMo and NiW carbide catalysts developed in this work with the corresponding nickel carbide and reduced nickel monometallic catalysts with the same nickel content would be very useful for a more rigorous evaluation of the former catalysts. Such a comparison must be reported in the near future. Concerning NiMo phosphide catalysts supported on silica the activity seems to be not influenced by the Ni/Mo ratio, while the SDO pathway can be tuned by altering this ratio as well as the calcination temperature of the precursor material. The suppression of deCO and the acceleration of HDO can be proved useful for facing the methanation problem related to nickel catalysts.

3.9. Influence of hydrogen partial pressure on the SDO over Ni catalysts

It is well known that quick deactivation of catalysts takes place in the absence of hydrogen that require multiple regeneration. Thus in this section we are going to provide a short resume of contributions dealing with the catalytic performance of Ni catalysts in the absence of hydrogen and then we will review a work dealing with the influence of hydrogen partial pressure on the SDO over Ni catalysts.

As already mentioned (Section 3.1) the first work dealing with natural triglycerides transformation to green diesel over Ni catalysts was reported by Snåre et al. [94]. They studied the deoxygenation of stearic acid over a lot of metallic catalysts in the absence of hydrogen which resulted to rather very low catalytic performance concerning the nickel catalysts.

The second relevant work was reported by Morgan et al. [106]. They studied the deoxygenation of tristearin, triolein and soybean oil over a 20 wt% Ni/C catalyst under N_2. Moreover, they compared the catalytic performance of the nickel catalyst with two typical noble metal catalysts supported on the same support (5% Pd/C and 1% Pt/C). The conversion of triglycerides to hydrocarbons obtained over the nickel catalyst was considerably higher than that obtained over the platinum and palladium catalyst. These results are not in agreement with those mentioned before for the catalysts supported on oxidic supports [94]. This could be attributed to the quite small nickel crystals obtained on the very high surface area of active carbon.

Taking into account the superior activity of the Ni catalyst with respect to Pd and Pt catalysts both for triglycerides conversion and cracking of the fatty acid chains to light hydrocarbons Morgan et al. [228] extended their investigation on the deoxygenation of triolein and soybean oil under nitrogen atmosphere using a nickel catalyst supported on γ-alumina (Ni/Al_2O_3), as well as Ni–Al, Ni–Mg–Al and Mg–Al layered double hydroxides (LDH). Obviously, catalysts of this type are more easily regenerated via burn-off of the coke than the nickel catalyst supported on carbon. The aforementioned LDH catalysts might be of interest, since the homogeneous mixing of Ni and Al potentially allows obtaining high nickel loadings and dispersions [229]. Moreover, these catalysts allow examining the effect of basicity on catalyst performance through the incorporation of Mg ions in the solid structure.

The catalytic deoxygenation of triolein and soybean oil over the tested catalysts yielded gaseous, liquid and solid products. The liquid product largely prevailed in all cases whereas the solid fraction (coke, graphitized carbon) was very small in all cases. It is remarkable that the maximum (minimum) amount of the liquid (solid) product was obtained over the impregnated nickel catalyst.

In a recent study Santillan—Jimenez et al. [230] chose the most promising catalyst of the previous study, namely the Ni–Al layered double hydroxide catalyst, and the 20% Ni/Al_2O_3 catalyst (for comparison) in order to investigate the effect of the gaseous atmosphere(N_2, $10H_2/N_2$, H_2) on the catalytic behavior and stability. The conversions of stearic acid and tristearin to fuel-like hydrocarbons were used as probe reactions (Table 7, entry 1). Both the catalytic performance and the extent of catalyst fouling were found to show a marked dependence on the hydrogen partial pressure and on the Ni-specific surface area of the catalyst employed. The amenability of a representative spent catalyst to regeneration via calcination in air was also demonstrated. The regenerated catalyst was observed to outperform the fresh formulation when tested for activity in the conversion of lipids to fuel-like hydrocarbons. This is attributed to the formation of strong basic sites – which are capable of catalyzing the deoxygenation of lipids – during the regeneration process. The fact that inexpensive Ni-based catalysts capable of affording good yields of fuel-like hydrocarbons can be regenerated by treatment in hot air makes these formulations interesting from an industrial standpoint.

Summarizing the most important findings of this sub-section we can conclude that the hydrogen partial pressure is crucial for the catalytic performance of nickel catalysts.

3.10. Stability of Ni catalysts upon SDO of natural triglycerides

Ni-catalysts are known to produce carbon deposits intensively during hydrocarbons conversion at elevated temperatures. This leads to their faster deactivation compared with noble metal catalysts. Also CO evolved as a result of triglycerides decarbonylation may poison Ni catalysts. Since the production of renewable fuels in large amounts may be done only in reactors working in continuous mode the information about stability of Ni-catalysts is important. Thus in this section this issue will be presented based on available data.

It seems that the stability of Ni catalysts used for green diesel production could be improved by: (a) using suitable support (as already mentioned a very active 10% Ni/ZrO_2 catalyst tested in the SDO of micro-algae oil by the group of Lercher was not deactivated for a time on stream equal to 72 h [111]), (b) using Ni_2P instead of metallic Ni (See for example, the behavior of Ni_2P/SAPO-11 and Ni/SAPO-11 catalysts tested by Zhao et al. [176] for the SOD of methyl laurate. Also, as it is proved by Zarchin et al. [178] Ni_2P supported on silica or HY maintain its SDO activity for >600 h though on the later support a diminution of hydrocracking activity is observed after 150 h on stream). (c) doping (Ce doped NiMo non sulfided catalysts supported on alumina exhibited constant yield for at least 160 h on stream upon transformation of Jatropha oil to green diesel [183]. P in Ni-HPW(30%)/nHA catalyst maintained the conversion of Jatropha oil stable for at least 200 h on steam [188]. La has a very positive effect on the reduction of the coke formed on NiW/nHA, NiW/Al_2O_3 and NiW/HY catalysts [231]) (d) using bimetallic active phase ($NiCu/ZrO_2$ catalysts proved to be quite stable, with low sintering and little coking during HDO of bio-oils produced via pyrolysis of Chlorella and *Nannochloropsis* sp. [232]).

Table 7
An overview of the reactant, catalysts, preparation, characterization and reaction conditions for deoxygenation under various hydrogen partial pressures.

Entry/Refs.	Reactant	Catalyst/preparation	Characterization	Reaction conditions
1/[230]	Stearic acid (SA) and tristearin (TS) in dodecane	20% Ni/γ-Al_2O_3 s.-i.w.i. Ni–Al layered double hydroxide (LDH) $[Ni_{0.67}Al_{0.33}(OH)_2][CO_3]_{0.17}\cdot mH_2O$ c.p. of metal nitrate salts with a mixture of NaOH and Na_2CO_3 at pH 10	N_2-physisorption XRD TPR CO_2-TPD TGA	SBR, mass of catalyst: 0.5 g For SA: (temperature: 300 °C, pressure: 9.2 bar, time: 1.5 h) For TS: (temperature: 355 °C, pressure: 39.5 bar, time: 6 h) Reactant: 1.75 g Solvent: 25 g Gas (N_2, 10% H_2/N_2, H_2) flow: 70 mL Stirring rate: 1000 rpm

4. Concluded remarks and future perspectives

The critical review attempted in this contribution allows elaborating a synthetic picture concerning the development of nickel based catalysts for the transformation, by hydrotreatment, of natural triglycerides into hydrocarbons in the diesel range. In spite of the early rather bad predictions, the work done in the last years indicated the potential suitability of these quite cheap catalysts in the green diesel production. The principal lines of the research in this domain are now clearly emerged. These concern catalytic supports, promoters and nickel loading, the SDO mechanism, the effect of preparation method, the use of other nickel formulations beside the metallic nickel supported nanoparticles (nickel phosphides), the use of bimetallic catalysts with Mo and W in the reduced state as well as nitrides, carbides and phosphides, the direct comparison of the nickel based non-sulphided catalysts with the conventional CoMo, NiMo and NiW hydrotreatment catalysts and noble metals and the use of catalysts in an atmosphere with lower or no hydrogen content.

The simultaneous achievement of high activity, selectivity for hydrocarbons in the diesel range with small amounts of branched hydrocarbons for obtaining good pour properties together with high catalyst stability and low hydrogen demand is not, in effect, an easy task. However, considerable progress has been pointed out towards this ambitious goal. It seems that supports with high surface area (>250 $m^2\ g^{-1}$), medium acidity and mesoporous structure are suitable for the preparation of mono-metallic nickel catalysts with high activity and selectivity for linear hydrocarbons in the diesel range. In contrast, nickel based catalysts supported on zeolites with high acidity and narrow pores though very active they favor extended hydrocracking of the natural triglycerides. The use of reducible supports (simple TiO_2, ZrO_2 and CeO_2 oxides or mixed ones) of high surface area (>150 $m^2\ g^{-1}$) will presumably results to more effective SDO catalysts.

A problem with the nickel monometallic catalysts is that they favor deCO and the subsequent methanation of the resulting CO, which is a quite hydrogen consuming route with respect to HDO. It seems that the use of nickel phosphide or, mainly, NiMo phosphide catalysts with proper Ni/Mo ratio results to the impressive inhibition of deCO and the acceleration of HDO. Moreover, a decrease in the extent of methanation seems to be achieved using a suitable promoter (e.g., copper). However, very few studies concerning the effect of promoters in nickel monometallic catalysts have been reported so far and the subject is indeed open for further research. This should include the study of bimetallic catalysts of basic metals (e.g., NiCo, NiFe and NiCu). Quite promising are the studies devoted to the addition of promoters (La, Ce, P) in the traditional NiMo and NiW hydrotreatment catalysts working in their reduced form. The target to reach the activity of the corresponding sulphided catalysts seems to be obtained. However, a considerable progress is expected concerning this kind of catalysts by investigating the best Ni/Mo or Ni/W ratio which is not necessarily the critical ratio of the sulphided hydrotreatment catalysts.

The achievement of considerable isomerization activity without extending cracking is perhaps a very difficult task. Thus, in spited of the progress pointed out we need much more work in order to obtain this goal in one step process.

Only few studies have been devoted to the preparation method. Most of the preparations have been mainly limited to the application of some kind of impregnation. The application of the co-precipitation or co-gelation methods with a careful control of the preparation parameters is expected leading to the development of catalyst with high nickel content (in the range 30–60% instead of about 5–20% frequently reported so far) and high surface area (>250$m^2\ g^{-1}$), namely to catalysts with higher active surface.

Considerable progress has been obtained concerning the SDO mechanism. The two of the three main routes (deCO, HDO) pass from common initial steps (triglyceride → fatty acid → aldehyde → alcohol). The intermediate aldehyde is decarbonylated (deCO) whereas the corresponding alcohol, being in equilibrium with aldehyde, is dehydrated and the resulting alkene is hydrogenated (HDO). The metallic nickel nanoparticles favor deCO. The whole SDO involves several additional routes besides the aforementioned principal ones as the direct deCO_2 of the intermediate fatty acid, the hydrolysis of the triglycerides by the water produced through the HDO, the esterification of the intermediate alcohols and fatty acids, the etherification of the alcohols as well as cracking and isomerizations. The change of the support, the formulation of the supported nanoparticles and the use of promoters and bimetallic phases does not affect considerably the main characteristics of the SDO mechanism but rather the relative contribution of each pathway and individual step in the whole mechanism. There is no doubt that more knowledge will be gained in the next few years concerning the SDO mechanism.

A final point concerns the evaluation of the catalysts studied by various groups under different experimental conditions. For a comparative evaluation the reader has to pay attention on several important experimental details illustrated in the tables, besides the temperature and hydrogen pressure. Specifically, the LHSV value when used FBR (taking into account, in addition, the concentration of the reactant in the feed) as well as the mass of the reactant to the catalyst ratio when BR or SBR have been used are actually very important parameters for comparing catalytic performances reported by different groups.

References

[1] N. Armaroli, V. Balzani, Angew. Chem. Int. Ed. 46 (2007) 52–66.
[2] K. Li, S. Liu, X. Liu, Int. J. Energy Res. 8 (2014) 965–977.
[3] P. Kallio, A. Pasztor, M.K. Akhtar, P.R. Jones, Curr. Opin. Biotechnol. 26 (2014) 50–55.
[4] R. Harun, J.W.S. Yip, S. Thiruvenkadam, W.A.W.A.K. Ghani, T. Cherrington, M.K. Danquah, Biotechnol. J. 9 (2014) 73–86.

[5] P. Panagiotopoulou, C. Papadopoulou, H. Matralis, X. Verykios, WIRES Energy Environ. 3 (2014) 231–253.
[6] S. Moka, M. Pande, M. Rani, R. Gakhar, M.J. Sharma Rani, A.N. Bhaskarwa, Renewable Sustainable Energy Rev. 32 (2014) 697–712.
[7] R.O.M.A. de Souza, L.S.M. Miranda, R. Luque, Green Chem. 16 (5) (2014) 2386–2405.
[8] G. Kocar, N. Civas, Renewable Sustainable Energy Rev. 28 (2013) 900–916.
[9] R. Razeghifard, Photosynth. Res. 117 (2013) 207–219.
[10] V.B. Borugadda, V.V. Goud, Renewable Sustainable Energy Rev. 16 (2012) 4763–4784.
[11] A.F. Lee, J.A. Bennett, J.C. Manayil, K. Wilson, Chem. Soc. Rev. 43 (2014) 7887–7916.
[12] B. Bharathiraja, M. Chakravarthy, R.R. Kumar, D. Yuvaraj, J. Jayamuthunagai, R.P. Kumar, S. Palani, Renewable Sustainable Energy Rev. 38 (2014) 368–382.
[13] T.M.Y. Khan, A.E. Atabani, I.A. Badruddin, A. Badarudin, M.S. Khayoond, S. Triwahyono, Renewable Sustainable Energy Rev. 37 (2014) 840–851.
[14] K. Dutta, A. Daverey, J.G. Lin, Renewable Energy 69 (2014) 114–122.
[15] R. Mythili, P. Venkatachalam, P. Subramanian, D. Uma, Int. J. Energy Res. 38 (2014) 1233–1259.
[16] E. Uggetti, B. Sialve, E. Trably, J.P. Steyer, Biofuel Bioprod. Biorefin. 8 (2014) 516–529.
[17] V.S. Yaliwal, N.R. Banapurmath, N.M. Gireesh, P.G. Tewari, Renewable Sustainable Energy Rev. 34 (2014) 608–627.
[18] T. Meyer, E.A. Edwards, Water Res. 65 (2014) 321–349.
[19] R. Kothari, A.K. Pandey, S. Kumar, V.V. Tyagi, S.K. Tyagi, Renewable Sustainable Energy Rev. 39 (2014) 174–195.
[20] E.U. Kiran, A.P. Trzcinski, W.J. Ng, Y. Liu, Fuel 134 (2014) 389–399.
[21] C. Zhang, H. Su, J. Baeyens, T. Tan, Renewable Sustainable Energy Rev. 38 (2014) 383–392.
[22] J. Mata-Alvarez, J. Dosta, M.S. Romero-Güiza, X. Fonoll, M. Peces, S. Astals, Renewable Sustainable Energy Rev. 36 (2014) 412–427.
[23] A.J. Ward, D.M. Lewis, B. Green, Algal Res. 5 (2014) 204–214.
[24] P.M. Christy, L.R. Gopinath, D. Divya, Renewable Sustainable Energy Rev. 34 (2014) 167–173.
[25] Y. Liu, O. Ersen, C. Meny, F. Luck, C. Pham-Huu, ChemSusChem 7 (2014) 1218–1239.
[26] S. Li, J. Gong, Chem. Soc. Rev. 43 (2014) 7245–7256.
[27] W. Kiatkittipong, S. Phimsen, K. Kiatkittipong, S. Wongsakulphasatch, N. Laosiripojana, S. Assabumrungrat, Fuel Process. Technol. 116 (2013) 16–26.
[28] H. Pucher, N. Schwaiger, R. Feiner, P. Pucher, L. Ellmaier, M. Siebenhofer, Int. J. Energ. Res. 38 (2014) 1964–1974.
[29] N. Ibrahim, S.K. Kamarudin, L.J. Minggu, J. Power Sources 259 (2014) 33–42.
[30] S. Dutta, S. Pal, Biomass Bioenergy 62 (2014) 182–197.
[31] A.H. Zacher, M.V. Olarte, D.M. Santosa, D.C. Elliott, S.B. Jones, Green Chem. 16 (2014) 491–515.
[32] D. Karadag, O.E. Koroglu, B. Ozkaya, M. Cakmakci, S. Heaven, C. Banks, J. Chem. Technol. Biotechnol. 89 (2014) 1627–1636.
[33] S. Dutta, J. Ind. Eng. Chem. 20 (2014) 1148–1156.
[34] M.E. Nissila, C.-H. Lay, J.A. Puhakka, Biomass Bioenergy 67 (2014) 145–159.
[35] E.F. Aransiola, T.V. Ojumu, O.O. Oyekola, T.F. Madzimbamuto, D.I.O. Ikhu-Omoregbe, Biomass Bioenergy 61 (2014) 276–297.
[36] C.D.M. de Araújo, C.C. de Andrade, E.D.E. Silva, F.A. Dupas, Renew. Sust. Energ. Rev. 27 (2013) 445–452.
[37] I.M. Lokman, U. Rashid, R. Yunus, Y.H. Taufiq-Yap, Catal. Rev. 56 (2014) 187–219.
[38] S. Bezergianni, A. Dimitriadis, Renewable Sustainable Energy Rev. 21 (2013) 110–116.
[39] M.K. Lam, K.T. Lee, A.R. Mohamed, Biotechnol. Adv. 28 (2010) 500–518.
[40] A. Mazubert, M. Poux, J. Aubin, Chem. Eng. J. 233 (2013) 201–223.
[41] S. Pinzi, D. Leiva-Candia, I. López-García, M.D. Redel-Macías, M.P. Dorado, Biofuels Bioprod. Biorefin. 8 (2014) 126–143.
[42] E. Santacesaria, G. Martinez Vicente, M. Di Serio, R. Tesser, Catal. Today 195 (2012) 2–13.
[43] Z. Yaakob, M. Mohammad, M. Alherbawi, Z. Alam, K. Sopian, Renewable Sustainable Energy Rev. 18 (2013) 184–193.
[44] A. Banerjee, R. Chakraborty, Resour. Conserv. Recycl. 53 (2009) 490–497.
[45] S.B. Glisic, A.M. Orlović, Renewable Sustainable Energy Rev. 31 (2014) 708–725.
[46] I.B. Banković-Ilić, I.J. Stojković, O.S. Stamenković, V.B. Veljkovic, Y.-T. Hung, Renewable Sustainable Energy Rev. 32 (2014) 238–254.
[47] G.G. Muciño, R. Romero, A. Ramírez, S.L. Martínez, R. Baeza-Jiménez, R. Natividad, Fuel 138 (2014) 143–148.
[48] R.A. Lee, J.M. Lavoie, Anim. Front 3 (2013) 6–11.
[49] R. Dillschneider, C. Steinweg, R. Rosello-Sastre, C. Posten, Bioresour. Technol. 142 (2013) 647–654.
[50] Y. Chisti, Trends Biotechnol. 26 (2008) 126–131.
[51] I.T.D. Cabanelas, Z. Steinweg, F.A. Chinalia, C.O. Souza, J.A. Perales, P.F. Almeida, J.I. Druzian, I.A. Nascimento, Appl. Energy 109 (2013) 283–290.
[52] M.K. Ji, R.A.I. Abou-Shanab, S.H. Kim, E.S. Salama, S.H. Lee, A.N. Kabra, Y.S. Lee, S. Hong, B.H. Jeon, Ecol. Eng. 58 (2013) 142–148.
[53] I. Rawat, V. Bhola, R.R. Kumar, F. Bux, Environ. Technol. 34 (2013) 1765–1775.
[54] V. Bhola, F. Swalaha, R. Ranjith Kumar, M. Singh, F. Bux, Int. J. Environ. Sci. Technol. 11 (2014) 2103–2118.
[55] M.F.M. Yusoff, X. Xu, Z. Guo, J. Am. Oil Chem. Soc. 91 (2014) 525–531.
[56] D.E. Lopez, J.G. Goodwin Jr., D.A. Bruce, E. Lotero, Appl. Catal. A 295 (2005) 97–105.
[57] M.K. Lam, A.R. Mohamed, Appl. Catal. B 93 (2009) 134–139.
[58] L.J. Konwar, J. Boro, D. Deka, Renewable Sustainable Energy Rev. 29 (2014) 546–564.
[59] Y.M. Sani, W.M.A.W. Daud, A.R.A. Aziz, Appl. Catal. A 470 (2014) 140–161.
[60] M. Farooq, A. Ramli, D. Subbarao, J. Cleaner Prod. 59 (2013) 131–140.
[61] P. Yin, W. Chen, W. Liu, H. Chen, R.J. Qu, X.G. Liu, Q.H. Tang, Q. Xu, Bioresource Technol. 140 (2013) 146–151.
[62] Q. Zhao, H. Wang, H.W. Zheng, Z. Sun, W. Shi, S.T. Wang, X.H. Wang, Z.J. Jiang, Catal. Sci. Technol. 3 (2013) 2204–2209.
[63] L. Diaz, M.E. Borges, J. Agric. Food Chem. 60 (2012) 7928–7933.
[64] M.E. Borges, L. Diaz, Renewable Sustainable Energy Rev. 16 (2012) 2839–2849.
[65] B. Dou, Y. Song, C. Wang, H. Chen, Y. Xu, Renewable Sustainable Energy Rev. 30 (2014) 950–960.
[66] E.A. Sanchez, R.A. Comelli, Int. J. Hydrogen Energy 39 (2014) 8650–8655.
[67] C.H. Zhou, H. Zhao, D.S. Tong, L.M. Wu, W.H. Yu, Catal. Rev. Sci. Eng. 55 (2013) 369–453.
[68] Y.C. Lin, Int. J. Hydrogen Energy 38 (2013) 2678–2700.
[69] A. Montebelli, C.G. Visconti, G. Groppi, E. Troncon, S. Kohler, H.J. Venvik, R. Myrstad, Appl. Catal. A 481 (2014) 96–103.
[70] J.M. Beiramar, A. Griboval-Constant, A.Y. Khodakov, ChemCatChem 6 (2014) 1788–1793.
[71] S. Kuld, C. Conradsen, P.G. Moses, I. Chorkendorff, J. Sehested, Angew. Chem. Int. Ed. 53 (2014) 5941–5945.
[72] A. Bansode, A. Urakawa, J. Catal. 309 (2014) 66–70.
[73] The European standards organization (CEN): European fuel standards—EN 590 (diesel), EN 14 214 (biodiesel). European Committee for Standardization (CEN), Brussels 2008(EN14214) 2004 (EN590).
[74] I. Kubickova, D. Kubicka, Waste Biomass Valorization 1 (2010) 293–308.
[75] C. Zhao, T. Brück, J.A. Lercher, Green Chem. 15 (2013) 1720–1739.
[76] R.W. Gosselink, S.A.W. Hollak, S.-W. Chang, J. van Haveren, K.P. de Jong, J.H. Bitter, D.S. van Es, ChemSusChem. 6 (2013) 1576–1594.
[77] L. Hermida, A.Z. Abdullah, A.R. Mohamed, Renewable Sustainable Energy Rev. 42 (2015) 1223–1233.
[78] S.N. Naik, V.V. Goud, P.K. Rout, A.K. Dalai, Renewable Sustainable Energy Rev. 14 (2010) 578–597.
[79] T.V. Choudhary, C.B. Phillips, Appl. Catal. A 397 (2011) 1–12.
[80] S. Chen, Int. J. Clean Coal Energy 1 (2012) 43–55.
[81] M. Mohammad, T.K. Hari, Z. Yaakob, Y.C. Sharma, K. Sopian, Renewable Sustainable Energy Rev. 22 (2013) 121–132.
[82] S.-Y. No, Fuel 115 (2014) 88–96.
[83] J. Calero, D. Luna, E.D. Sancho, C. Luna, F.M. Bautista, A.A. Romero, A. Posadillo, J. Berbel, C. Verdugo-Escamilla, Renewable Sustainable Energy Rev. 42 (2015) 1437–1452.
[84] N. Mo, P.E. Savage, ACS Sustainable Chem. Eng. 2 (2014) 88–94.
[85] V.R. Wiggers, G.R. Zonta, A.P. França, D.R. Scharf, E.L. Simionatto, L. Ender, H.F. Meier, Fuel 107 (2013) 601–608.
[86] R. Černý, M. Kubů, D. Kubička, Catal. Today 204 (2013) 46–53.
[87] D. Kubicka, I. Kubickova, J. Cejka, Catal. Rev. Sci. Eng. 55 (2013) 1–78.
[88] S.A.P. da Mota, A.A. Mancio, D.E.L. Lhamas, D.H. de Abreu, M.S. da Silva, W.G. dos Santos, D.A.R. de Castro, R.M. de Oliveira, M.E. Araújo, L.E.P. Borges, N.T. Machado, J. Anal. Appl. Pyrol. 110 (2014) 1–11.
[89] Z.D. Yigezu, K. Muthukumar, Energy Convers. Manag. 84 (2014) 326–333.
[90] T. Morgan, E. Santillan-Jimenez, A.E. Harman-Ware, Y. Ji, D. Grubb, M. Crocker, Chem. Eng. J. 189–190 (2012) 346–355.
[91] R. Fréty, M.D.C. da Rocha, S.T. Brandão, L.A.M. Pontes, J.F. Padilha, L.E.P. Borges, W.A. Gonzalez, J. Braz. Chem. Soc. 22 (2011) 1206–1220.
[92] K. Kon, W. Onodera, S. Takakusagi, K. Shimizu, Catal. Sci. Technol. 4 (2014) 3705–3712.
[93] K. Kandel, J.W. Anderegg, N.C. Nelson, U. Chaudhary, I.I. Slowing, J. Catal. 314 (2014) 142–148.
[94] M. Snåre, I. Kubickova, P. Maki-Arvela, K. Eranen, D.Y. Murzin, Ind. Eng. Chem. Res. 45 (2006) 5708–5715.
[95] V.A. Yakovlev, S.A. Khromova, O.V. Sherstyuk, V.O. Dundich, D. Yu Ermakov, V.M. Novopashina, M. Yu Lebedev, O. Bulavchenko, V.N. Parmon, Catal. Today 144 (2009) 362–366.
[96] V.O. Dundich, S.A. Khromova, D. Yu Ermakov, M. Yu Lebedev, V.M. Novopashina, V.G. Sister, A.I. Yakimchuk, V.A. Yakovlev, Kinet. Catal. 51 (2010) 704–709.
[97] S. Bezergianni, A. Dimitriadis, G. Meletidis, Fuel 125 (2014) 129–136.
[98] S. Bezergianni, A. Dimitriadis, D. Karonis, Fuel 136 (2014) 366–373.
[99] M. Al-Sabawi, J. Chen, Energy Fuels 26 (2012) 5373–5399.
[100] George W. Huber, P. O'Connor, A. Corma, Appl. Catal. A 329 (2007) 120–129.
[101] S. Bezergianni, A. Kalogianni, I.A. Vasalos, Bioresour. Technol. 100 (2009) 3036–3042.
[102] D. Kubička, J. Horáček, M. Setnička, R. Bulánek, A. Zukal, I. Kubičková, Appl. Catal. B 145 (2014) 101–107.
[103] A. Vonortas, N. Papayannakos, WIREs Energy Environ. 3 (2014) 3–23.
[104] T.N. Kalnes, K.P. Koers, T. Marker, D.R. Shonnard, Sustainable Energy 28 (2009) 111–120.
[105] S. Mikkonen, T. Hartikka, M. Kuronen, P. Saikkonen In, HVO, in: In HVO, Hydrotreated Vegetable Oil—A Premium Renewable Biofuel for Diesel Engines, Neste Oil Proprietary Publication, 2012.

[106] T. Morgan, D. Grubb, E. Santillan-Jimenez, M. Crocker, Top. Catal. 53 (2010) 820–829.
[107] S. Lestari, P. Maki-Arvela, K. Eranen, J. Beltramini, G.Q.M. Lu, D.Y. Murzin, Catal. Lett. 134 (2010) 250–257.
[108] B. Rozmyslowicz, P. Maki-Arvela, S. Lestari, O.A. Simakova, K. Eranen, I.L. Simakova, D.Y. Murzin, T.O. Salmi, Top. Catal. 53 (2010) 1274–1277.
[109] P. Maki-Arvela, B. Rozmyslowicz, S. Lestari, O. Simakova, K. Eranen, T. Salmi, D.Y. Murzin, Energy Fuels 25 (2011) 2815–2825.
[110] B. Peng, Y. Yao, C. Zhao, J.A. Lercher, Angew. Chem. Int. Ed. 51 (2012) 2072–2075.
[111] B. Peng, X. Yuan, C. Zhao, J.A. Lercher, J. Am. Chem. Soc. 134 (2012) 9400–9405.
[112] B. Peng, C. Zhao, S. Kasakov, S. Foraita, J.A. Lercher, Chem. Eur. J. 19 (2013) 4732–4741.
[113] H. Zuo, Q. Liu, T. Wang, N. Shi, J. Liu, L. Ma, J. Fuel Chem. Techn. 40 (2012) 1067–1073.
[114] H. Zuo, Q. Liu, T. Wang, L. Ma, Q. Zhang, Q. Zhang, Energy Fuels 26 (2012) 3747–3755.
[115] Q. Liu, H., Zuo, T., Wang, L., Ma, Q. Zhang, Appl. Catal. A: Gen. 468 (2013) 68–74.
[116] Q. Liu, H. Zuo, Q. Zhang, T. Wang, L. Ma, Chinese J, Catal 35 (2014) 748–756.
[117] C. Ochoa-Hernández, Y. Yang, P. Pizarro, V.A. de la Peña O'Shea, J.M. Coronado, D.P. Serrano, Catal, Today 210 (2013) 81–88.
[118] N. Shi, Q. Liu, T. Jiang, T. Wang, L. Ma, Q. Zhang, X. Zhang, Catal. Commun. 20 (2012) 80–84.
[119] P. Kumar, S.R. Yenumala, S.K. Maity, D. Shee, Appl. Catal. A 471 (2014) 28–38.
[120] V.C.S. Palla, D. Shee, S.K. Maity, RSC Adv. 4 (2014) 41612–41621.
[121] S. Krompiec, J. Mrowiec-Białoń, K. Skutil, A. Dukowicz, L. Pająk, A.B. Jarzębski, J. Non-Cryst. Solids 315 (2003) 297–303.
[122] K. Bourikas, C. Kordulis, A. Lycourghiotis, Chem. Rev. 114 (2014) 9754–9823.
[123] T. Yokoyama, T. Setoyama, N. Fujita, M. Nakajima, T. Maki, Appl. Catal. A 88 (1992) 149–161.
[124] R. Pestman, R.M. Koster, E. Boellaad, A.M. van der Kraan, V. Ponec, J. Catal. 174 (1998) 142–152.
[125] T. Yokoyama, N. Yamagata, Appl. Catal. A 221 (2001) 227–239.
[126] R.D. Haley, M.S. Tikhov, R.M. Lambert, Catal. Lett. 76 (2001) 125–130.
[127] K.I. Gursahani, R. Alcala, R.D. Cortright, J.A. Dumesic, Appl. Catal. A 222 (2001) 369–392.
[128] S.K. Kim, J.Y. Han, H. Lee, T. Yum, Y. Kim, J. Kim, Appl. Energy 116 (2014) 199–205.
[129] R. Alcala, M. Mavrikakis, J.A. Dumesic, J. Catal. 218 (2003) 178–190.
[130] C. Dupont, R. Lemeur, A. Daudin, P. Raybaud, J. Catal. 279 (2011) 276–286.
[131] R. Kaewmeesri, A. Srifa, V. Itthibenchapong, K. Faungnawakij, Energy Fuels 29 (2015) 833–840.
[132] W. Song, C. Zhao, J.A. Lercher, Chem. Eur. J. 19 (2013) 9833–9842.
[133] K. Bourikas, C. Kordulis, A. Lycourghiotis, Catal. Rev. Sci. Eng. 48 (2006) 363–444.
[134] L.A.M. Hermans, J.W. Geus, Preparation of Catalysts II, in: P. Delmon, P.A. Jacobs, G. Poncelet (Eds.), Elsevier, Amsterdam, 1979, p. 113.
[135] M. Han, Q. Liu, J. He, Y. Song, Z. Xu, J. Zhu, J. Adv. Mater. 19 (2007) 1096–1100.
[136] Z. Liu, Y. Wang, J. Li, R. Zhang, RSC Adv. 4 (2014) 13280–13292.
[137] S.-C. Qi, X.-Y. Wei1, Z.-M. Zong, J. Hayashi, X.-H. Yuan, L.-B. Sun, ChemCatChem 5 (2013) 3543–3547.
[138] S.M. Sajjadi, M. Haghighi, A.A. Eslami, F. Rahmani, J. Sol Gel Sci. Technol. 67 (2013) 601–617.
[139] S.C. Qi, X.Y. Wei, Z.M. Zong, Y.K. Wang, RSC Adv. 3 (2013) 14219–14232.
[140] B. Roy, K. Artyushkova, H.N. Pham, L. Li, A.K. Datye, C.A. Leclerc, Int. J. Hydrogen Energy 37 (2012) 18815–18826.
[141] B. Roy, U. Martinez, K. Loganathan, A.K. Datye, C.A. Leclerc, Int. J. Hydrogen Energy 37 (2012) 8143–8153.
[142] M.V. Bykova, D.Yu. Ermakov, V.V. Kaichev, O.A. Bulavchenko, A.A. Saraev, M. Yu Lebedev, V.A. Yakovlev, Appl. Catal. B 113–114 (2012) 296–307.
[143] P.G. Savva, K. Goundani, J. Vakros, K. Bourikas, Ch. Fountzoula, D. Vattis, A. Lycourghiotis, Ch. Kordulis, Appl. Catal. B 79 (2008) 199–207.
[144] G. Onyestyak, S. Harnos, A. Szegedi, D. Kallo, Fuel 102 (2012) 282–288.
[145] B. Veriansyah, J.Y. Han, S.K. Kim, S.-A. Hong, Y.J. Kim, J.S. Lim, Y.-W. Shu, S.-G. Oh, J. Kim, Fuel 94 (2012) 578–585.
[146] S.K. Kim, S. Brand, H. Lee, Y. Kim, J. Kim, Chem. Eng. J. 228 (2013) 114–123.
[147] E. Santillan-Jimenez, T. Morgan, J. Lacny, S. Mohapatra, M. Crocker, Fuel 103 (2013) 1010–1017.
[148] A. Srifa, K. Faungnawakij, V. Itthibenchapong, S. Assabumrungrat, Chem. Engin. J. (2014), http://dx.doi.org/10.1016/j.cej.2014.09.106
[149] N. Chen, S. Gong, H. Shirai, T. Watanabe, E.W. Qian, Appl. Catal. A 466 (2013) 105–115.
[150] I. Simakova, O. Simakova, P. Maki-Arvela, A. Simakov, M. Estrada, D.Y. Murzin, Appl. Catal. A 355 (2009) 100–108.
[151] E. Santillan-Jimenez, T. Morgan, J. Shoup, A.E. Harman-Ware, M. Crocker, Catal. Today 237 (2014) 136–144.
[152] K. Murata, Y. Liu, M. Inaba, I. Takahara, Energy Fuels 24 (2010) 2404–2409.
[153] X. Wang, P. Clark, S.T. Oyama, J. Catal. 208 (2002) 321–331.
[154] M. Lu, A. Wang, X. Li, X. Duan, Y. Teng, Y. Wang, C. Song, Y. Hu, Energy Fuels 21 (2007) 554–560.
[155] X. Liu, J. Chen, J. Zhang, Ind. Eng. Chem. Res. 47 (2008) 5362–5368.
[156] J.A. Cecilia, I. Jimenez-Morales, A. Infantes-Molina, E. Rodríguez-Castellon, A. Jimenez-Lopez, J. Mol. Catal. A 368 (2013) 78–87.
[157] S.F. Zaman, K.J. Smith, Appl. Catal. A 378 (2010) 59–68.
[158] X. Song, Y. Ding, W. Chen, W. Dong, Y. Pei, J. Zang, L. Yan, Y. Lu, Chin. J. Catal. 33 (2012) 1938–1944.
[159] R. Cheng, Y. Shu, M. Zheng, L. Li, J. Sun, X. Wang, T. Zhang, J. Catal. 249 (2007) 397–400.
[160] P. Liu, J.A. Rodriguez, Y. Takahashi, K. Nakamura, J. Catal. 262 (2009) 294–303.
[161] H.Y. Zhao, D. Li, P. Bui, S.T. Oyama, Appl. Catal. A 391 (2011) 305–310.
[162] V.M.L. Whiffen, K.J. Smith, Energy Fuels 24 (2010) 4728–4737.
[163] K. Li, R. Wang, J. Chen, Energy Fuels 25 (2011) 854–863.
[164] J.A. Cecilia, A. Infantes-Molina, E. Rodríguez-Castellon, A. Jimenez-Lopez, S.T. Oyama, Appl. Catal. B 136 (2013) 140–149.
[165] P. Liu, J.A. Rodriguez, Y. Takahashi, K. Nakamura, J. Catal. 262 (2009) 294–303.
[166] S.T. Oyama, X. Wang, Y.-K. Lee, K. Bando, F.G. Requejo, J. Catal. 210 (2002) 207–217.
[167] P. Liu, J.A. Rodriguez, T. Asakura, J. Gomes, K. Nakamura, J. Phys. Chem. B 109 (2005) 4575–4583.
[168] Y. Yang, C. Ochoa-Hernandez, P. Pizarro, V.A. de la Pena O'shea, J.M. Coronado, D.P. Serrano, Top. Catal. 55 (2012) 991–998.
[169] Y. Yang, C. Ochoa-Hernandez, V.A. de la Pen˜a O'shea, J.M. Coronado, D.P. Serrano, ACS Catal. 2 (2012) 592–598.
[170] Y. Yang, J. Chen, H. Shi, Energy Fuels 27 (2013) 3400–3409.
[171] H. Shi, J. Chen, Y. Yang, S. Tian, Fuel Process Technol. 118 (2014) 161–170.
[172] O.I. Şenol, E.M. Ryymin, T.R. Viljava, A.O.I. Krause, J. Mol Catal. A 277 (2007) 107–122.
[173] E. Laurent, B. Delmon, Appl. Catal. A 109 (1994) 77–96.
[174] E. Laurent, B. Delmon, Appl. Catal. A 109 (1994) 97–115.
[175] J. Huang, J. Chen, Chin. J. Catal. 33 (2012) 790–796.
[176] S. Zhao, M. Li, Y. Chu, J. Chen, Energy Fuels 28 (2014) 7122–7132.
[177] J. Chen, H. Shi, L. Li, K. Li, Appl. Catal. B 144 (2014) 870–884.
[178] R. Zarchin, M. Rabaev, R. Vidruk-Nehemya, M.V. Landau, M. Herskowitz, Fuel 139 (2015) 684–691.
[179] M. Herskowitz, M.V. Landau, Y. Reizner, D. Berger, Fuel 111 (2013) 157–164.
[180] S. Lestari, P. Mäki-Arvela, J. Beltramini, G.Q.M. Lu, D.Y. Murzin, ChemSusChem 2 (2009) 1109–1119.
[181] J. Liu, C. Liu, G. Zhou, S. Shen, L. Rong, Green Chem. 14 (2012) 2499–2505.
[182] J. Liu, S. Yoda, J. He, L. Deng, K. Fan, L. Rong, Chem. Lett. 43 (2014) 310–312.
[183] J. Liu, K. Fan, W. Tian, C. Liu, L. Rong, Int. J. Hydrogen Energy 37 (2012) 17731–17737.
[184] T. Kimura, H. Imai, X. Li, K. Sakashita, S. Asaoka, S.S. Al-Khattaf, Catal. Lett. 143 (2013) 1175–1181.
[185] C. Liu, J. Liu, G. Zhou, W. Tian, L. Rong, J. Taiwan Inst. Chem. Eng. 44 (2013) 221–227.
[186] C. Liu, J. Liu, G. Zhou, W. Tian, L. Rong, Environ. Prog. Sustainable 32 (2013) 1240–1246.
[187] G. Zhou, Y. Hou, L. Liu, H. Liu, C. Liu, J. Liu, H. Qiao, W. Liu, Y. Fan, S. Shen, L. Rong, Nanoscale 4 (2012) 7698–7703.
[188] K. Fan, J. Liu, X. Yang, L. Rong, Int. J. Hydrogen Energy 39 (2014) 3690–3697.
[189] S.J. Reaume, N. Ellis, Energies 6 (2013) 619–633.
[190] J.A. Martens, D. Verboekend, K. Thomas, G. Vanbutsele, J.P. Gilson, J. Perez-Ramırez, ChemSusChem 6 (2013) 421–425.
[191] S.V. Konnov, I.I. Ivanova, O.A. Ponomareva, V.I. Zaikovskii, Microporous Mesoporous Mater. 164 (2012) 222–231.
[192] J. Hancsok, M. Krar, S. Magyar, L. Boda, A. Hollo, D. Kallo, Microporous Mesoporous Mater. 101 (2007) 148–152.
[193] P. Simacek, D. Kubicka, I. Kubickova, F. Homola, M. Pospısil, J. Chudoba, Fuel 90 (2011) 2473–2479.
[194] A. Ivanov, T. Vasina, V. Nissenbaum, L. Kustov, M. Timofeeva, J. Houzvicka, Appl. Catal. A 259 (2004) 65–72.
[195] B. Gagea, Y. Lorgouilloux, Y. Altintas, P. Jacobs, J. Martens, J. Catal. 265 (2009) 99–108.
[196] B. Qiu, X. Yi, L. Lin, W. Fang, H. Wan, Catal. Today 131 (2008) 464–471.
[197] H. Jin, X. Yi, X. Sun, B. Qiu, W. Fang, W. Weng, H. Wan, Fuel 89 (2010) 1953–1960.
[198] M. Roussel, J.-L. Lemberton, M. Guisnet, T. Cseri, E. Benazzi, J. Catal. 218 (2003) 427–437.
[199] M. Roussel, S. Norsic, J.-L. Lemberton, M. Guisnet, T. Cseri, E. Benazzi, Appl. Catal. A 279 (2005) 53–58.
[200] Y. Villasana, Y. Escalante, J.E. Rodríguez Nuñez, F.J. Méndez, S. Ramírez, M.A. Luis-Luis, E. Cañizales, J. Ancheyta, J.L. Brito, Catal. Today 220–222 (2014) 318–326.
[201] Y. Villasana, F. Ruscio-Vanalesti, C. Pfaff, F.J. Méndez, M.Á. Luis-Luis, J.L. Brito, Fuel 110 (2013) 259–267.
[202] W. Zhang, Y. Zhang, L. Zhao, W. Wei, Energy Fuels 24 (2010) 2052–2059.
[203] H. Zhao, S.T. Oyama, H.-J. Freund, R. Włodarczyk, M. Sierka, Appl. Catal. B 164 (2015) 204–216.
[204] J.A. Cecilia, A. Infantes-Molina, E. Rodríguez-Castellón, A. Jiménez-López, S.T. Oyama, Appl. Catal. B 136–137 (2013) 140–149.
[205] E. Furimsky, Appl. Catal. A 240 (2003) 1–28.
[206] W. Zhang, Y. Zhang, L. Zhao, W. Wei, Energy Fuels 24 (2010) 2052–2059.
[207] B. Diaz, S.J. Sawhill, D.H. Bale, R. Main, D.C. Phillips, S. Korlann, R. Self, M.E. Bussell, Catal. Today 86 (2003) 191–209.
[208] S. Ramanathan, S.T. Oyama, J. Phys. Chem. 99 (1995) 16365–16372.
[209] L.A. Santillan-Vallejo, J.A. Melo-Banda, A.I. Reyes de la Torre, G. Sandoval-Robles, J.M. Domínguez, A. Montesinos-Castellanos, J.A. de los Reyes-Heredia, Catal. Today 109 (2005) 33–41.

[210] S.T. Oyama, T. Gott, H. Zhao, Y.-K. Lee, Catal. Today 143 (2009) 94–107.
[211] E. Furimsky, Catal. Today 217 (2013) 13–56.
[212] J. Monnier, H. Sulimma, A. Dalai, G. Caravaggio, Appl. Catal. A 382 (2010) 176–180.
[213] J. Han, J. Duan, P. Chen, H. Lou, X. Zheng, H. Hong, Green Chem. 13 (2011) 2561–2568.
[214] J. Han, J. Duan, P. Chen, H. Lou, X. Zheng, H. Hong, ChemSusChem 5 (2012) 727–733.
[215] W. Zhang, Y. Zhang, L. Zhao, W. Wei, Energy Fuels 24 (2010) 2052–2059.
[216] H. Wang, S. Yan, S.O. Salley, K.Y. Simon Ng, Ind. Eng. Chem. Res. 51 (2012) 10066–10073.
[217] J.S. Lee, S.T. Oyama, M. Boudart, J. Catal. 106 (1987) 125–133.
[218] E. Iglesia, F.H. Ribeiro, M. Boudart, J.E. Baumgartner, Catal. Today 15 (1992) 307–337.
[219] J.S. Lee, M. Boudart, Catal. Lett. 20 (1993) 97–106.
[220] J.B. Claridge, A.P.E. York, A.J. Brungs, M.L.H. Green, Chem. Mater. 12 (2000) 132–142.
[221] H. Wang, S. Yan, S.O. Salley, K.Y. Simon Ng, Fuel 111 (2013) 81–87.
[222] R. Sotelo-Boyas, Y. Liu, T. Minowa, Ind. Eng. Chem. Res. 50 (2010) 2791–2799.
[223] S. Wu, J. Huang, T. Wu, K. Song, H. Wang, L. Xing, H. Xu, L. Xu, J. Guan, Q. Kan, Chin. J. Catal. 27 (2006) 9–14.
[224] B. Al Alwan, E. Sari, S.O. Salley, K.Y. Simon Ng, Ind. Eng. Chem. Res. 53 (2014) 6923–6933.
[225] M.Q. Zhao, R.M. Crooks, Chem. Mater. 11 (1999) 3379–3385.
[226] J. Chen, Y. Yang, H. Shi, M. Li, Y. Chu, Z. Pan, X. Yu, Fuel 129 (2014) 1–10.
[227] Z. Pan, R. Wang, M. Li, Y. Chu, J. Chen, J. Energy Chem. 24 (2015) 77–86.
[228] T. Morgan, E. Santillan-Jimenez, A.E. Harman-Ware, Y. Ji, D. Grubb, M. Crocker, Chem. Eng. J. 189–190 (2012) 346–355.
[229] J.-T. Feng, Y.-J. Lin, D.G. Evans, X. Duan, D.-Q. Li, J. Catal. 266 (2009) 351–358.
[230] E. Santillan-Jimenez, T. Morgan, J. Shoup, A.E. Harman-Ware, M. Crocker, Catal. Today 237 (2014) 136–144.
[231] K. Fan, X. Yang, J. Liu, L. Rong, RSC Adv. 5 (2015) 33339–33346.
[232] Q. Guo, M. Wu, K. Wang, L. Zhang, X. Xu, Ind. Eng. Chem. Res. 54 (2015) 890–899.